EAST BAY
MUNICIPAL UTILITY DISTRICT

Pardee Reservoir Enlargement Project
PRELIMINARY DESIGN REPORT

Volume 6
SEISMOTECTONIC EVALUATION STUDY

June 1998

HCG
Pardee Project Team

EBMUD *EAST BAY MUNICIPAL UTILITY DISTRICT*

PARDEE RESERVOIR ENLARGEMENT PROJECT
PRELIMINARY DESIGN REPORT

Volume 6

SEISMOTECTONIC EVALUATION REPORT

June 1998

Prepared for

EAST BAY MUNICIPAL UTILITY DISTRICT
375 Eleventh Street
Oakland California, 94607
(510) 835-3000

Submitted By

HCG
Pardee Project Team
HDR Engineering Inc.
Christensen Associates Inc.
ΦGEI Consultants Inc.

Project Office
505 Fourteenth Street – Suite 940
Oakland , California, 94612
(510) 986-1880

MATERIALS ENGINEERING

Pardee Reservoir Enlargement Project
PRELIMINARY DESIGN REPORT

LIST OF REPORT VOLUMES

Volume

1. SUMMARY TECHNICAL REPORT
2. (Not Used)
3. COST ESTIMATE
4. CONCEPTUAL DESIGN REPORT
5. CONCEPTUAL DESIGN BASIS MEMORANDA
6. SEISMOTECTONIC EVALUATION STUDY
7. CONCRETE DAMS
   STRESS & STABILITY ANALYSIS
8. PARDEE DAM SITE
   GEOLOGY & GEOTECHNICAL DATA REPORT
9. JACKSON CREEK DAM SITE
   GEOLOGY & GEOTECHNICAL REPORT
10. DOWNSTREAM DAM SITE
    GEOLOGY & GEOTECHNICAL REPORT
11. CONSTRUCTION MATERIALS REPORT
12. HYDROLOGIC STUDIES
13. RESERVOIR OPERATIONS STUDIES DATA
14. RAISED INTAKE TOWER
    PRELIMINARY SEISMIC ANALYSIS & STRUCTURAL DESIGN

PARDEE RESERVOIR ENLARGEMENT PROJECT
PRELIMINARY DESIGN REPORT

VOLUME 6
SEISMOTECTONIC EVALUATION STUDY

CONTENTS

EXHIBITS

TABLES

APPENDICES

1. INTRODUCTION

1.1 BACKGROUND

The East Bay Municipal Utility Water District (EBMUD) has embarked on a water supply management program to investigate alternatives to meet water supply needs for projected population increases and drought security. One alternative project is the Pardee Reservoir Enlargement Project.

Pardee Dam and Reservoir are owned and operated by EBMUD for the primary purpose of municipal water supply. Reservoir enlargement options that would raise the normal reservoir water surface by about 40 to 70 feet are currently being considered.

This report presents a summary of pertinent geological issues pertaining to fault capability in the vicinity of Pardee Reservoir, seismic response spectra recommended for preliminary design, and associated ground motion acceleration time histories for preliminary design.

This study is not intended to be a complete characterization of seismotectonic sources affecting structures in the western Sierra Nevada. It does not include a detailed explanation of Cenozoic and Quaternary stratigraphy in the western Sierra Nevada foothills and central San Joaquin Valley, nor characterizations of far-field seismic sources, which include active faults beyond the Pardee study area such as the Sierra Nevada frontal fault zone, Coast Range thrust fault, and San Andreas fault system. However, contribution of far-field seismic sources identified in other studies were considered in the probabilistic hazard analyses.

A summary of pertinent geologic issues pertaining to fault capability in the vicinity of Pardee Dam are presented. Explanations of Cenozoic and Quaternary geology, soil stratigraphy of the western Sierra Nevada, regional seismic courses, and historic seismicity are contained in Dames and Moore (1993) and U. S. Army Corps of Engineers (1995).

1.2 PURPOSE

The purposes of this study are to:

1. Briefly describe the tectonic setting of the western Sierra Nevada.
2. Identify and evaluate near-field seismic sources likely to affect the Pardee Reservoir Enlargement Project.

3. Determine design ground motions at the existing Pardee Dam site, the downstream dam site, the Jackson Creek Dam site, and the existing outlet tower for use in preliminary design.
4. Recommended additional seismotectonic studies for final design.

1.3 SCOPE OF WORK

The scope of work consisted of:

1. Review of published geologic maps.
2. Review and analysis of previous investigative findings, including maps, reports, trench logs (i.e., Corps of Engineers, 1995), and unpublished geomorphic profiles (Pacific Gas and Electric Company).
3. Stereoscopic examination of aerial photographs for the years 1971, 1987, 1991, 1992, 1995 and 1996.
4. Preliminary design-level geologic mapping of an approximately 3-square-mile area west of Pardee Reservoir.
5. Reconnaissance-level geologic mapping of an approximately 25-square-mile area generally north and west of Pardee Reservoir.
6. Interpretation and analysis of existing and newly acquired data and characterization of near-field seismic sources.
7. Estimation of ground motions at the existing Pardee Dam site, downstream dam sites, Jackson Creek Dam site, and existing outlet tower site.
8. Formulation of site specific response spectra.
9. Development of design acceleration time histories.

2. GEOLOGIC SETTING

Pardee Reservoir is in the western Sierra Nevada, near the margin with the Central Valley. Together, the Central Valley and Sierra Nevada form a single tectonic province termed the "Sierran Block," which is a block of basement rocks tilted downward to the west, situated between the California Coast Ranges to the west and the Basin and Range province to the east. Regional tectonic features are shown on Exhibit 2-1.

Bedrock in the western Sierra Nevada consists of metamorphosed volcanic and sedimentary rocks that provide evidence of Paleozoic and Mesozoic continental growth. Oblique convergence between the North American plate and an oceanic plate (perhaps the proto-Farallon plate) was the driving mechanism for this terrane accretion, which culminated with the Nevadan Orogeny in late Jurassic time between 163 and 143 million years ago (Graymer and Jones, 1994). The principal terrane boundaries near Pardee Reservoir are the Melones fault zone and Bear Mountains fault zone. These two pronounced fault zones separate the bedrock complex of the western Sierra Nevada into three northwest-trending tectonic terranes, as shown on Exhibit 2-2. From east to west, the three tectonic terranes are:

1. The Calaveras Terrane, which is composed of Paleozoic-age rocks (245-570 million years old).

2. The Placerville Belt (equivalent to the Central Belt of Clark, 1964), an approximately 7-kilometer-wide zone of Mesozoic-age (65-245 million years old), metavolcanic and metasedimentary rocks bounded by the Melones (on the east) and Bear Mountains (on the west) fault zones.

3. The Western Belt, which is located west of the Bear Mountains fault zone and is composed of Mesozoic-age, metavolcanic, and metasedimentary rocks similar to that of the Placerville Belt.

Pardee Reservoir is in the Western Belt. The Western Belt comprises three Mesozoic-age bedrock formations, the Copper Hill Volcanics, Salt Springs Slate, and Gopher Ridge Volcanics. The regional geology in the vicinity of Pardee Reservoir is shown in section on Exhibit 2-3 and in plan on Exhibit 2-4.

Tertiary bedrock units of the Ione, Valley Springs, and Mehrten Formations locally overlie the Mesozoic rocks in the vicinity of Pardee Reservoir.

The Eocene-age Ione Formation (40 million years old) is the oldest Tertiary unit in the region, and consists of quartz-rich sandstone and conglomerate and kaolinitic claystone. The Ione Formation is a local source of sand and gravel, lignitic coal and pottery-grade clay.

The Oligocene- to Miocene-age Valley Springs Formation (20-25 million years old) consists of interbedded fluvial deposits (siltstone, sandstone and conglomerate) and rhyolitic tuffs. Rhyolitic tuffs south of Pardee Reservoir have been dated to be 22 to 23 million years old (Dames & Moore, 1993) and are particularly useful in evaluating late Cenozoic deformation.

The Miocene- to Pliocene-age Mehrten Formation (4.6-10 million years old) consists of volcaniclastic sediments, volcanic agglomerates, tuffs and local lava flows deposited in stream channels. The Mehrten deposits are highly resistant to erosion and Mehrten-filled, Cenozoic-age stream channels form a series of discontinuous linear ridges that strike roughly perpendicular to the regional structure. The Table Mountain Latite, which forms a prominent southwest-trending series of ridges approximately 40 km south of Pardee Reservoir, is an older member of the Mehrten Formation.

2.1 FOOTHILLS FAULT SYSTEM

The Foothills fault system is a wide zone of faulting located along the western slopes of the central Sierra Nevada. The Foothills fault system includes the Melones and Bear Mountains fault zones and other recently recognized faults to the west that together form a fault system extending a distance of approximately 230 km, from Mariposa northwestward to Oroville. The closest faults to Pardee Dam that appear to exhibit late Cenozoic activity are shown on Exhibit 2-4. These are the Youngs Creek fault (4000 meters east); Devils Gate fault (1070 meters east); Waters Peak fault (152 meters west); and Ione fault (1370 meters west).

Late Cenozoic faulting in the western Sierra has taken place primarily along pre-existing zones of weakness that are relics from the Mesozoic-age Nevadan Orogeny and resulted from a strong pulse of uplift and westward-tilting of the Sierran Block. Uplift of the modern Sierra Nevada is estimated to have begun approximately 4 to 7 million years ago (Unruh, 1991; Pacific Gas and Electric Company, in progress). Based on progressive tilting of the Miocene-age Mehrten Formation, the onset of relatively continuous uplift appears to have occurred during deposition of the uppermost part of the Mehrten Formation, which has been estimated to be between 4.6 and 5.7 million years old (Woodward-Clyde Consultants, 1978). Based on this tilting and the estimated age of the Mehrten Formation, 5 million years is generally selected as the initial time of uplift and the basis for slip rate determination for late Cenozoic faults within the Sierran Block.

The Melones fault zone was the primary structure of the ancestral Foothills fault system, and is considered to be the most active component of the fault system in modern time (last 2 million years). Both the Melones and Bear Mountains fault zones appear to be more continuous than faults located further west. Faults in the northwestern portion of the Foothills belt (e.g., Oroville area) appear to have more pronounced geomorphic expression than the central and southern portions of the belt, reflecting greater activity in the northwestern portion of the Foothills fault system.

2.1.1 REGIONAL SEISMICITY

Compared to surrounding regions, the Sierran Block is characterized by a low level of seismicity. The Sierran Block is considered to be a relatively stable crustal block between the San Andreas fault system and the Basin and Range (Pacific Gas and Electric, unpublished; Urhammer, 1991). Although compilation and analysis of earthquake seismicity was not part of this study, a review of published reports indicates that earthquake focal mechanisms show a pattern of oblique slip to dextral slip on northwest-striking faults and a pattern of normal dip-slip on north-striking faults in the Sierra Nevada (Pacific Gas and Electric Company, unpublished; Wong and Savage, 1983; Hill and others, 1991).

The largest recorded historic earthquake along the Foothills fault system was the Oroville earthquake of August 1, 1975 (magnitude = 5.7). This earthquake, centered approximately 150 km northwest of Pardee Reservoir, provides direct seismologic evidence that portions of the Foothill fault system are active. The earthquake was dominantly normal dip-slip, with the west side down, and a focal depth of 8 km (Bolt, 1977). However, earthquake focal mechanisms also indicate a strike-slip component of movement (lateral-to-vertical ratio of 0.4:1, Wallace, 1990). Surface rupturing was associated with a trace of the Cleveland Hill fault, and extended for a distance of 5.7 km. Surface displacement measurements indicated 4 cm of right-lateral strike-slip and 5 cm of normal dip-slip movement (Hart and Rapp, 1975).

2.1.2 STYLE OF LATE CENOZOIC DEFORMATION

The rate and style of tectonic deformation in the Sierran Block is influenced by northwest motion of the Pacific plate relative to the North American plate and crustal extension in the Basin and Range. Approximately 75 percent of the dextral plate motion (i.e., about 36 mm of the total 48 mm/year) between the Pacific and North American plates is accommodated by the San Andreas fault system. The remaining 25 percent (12 mm) is accommodated by deformation east of, and partly within, the Sierran Block with much of the movement believed to be accommodated by faults in the Greater Walker Lane tectonic belt. The Greater Walker Lane tectonic belt is considered to be the transition between the Sierran Block and the Basin and Range, as shown on Exhibit 2-1. Although regionally the Sierran Block is not considered a significant contributor to plate boundary motion, the presence of diffuse seismicity indicates ongoing, low-level tectonic activity within the Sierran Block from east-west crustal extension and dextral strike-slip motion.

Late Cenozoic deformation, manifested as extensional and dextral displacements, has occurred locally along reactivated fault segments within the Foothills fault system. This has been demonstrated by geomorphic analyses and paleoseismic trench studies (e.g., Pacific Gas and Electric Company, unpublished; Woodward-Clyde Consultants, 1978). The previously identified studies indicate that Cenozoic faulting may involve a component of strike-slip movement, but slip rate estimates only pertain to normal slip movement. Based on our field mapping of several fault exposures, development of criteria to assess sense of slip in exposed faults, and geomorphic analysis designed to

evaluate apparent tectonic offset of Tertiary paleostream channel deposits, it appears that the Cenozoic style of movement for the central Foothills fault system includes a significant component of dextral strike slip in addition to normal slip.

A geomorphic analysis of the surface of the Table Mountain Latite was conducted as part of this study to constrain the strike-slip component of Cenozoic deformation along the Foothills fault system. The Table Mountain Latite, which is about 9.6 million years old, forms a series of resistant ridges adjacent to the modern Stanislaus River approximately 40 km southeast of Pardee Dam. These ridges are the remnants of a Tertiary stream channel that was filled by volcanic flows that now are elevated above the surrounding topography because of preferential erosion of the surrounding, less resistant rocks. Several late Cenozoic faults that displace the Table Mountain Latite were previously identified based on geomorphic analysis and subsurface investigations for the New Melones Dam and Stanislaus Nuclear Power Plant (Woodward-Clyde Consultants, 1978). Paleoseismic trench data indicate that movement of these faults is predominantly normal-slip, with an unknown component of strike-slip.

Surface topography provides a good approximation of the former channel axis because of the resistant nature of the latite. The channel axis is displaced laterally at four locations in the area examined. All four of these locations coincide with previously identified faults or steep monoclinal folds as shown on Exhibit 2-5. The strike-slip component of movement was computed by measuring apparent displacements of the channel axis. Lateral offset of the channel axis appears to vary from about 250 to 600 meters. If the lateral offsets were solely the result of dextral strike-slip deformation over the past 5 million years, average lateral slip rates would be 0.05 to 0.12 mm/year. The actual slip rate would likely be less than the computed slip rate, because channel sinuosity and normal-slip deformation may affect apparent lateral offset, and deformation may have been initiated prior to 5 million years ago.

Ridges capped by the Mehrten Formation also were examined as part of this study to constrain possible slip rates of faults in the Pardee Reservoir area. Relationships between five northwest-trending faults and several southwest-trending linear ridges in the Valley Springs area southeast of Pardee Reservoir are shown on Exhibit 2-6. Prominent linear ridges are assumed to accurately denote axes of paleostream channels that were filled by volcaniclastic sediments. Paleostream channel axes in the Valley Springs area cannot be established as confidently as at Table Mountain because of the lack of continuity and the sporadic distribution of Mehrten exposures. Lateral offsets of the ridges appear to vary from approximately 600 to 1200 meters, which are larger than apparent offsets observed at Table Mountain. Larger apparent lateral offsets in the Valley Springs area are most likely due to problems associated with reconstructing paleochannel axes than from greater fault slip rates. Palinspastic reconstruction of the paleostream channels in the Mehrten Formation at both locations indicates a pattern of dextral strike-slip along the northwest-trending faults.

A Mehrten Formation exposure north of Lake Amador, where a trace of the Devils Gate fault has been mapped, was also examined and is presented on Exhibit 2-7. Based on reconstruction of probable Mehrten-age channels, dextral strike-slip displacements of approximately 150 to 450 meters were computed at this location. Based on this geomorphic reconstruction and an assumption that faulting was initiated approximately 5 million years ago, the computed late Cenozoic strike-slip rate across this fault trace is in the range of 0.03 to 0.09 mm/year.

Seismologic evidence of a dextral strike-slip component to the Foothills fault system includes earthquake focal mechanisms indicating oblique-slip and strike-slip faulting events in the north-central Sierra Nevada (Hill and others, 1991; Wong and Savage, 1983). Surface rupture associated with the 1975 Oroville earthquake produced a 0.8:1 lateral-to-vertical slip ratio, and right-lateral displacements generally were greater than vertical displacements along most of the rupture trace (Hart and Rapp, 1975).

Oblique-slip to strike-slip deformation is recognized in trenches on several faults in the south-central portion of the Foothills fault system as follows:

1. Trenches excavated across the Youngs Creek, Negro Jack Point and Rawhide Flat East faults exposed "flower structures," which are typically indicative of strike-slip faults (Woodward-Clyde Consultants, 1978).

2. Slickensided surfaces identified in a trench across the Waters Peak fault indicate a lateral-to-vertical slip ratio of 1:1 to 2:1 (William Lettis and Associates, 1994).

3. A lateral-to-vertical slip ratio of 1.8:1 was measured in Mehrten deposits offset by the Maidu East fault near the Auburn Dam site (Woodward-Clyde Consultants, 1977).

According to previous investigators (Schwartz, D., 1997; Page, W. P., 1997), faults in the eastern portion of the Foothills fault system (i.e., Melones fault zone) appear to be more continuous, more active, and characterized by dominantly normal-slip movement compared to faults in the western portion of the fault system. Based on the information presented above, it is concluded that:

1. Dextral strike-slip is a significant, and possibly the dominant, component of Cenozoic deformation for northwesterly trending faults in the western portion of the Foothills fault system.

2. Cenozoic movement on northerly trending faults may be predominantly characterized by normal-slip.

3. Geomorphic reconstruction is a less precise method of estimating slip rates than fault movement indicators observed in paleoseismic trenches; however, the geomorphic reconstruction analysis indicates a consistent pattern of

dextral strike-slip across the faults examined for this study. Seismicity and limited paleoseismic trenching data also support a significant component of strike-slip deformation.

2.2 FAULTS IN THE PARDEE RESERVOIR AREA

2.2.1 YOUNGS CREEK FAULT

The Youngs Creek fault was identified in previous studies as having late Cenozoic displacement on the basis of moderately strong to strong geomorphic expression and a 5-meter vertical displacement of the Mehrten Formation in trenches excavated by Woodward-Clyde Consultants (1978). Faults exposed in the trenches display down-to-the-east movement.

The Youngs Creek fault is characterized as a 30- to 60-meter-wide zone of intensely sheared and slickensided serpentinite and displaced Tertiary deposits that is close to the western contact of a melange zone that forms the contact between the Western Belt and the Placerville Belt tectonic terranes (Corps of Engineers, 1995). Both William Lettis & Associates (1994) and Page (1994) believe that sufficient colluvium was exposed in the Corps of Engineers' trench to demonstrate that no displacement occurred in the past 14,000 to 60,000 years. In contrast, the Corps of Engineers' report states that the trench did not expose sufficient soil cover to allow an assessment of fault activity.

Geologic field mapping of the Youngs Creek fault was not conducted as part of the Pardee Reservoir enlargement studies; however, geomorphic analyses were conducted using aerial photographs and topographic quadrangle maps. The Youngs Creek fault exhibits a strong to moderate geomorphic expression for a distance of approximately 22 km as shown on Exhibit 2-4. As shown on Exhibit 2-6, a strong lineament, which is indicative of late Cenozoic movement, is a short distance west of the fault trace trenched by Woodward-Clyde Consultants (1978) and the Corps of Engineers (1995). Based on geologic and geomorphic data, the late Cenozoic displacement is probably oblique (dextral strike-slip and down-to-the-east normal slip). Fault ruptures logged in Woodward-Clyde Consultants' Trench 2 (1978) are nearly vertical at depth and become slightly concave-upward (i.e., "flower structure"), which are typical of faulting produced by lateral slip.

The Youngs Creek fault may represent a segment of a longer fault zone aligned along the Bear Mountains fault zone that includes the Sunnybrook East fault to the northwest and other possible fault segments to the southeast. The length of the Sunnybrook East fault is estimated to be 8 km (Pacific Gas and Electric Company, unpublished).

2.2.2 DEVILS GATE FAULT

The Devils Gate fault was identified by previous investigators on the basis of strong geomorphic expression along the eastern margin of Pardee Reservoir and apparent offset

of late Cenozoic deposits at two locations to the northwest and southeast of the reservoir. Previous estimates of fault length ranged from 20 to 40 km (Earth Sciences Associates, 1992, and Dames and Moore, 1993). The longer fault length reflects the combined length of the Devils Gate fault and the Peoria Pass fault located at Table Mountain. Dames and Moore (1993) considered the two faults to be distinct segments of a single fault zone. Pacific Gas and Electric Company (unpublished) consider the Devils Gate fault to be one of several fault segments that form a 60 km fault zone extending southeastward to Table Mountain. Based on geomorphic mapping conducted for the Pardee Reservoir Enlargement Study, it appears that the primary trace of the Devils Gate fault forms a moderately strong to strong geomorphic lineament for a distance of approximately 22 km as shown on Exhibit 2.3. This lineament may represent the northern segment of a longer fault zone.

In addition to the primary trace of the Devils Gate fault, a second fault trace was identified east of the Jackson Creek Spillway, where a geomorphic lineament coincides with a faulted contact between the Copper Hills Volcanics and Salt Springs Slate formations, as shown on Exhibit 2-3. This fault trace, which is exposed about 340 meters south of the Jackson Creek Spillway at low reservoir levels, is characterized by drag folding indicative of strike-slip movement, which is associated with late Cenozoic movement.

The Devils Gate fault may coincide with the western edge of a shear zone referred to as the Spring Valley structure, which is part of the Bear Mountain fault zone located east of the town of Valley Springs (Woodward-Clyde Consultants, 1978). Based on a geomorphic profile, the Castle Rock Tuff member of the Valley Springs Formation was vertically offset (west side down) 12 meters. Woodward-Clyde Consultants (1978) attributed the offset to buried topographic relief rather than faulting. Recent re-interpretation of the geomorphic profile by Pacific Gas and Electric Company (unpublished) indicates that west-side-down offset may be the result of faulting.

According to Dames and Moore (1993), the top of the Mehrten Formation (i.e., ground surface) is vertically offset 12 meters across the Devils Gate fault north of Lake Amador, which is approximately 5 km northwest of Pardee Reservoir. Using a vertical displacement of 12 meters and an assumption that faulting was initiated 5 million years ago, the late Cenozoic normal-slip rate for the Devils Gate fault was calculated to be 0.002 mm/year. Geologic mapping conducted as part of this study, an evaluation of the Dames and Moore (1993) profile, and geomorphic profiles constructed by Pacific Gas and Electric Company (unpublished) do not indicate only normal-slip displacement across the postulated trace of the Devils Gate fault near State Highway 88. Palinspastic reconstruction of probable Mehrten-age channels indicate that approximately 150 to 450 meters of dextral strike-slip displacement may have occurred along the Devils Gate fault at the State Highway 88 location. The apparent late Cenozoic strike-slip rate of movement is in the range of 0.03 to 0.09 mm/year, based on the following assumptions: 1) 150 to 450 meters of strike-slip movement, 2) little to no channel sinuosity, and 3) faulting initiated 5 million years ago.

2.2.3 *WATERS PEAK FAULT*

The Waters Peak fault was identified by previous investigators on the basis of strong geomorphic expression, geomorphic profiles, and paleoseismic trenching. The fault is well expressed geologically, as well as geomorphically, in the Mokelumne River gorge and Mexican Gulch, where the fault strikes approximately N37-44W and dips steeply (64 to 70 degrees) to the northeast.

The Waters Peak fault forms a strong geomorphic lineament for a distance of approximately 15 km, from the northeast side of Waters Peak southward to near New Hogan Reservoir, as shown on Exhibit 2-4. Based on a lack of geologic and geomorphic indications of faulting north of Waters Peak, the northwestern end of the fault is considered to be in the vicinity of Stony Creek Road. The Waters Peak fault may be the northern segment of a longer fault zone that includes the Green Springs Run fault southeast of New Hogan Reservoir (Dames & Moore, 1993).

The Castle Rock tuff member (22 million years old) of the Valley Springs Formation is offset vertically 46 to 62 meters by the Waters Peak fault (Dames & Moore, 1993; Page, 1994). Using these vertical displacements and an assumption that faulting was initiated approximately 5 million years ago, the average late Cenozoic uplift rate for the Waters Peak fault ranges from 0.009 to 0.012 mm/year.

The Waters Peak fault was exposed in "Trench 3, Waters Peak Fault South," Corps of Engineers (1995). Fault planes exposed in the trench extend upward into Quaternary-age deposits that show late Quaternary displacement. The vertical offset at the top of the Quaternary-age faulted material is less than the offset at the base, which indicates repeated fault rupture events. Approximately 15 cm of displacement was measured at the uppermost faulted deposit, which may have an age of approximately 100,000 to 300,000 years. The fault exhibits both normal-slip and strike-slip displacement in Trench 3 (Corps of Engineers, 1995) and exposures observed in Mexican Gulch. The lateral to vertical slip ratio observed in the trench was estimated to be 1:1 to 2:1 (William Lettis & Associates, 1994).

The date of the last faulting event is unknown because of uncertainty in identifying the age of the lowermost (oldest) unfaulted deposit above the fault. The age of the unfaulted deposit is estimated as 20,000 to 70,000 years by the most detailed examination of the material (William Lettis & Associates, 1994). The Corps of Engineers investigators and reviewers judged the most recent movement of the Waters Peak fault to be more than 35,000 years ago.

2.2.4 *IONE FAULT*

The Ione fault was identified in previous studies on the basis of geomorphic expression, fault exposures in the Lake Amador spillway channel, and apparent vertical displacement of the Eocene-age Ione Formation (40 million years old). Earth Sciences Associates (1992) continued the lineament south to the town of Valley Springs; Dames & Moore

(1993) extended the fault south to Valley Springs Peak, but not as far south as the town of Valley Springs. Geomorphic expression of the Ione fault is characterized in this study as a 23-kilometer-long, west-facing escarpment that ends about 1.8 km northwest of the Mokelumne River, as shown on Exhibit 2-4.

The strong geomorphic lineament along the Ione fault zone coincides with a wide zone of faulting exposed in the Lake Amador spillway channel, approximately 7 km northwest of the Mokelumne River, as shown on Exhibit 2-7. Detailed mapping of exposures in the Lake Amador spillway channel were conducted as part of this study and are presented on Exhibit 2-8. Numerous shears and faults over a length of about 200 meters were identified within the Salt Springs Slate Formation. All of the faults observed in the Lake Amador spillway channel are aligned generally parallel to foliation, which has a northwesterly strike and steep east dip (average orientation of N15W strike and dip 80°E). Faults observed in the Lake Amador spillway channel are similar in orientation to the east-dipping fault exposed in the Corps of Engineers' "Trench 1, Ione Fault" (Corps of Engineers, 1995). Differences in materials exposed in the north and south trench walls indicate that the fault in Trench 1 may have experienced strike-slip displacement in addition to dip-slip movement. No westerly dipping normal fault was observed in the Lake Amador spillway channel or in the Corps of Engineers trenches, which is contradictory to the west-side-down normal fault postulated by the Corps of Engineers.

Dames and Moore (1993) reported that the Ione Formation was vertically offset (west side down) a distance of 185 meters across the Ione fault. Using a vertical offset of 185 meters and an assumption that faulting was initiated 5 million years ago, the computed average late Cenozoic uplift rate is 0.037 mm/year. Based on profiling from Waters Peak westward across the Ione fault to Jackson Valley, vertical displacement of the base of the Ione Formation is estimated to be approximately 76 meters. Using 76 meters of displacement and an assumption that faulting was initiated 5 million years ago, the computed average late Cenozoic uplift rate is 0.015 mm/year.

No geomorphic expression of faulting was observed between the southwestern edge of Waters Peak and the Mokelumne River, which is in dramatic contrast to the strong west-facing escarpment to the northwest. No evidence of Cenozoic faulting was identified between Mexican Gulch and Penn Mine, which is a distance of approximately 3 km from mapping rock exposures along the walls of the Mokelumne River gorge. The Waters Peak fault appears to end toward the north, just as the Ione fault appears to terminate to the south. If the style of movement on the Ione fault is primarily dextral strike-slip, it can be hypothesized that motion along the Ione fault may step over to the Waters Peak fault (i.e., left-stepping faults are consistent with dextral strike-slip motion). Direct evidence to support or negate this hypothesis is not available.

2.2.5 GEOMORPHIC LINEAMENTS

Several geomorphic lineaments were identified and evaluated for this study. Geomorphic expressions of these features vary from weak to strong and include discontinuous to

continuous (1 to 4 km in length) linear drainages, hillside benches, and vegetation lineaments. Several lineaments were identified along trends of the late Cenozoic faults discussed above. Other lineaments appear to be associated with soil or vegetation changes, formational contacts, interbedding of different geologic units, bedrock structure, and faults of unknown activity.

Only lineaments displaying at least moderately strong geomorphic expression and possible association with faults are depicted on Exhibit 2-4. Two of these lineaments cross the proposed Jackson Creek Dam site. The westernmost of these two lineaments, which approximately coincides with a lineament identified by Dames and Moore (1993), roughly follows the geologic contact between the Salt Springs Slate and Gopher Ridge Volcanics formations. This contact is considered to be unfaulted and could be the result of differential erosion along the contact. Faulting in the vicinity of the contact is also possible based on scattered quartz exposures observed in the area and association between quartz veins and other identified faults in the Pardee Reservoir area. Quartz veins also occur as dikes along fractures and fold axes. This western lineament closely parallels the Waters Peak fault (located approximately 700 meters west), and late Cenozoic faulting along this lineament is possible.

The easternmost lineament closely follows the geologic contact between the Copper Hills Volcanics and Salt Springs Slate formations. These formations are faulted at the single exposure of the contact observed during this study. The geomorphic lineament could be the result of recent faulting or differential erosion along an old faulted contact. It is our interpretation that this lineament is an active trace of the Devils Gate fault because: 1) the lineament closely parallels a mapped trace of the Devils Gate fault, which is approximately 350 meters east, and 2) drag folding indicative of late Cenozoic strike-slip movement was observed in the fault exposure about 340 meters south of the Jackson Creek Spillway.

Two additional lineaments were identified in the Campo Seco area, which is downstream from Pardee Dam and south of the Mokelumne River. The eastern lineament is characterized by several weak to moderately strong discontinuous features, including a vegetation lineament, linear drainage, and a hillside bench. The western lineament is a more westerly trending linear drainage and hillside saddle that appears to intersect the eastern lineament.

2.3 FAULT CAPABILITY AND MAXIMUM EARTHQUAKES

Criteria for estimating fault activity are slip rate, time of last fault movement, and characteristic amount of fault rupture. Magnitudes of earthquakes associated with specific active faults are estimated by considering the seismic setting and fault parameters such as style of movement, typical displacement amount, and anticipated length or area of fault rupture. According to guidelines established by the State of California Division of Safety of Dams (DSOD), faults that show evidence of displacement within the past 35,000 years are considered active seismic sources for the purpose of seismic design.

Faults that can be demonstrated not to have moved in the past 35,000 years can be considered inactive, and not likely to produce an earthquake during the life of the project. Inactive faults can be dismissed as seismogenic sources for seismic design.

Faults in the Foothills fault system are considered conditionally active seismic sources by the DSOD because evidence pertaining to recency of movement is inconclusive. Fault activity assessments in the Sierran foothills are difficult to resolve because of the scarcity of Quaternary-age deposits for measurement of slip rates and assessment of recency of faulting. Without Quaternary-age deposits it is difficult to distinguish geologically recent displacements from movements produced by geologically older and currently inactive faults. Seismogenic assessments in the western Sierra Nevada are based on deformation of late Cenozoic deposits, evaluation of subtle features in fault zones, and geomorphic expression. Repeated and geologically recent fault movement typically leads to strong geomorphic expression. Weak geomorphic expression of a fault indicates a very low rate, or lack, of recent faulting.

All four faults examined in this study: Youngs Creek, Devils Gate, Waters Peak, and Ione, are considered to be active for seismic design considerations based on strong geomorphic expression, apparent late Cenozoic style of deformation (i.e., lateral or extensional displacements), and uncertainty regarding the time of last fault movement. These four faults may be less active than faults in the eastern and northern portions of the Foothills fault system because they display more subtle geomorphic expression than faults associated with the Melones fault zone and faults in the Oroville area. It is possible that further study may determine that all or some of the faults in the Pardee Reservoir area are not active.

Characterization of the style of deformation is an essential component in understanding fault behavior. To account for the indications of oblique slip and dextral strike-slip deformation identified from geomorphic reconstructions of paleostream channels and seismicity records, as well as dominant dip-slip movement identified from paleoseismic trench measurements of slickensided fault surfaces that plunge steeply in the direction of fault dip, lateral-to-vertical slip ratios were developed for the faults in the Pardee Reservoir area. Maximum earthquake magnitudes were determined using magnitude-fault area relationships established by Wells and Coppersmith (1994). The following sections summarize the seismic hazard assessment of the four faults in the Pardee Reservoir area.

2.3.1 YOUNGS CREEK FAULT

Fault Activity: The Youngs Creek fault appears to have ruptured late Cenozoic-age deposits, and the last rupture event may have occurred more than 14,000 to 60,000 years ago. The Youngs Creek fault is considered to be an active seismic source for seismic design purposes because, based on available data, movement within the last 35,000 years could have occurred.

Earthquake Magnitude: The Youngs Creek fault exhibits a strong to moderate geomorphic expression for a distance of approximately 22 km. Based on a rupture length of 22 km and rupture width of 12 km, the maximum magnitude earthquake is computed to be 6.4 using the magnitude-fault area relationships established by Wells and Coppersmith (1994).

Slip Rate: The Youngs Creek fault has previously been characterized as displaying primarily normal fault movement by previous investigators. Based on re-interpretation of trench logs and examination of geomorphic features, a strong component of strike-slip deformation was identified. A lateral to vertical slip ratio of 2:1 and an average cumulative slip rate of 0.002 mm/year is estimated for the Youngs Creek fault.

2.3.2 DEVILS GATE FAULT

Fault Activity: The Devils Gate fault appears to have displaced late Cenozoic-age deposits, but has not been trenched. The timing of the last fault movement is unknown. The Devils Gate fault is considered to be an active seismic source for seismic design purposes because based on available data, movement within the last 35,000 years could have occurred.

Earthquake Magnitude: The Devils Gate fault exhibits a strong to moderate geomorphic expression for a distance of approximately 22 km. Based on a rupture length of 22 km and rupture width of 12 km, the maximum magnitude earthquake is estimated to be 6.4 using the magnitude-fault area relationships established by Wells and Coppersmith (1994).

Slip Rate: Drag folds observed at a fault exposure and palinspastic reconstruction of probable Mehrten-age channels indicate that the late Cenozoic strike-slip rate of movement is greater than the normal dip-slip rate. A lateral to vertical slip ratio of 5:1 for the Devils Gate fault and an average cumulative slip rate of 0.03 mm/year is estimated for the Devils Gate fault.

Fault Displacement: Fault displacement is a consideration for foundation design because a trace of the Devils Gate fault passes close to the proposed Jackson Creek dam. It has been demonstrated through mapping of fault ruptures and paleoseismic trenching of active faults that surface displacement varies along rupture traces. Based on the magnitude-displacement relationships established by Wells and Coppersmith (1994), the amount of displacement per earthquake event is estimated to be 10 to 40 cm for a magnitude 6.0 to 6.4 earthquake. Paleoseismic trench observations in the Waters Peak Fault South Trench indicate a displacement of 15 cm for the most recent rupturing event, which is consistent with the estimated range of 10 to 40 cm.

2.3.3 WATERS PEAK FAULT

Fault Activity: The Waters Peak fault has displaced late Quaternary deposits, and the most recent fault movement may have occurred between 20,000 to 70,000 years ago. The

Waters Peak fault is considered to be an active seismic source for seismic design purposes because, based on available data, movement within the last 35,000 years could have occurred.

Earthquake Magnitude: The Waters Peak fault exhibits a strong to moderate geomorphic expression for a distance of approximately 15 km. Based on a rupture length of 15 km and a rupture width of 12 km, the Waters Peak fault may generate an earthquake with a moment magnitude of approximately 6.3 using magnitude-fault area relationships established by Wells and Coppersmith (1994).

Slip Rate: Based on the estimated lateral to vertical slip ratio of 2:1 estimated from a trench exposure (William Lettis and Associates, 1994) and previous estimates of vertical displacement of Cenozoic deposits in the Valley Springs area, an average cumulative slip rate of about 0.02 mm/year (i.e., 0.018 to 0.024 mm/year) was computed for the Waters Peak fault.

2.3.4 IONE FAULT

Fault Activity: The Ione fault has displaced Cenozoic deposits and may have displaced late Quaternary deposits. The most recent fault movement may have occurred between 9,000 to 14,000 years ago. Based on available data, the Ione fault is considered to be an active seismic source for seismic design.

Earthquake Magnitude: The Ione fault exhibits a strong to moderate geomorphic expression for a distance of approximately 23 km. Based on a rupture length of 23 km and a rupture width of 12 km, the Ione fault may generate an earthquake with a moment magnitude of approximately 6.4, according to the magnitude-fault area relationship established by Wells and Coppersmith (1994).

Slip Rate: Cenozoic deposits appear to be vertically displaced approximately 76 meters across the Ione fault west of Waters Peak, which leads to a vertical slip rate of 0.015 mm/year over the past 5 million years. Faults exposed in the Lake Amador spillway channel and in the Corps of Engineers' trench exhibit both dip-slip and strike-slip directions of movement. For consistency with the dextral strike-slip pattern observed across other nearby faults, a lateral to vertical slip ratio of 2:1 was used for the Ione fault. Using a lateral to vertical slip ratio of 2:1 and identified displacements, an average cumulative slip rate of 0.03 mm/year is estimated for the Ione fault.

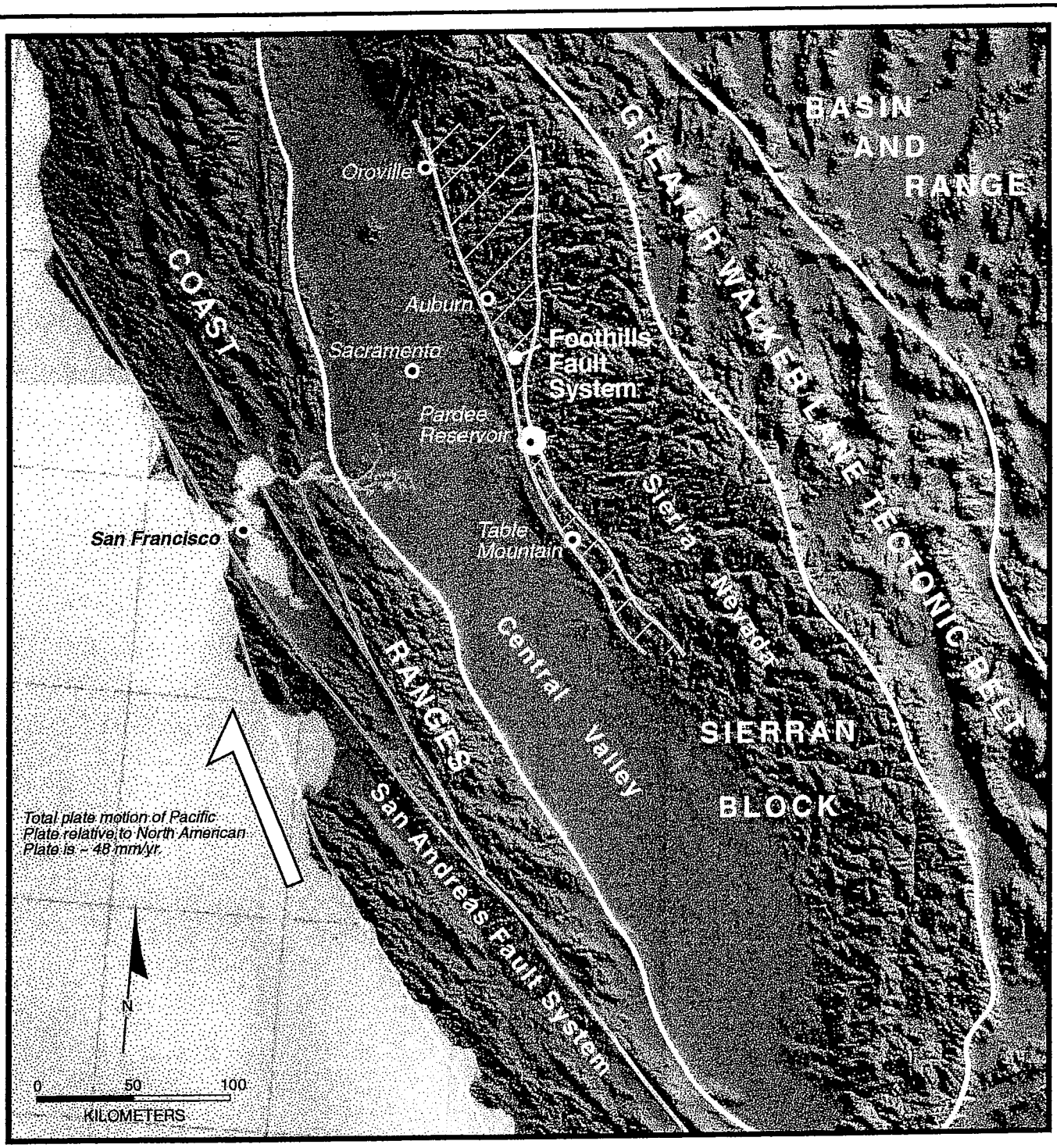

HCG

Pardee Project Team

HDR Engineering Inc.
Christensen Associates Inc.
ΦGHI Consultants Inc.

Pardee Reservoir Enlargement Project

REGIONAL TECTONIC MAP

VOLUME	Exhibit 2.1	
SCALE		REV.
DATE Dec. 1997		

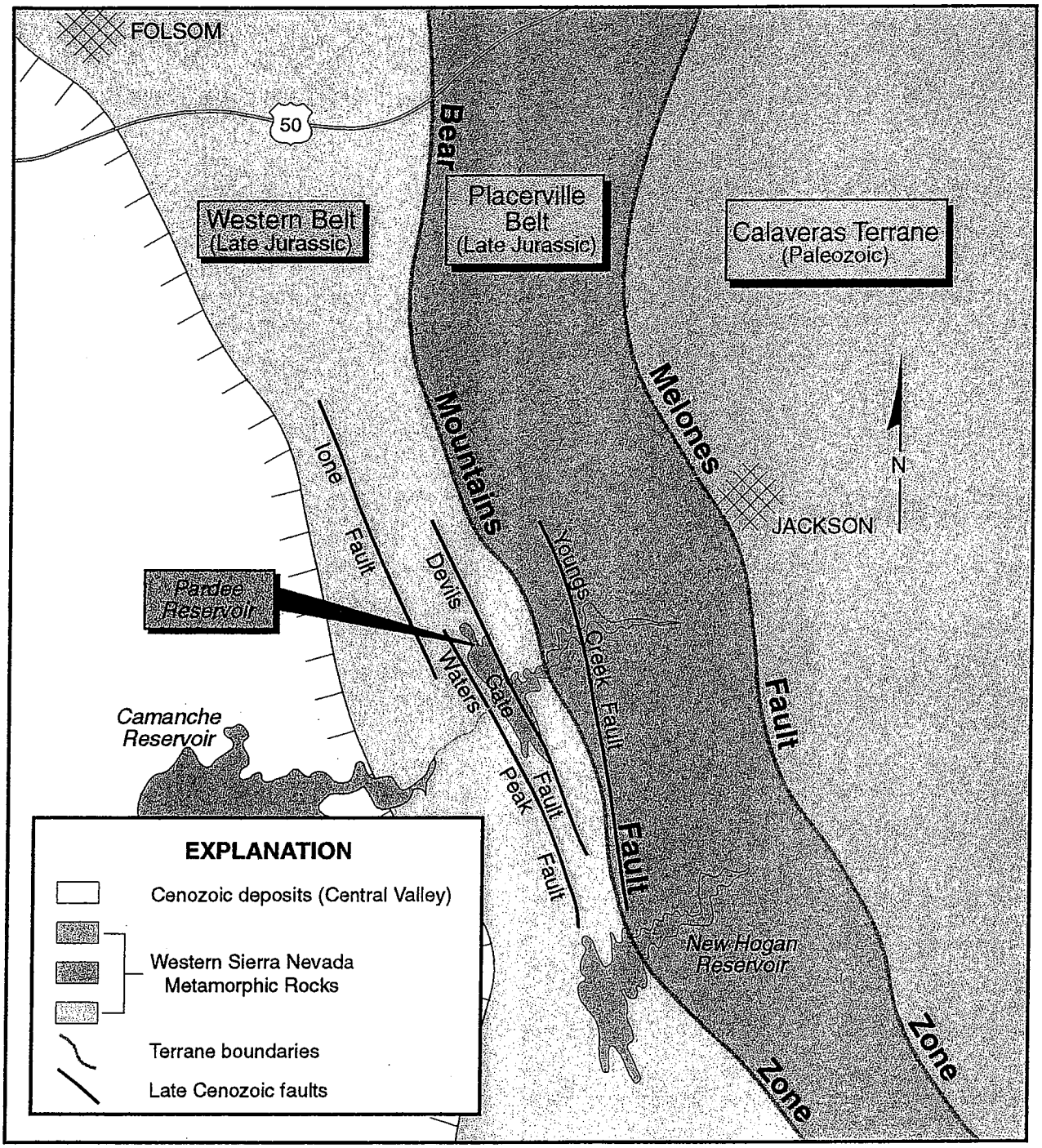

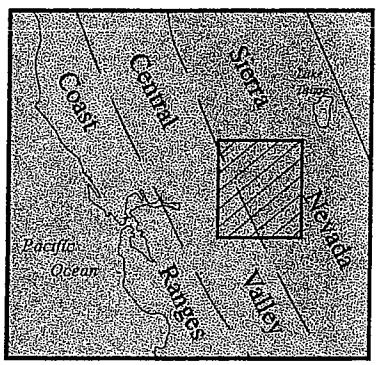

HCG

Pardee Project Team

HDR Engineering Inc.
Christensen Associates Inc.
GEI Consultants Inc.

Pardee Reservoir Enlargement Project

TECTONIC TERRANES OF THE WESTERN SIERRA NEVADA

VOLUME			
SCALE	Not to scale	Exhibit 2.2	
DATE	Dec. 1997		REV.

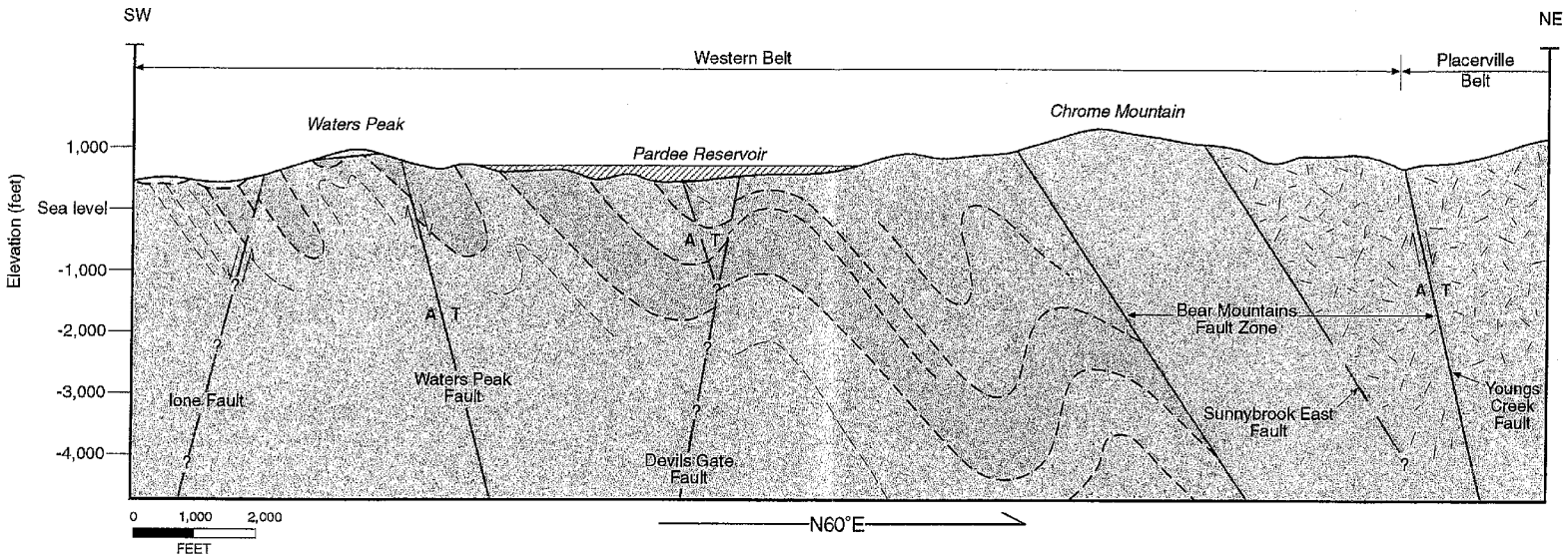

EXPLANATION

Eocene — Ione Formation

Copper Hills Volcanics Formation

Mesozoic — Salt Springs Slate Formation

Gopher Ridge Volcanics Formation

Ultramafics, Gabbro, Diorite

Melange (Paleozoic and Mesozoic)

A / T — Fault, late Cenozoic sense of slip where known shown with red arrows, A indicates movement away from observer, T indicates movement toward observer.

HCG

Pardee Project Team

HDR Engineering Inc.
Christensen Associates Inc.
ΦGEI Consultants Inc.

Pardee Reservoir Enlargement Project

REGIONAL GEOLOGIC CROSS SECTION

VOLUME
SCALE
DATE Dec. 1997

Exhibit 2.3

REV.

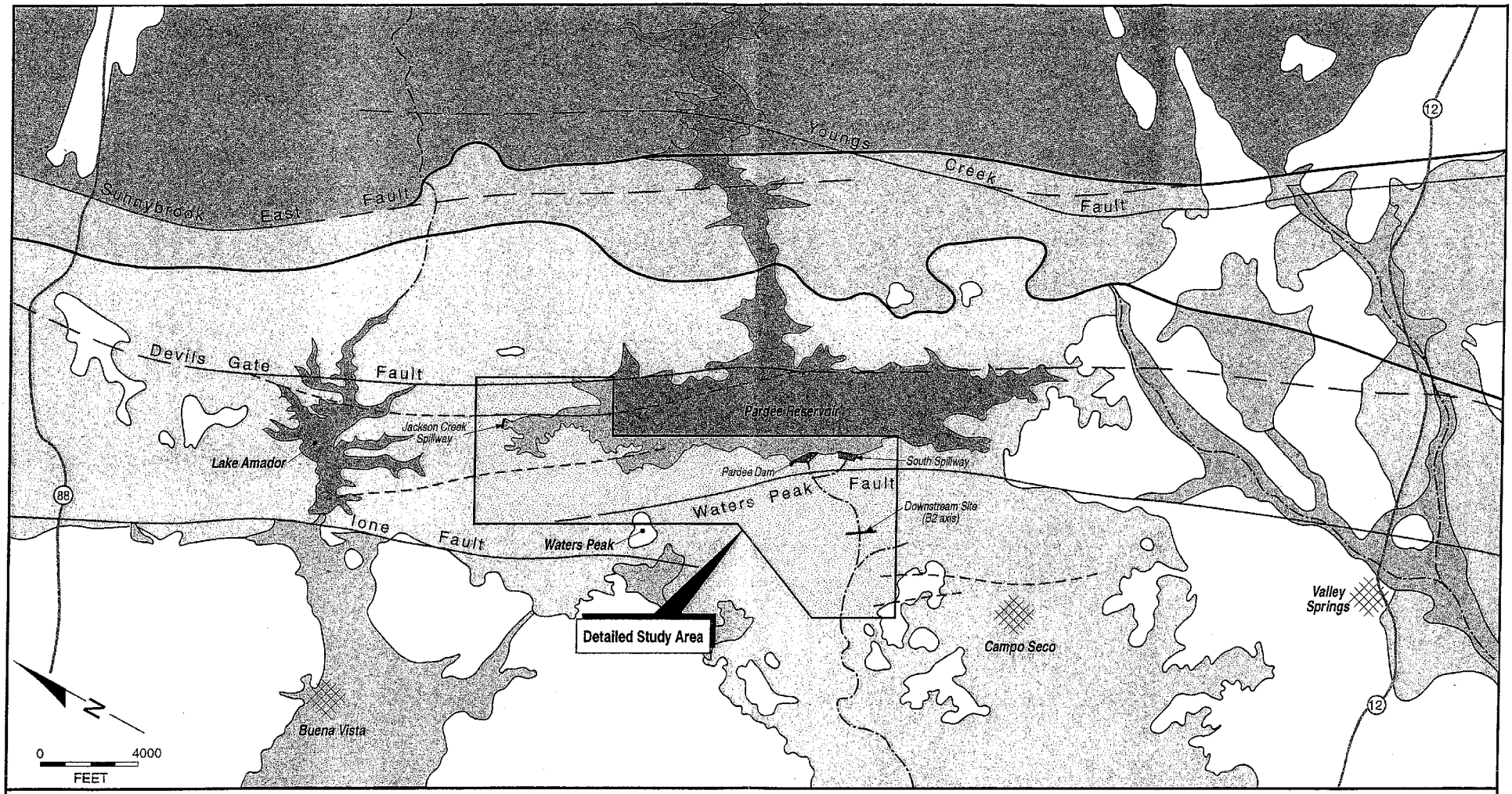

EXPLANATION

GEOLOGIC UNITS

- Quaternary deposits
- Tertiary units
- Mesozoic metamorphic rocks (Western Belt)
- Mesozoic metamorphic rocks (Placerville Belt)

SYMBOLS

- River or creek channel
- Geologic contact
- Bear Mountains fault zone (includes melange and ultramafic, gabbroic and dioritic rocks)
- Fault with probable or confirmed late Cenozoic activity, dashed where inferred
- Lineament with moderate geomorphic expression (possible fault)

Sources:
Bartow and Marchand (1979);
Clark (1964);
Marchand and Allwardt (1981);
and this study.

HCG

Pardee Project Team

HDR Engineering Inc.
Christensen Associates Inc.
©GH Consultants Inc.

Pardee Reservoir Enlargement Project

FAULT AND BEDROCK GEOLOGY MAP

VOLUME		
SCALE	Exhibit 2.4	
DATE Dec. 1997		REV.

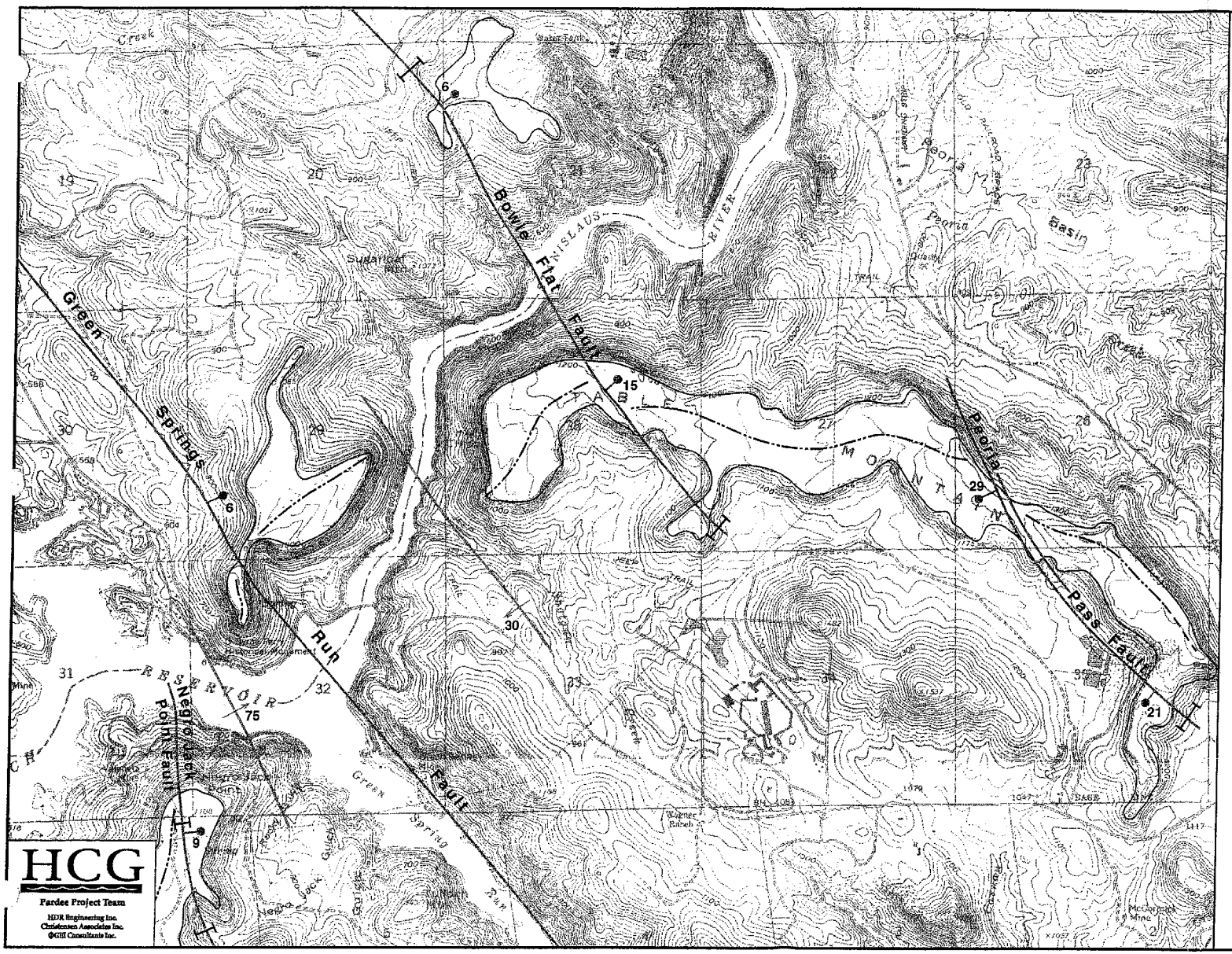

EXPLANATION

- Fault
- 29 — Height of fault scarp (meters), ball on downthrown side.
- Steep fold axis (possible fault).
- 75 — Elevation difference across fold axis (meters), arrow denotes down side.
- Trench site (WCC, 1978)
- Surface of Table Mountain Latite, showing interpreted paleochannel axis.

N

0 2000
FEET

Base map: New Melones Dam 7.5' Quadrangle

See Exhibit 2-1 for general location of Table Mountain Relative to Pardee Reservoir

HCG

Pardee Project Team

HDR Engineering Inc.
Christensen Associates Inc.
©Gill Consultants Inc.

Pardee Reservoir Enlargement Project

FAULT MAP OF TABLE MOUNTAIN

VOLUME		Exhibit 2.5	
SCALE			
DATE	Dec. 1997		REV.

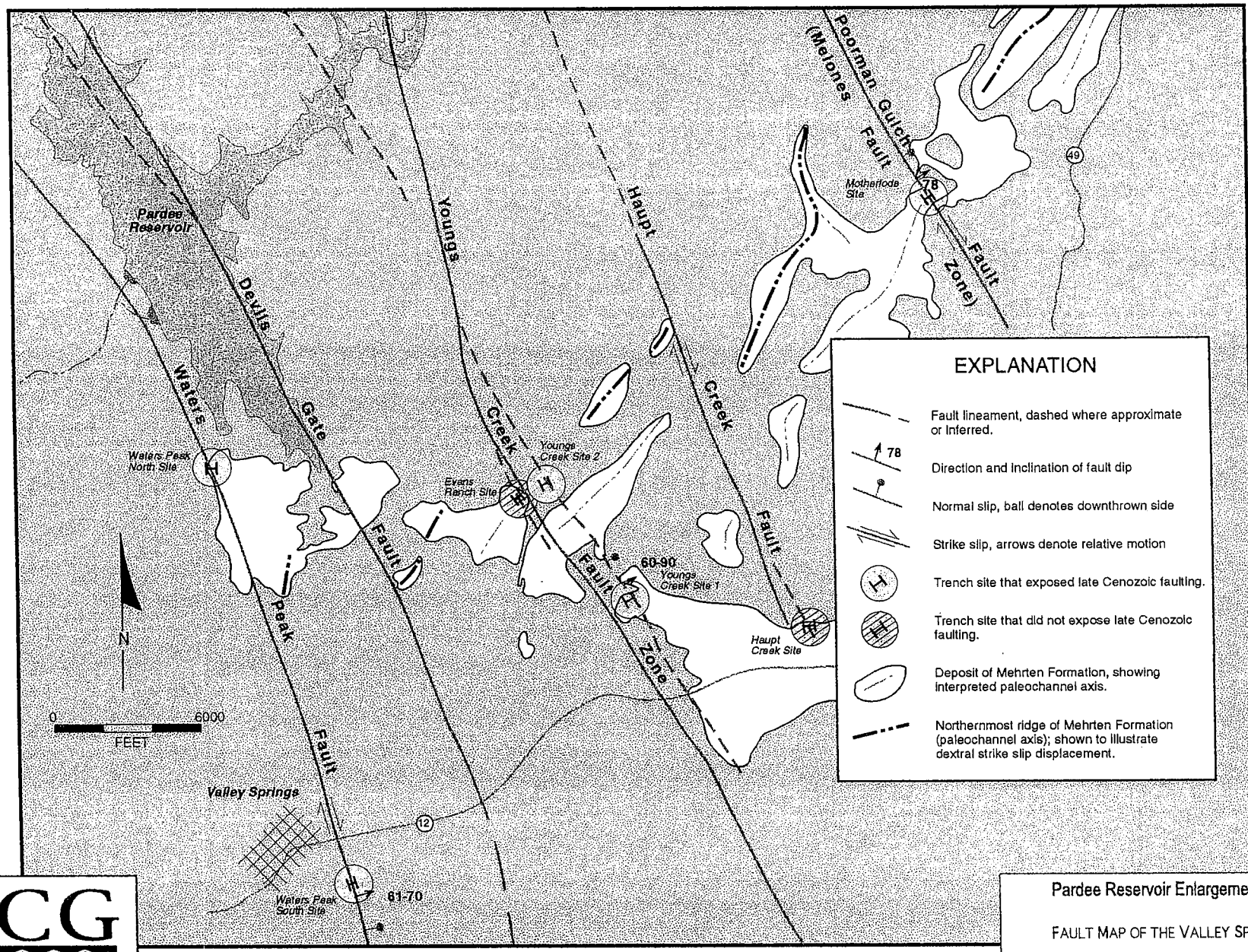

HCG

Pardee Project Team

HDR Engineering Inc.
Christensen Associates Inc.
ΦGEI Consultants Inc.

Note: Trench data from Woodward-Clyde Consultants (1978) and Corps of Engineers (1995)

Pardee Reservoir Enlargement Project

FAULT MAP OF THE VALLEY SPRINGS AREA

VOLUME		Exhibit 2.6	
SCALE			REV.
DATE	Dec. 1997		

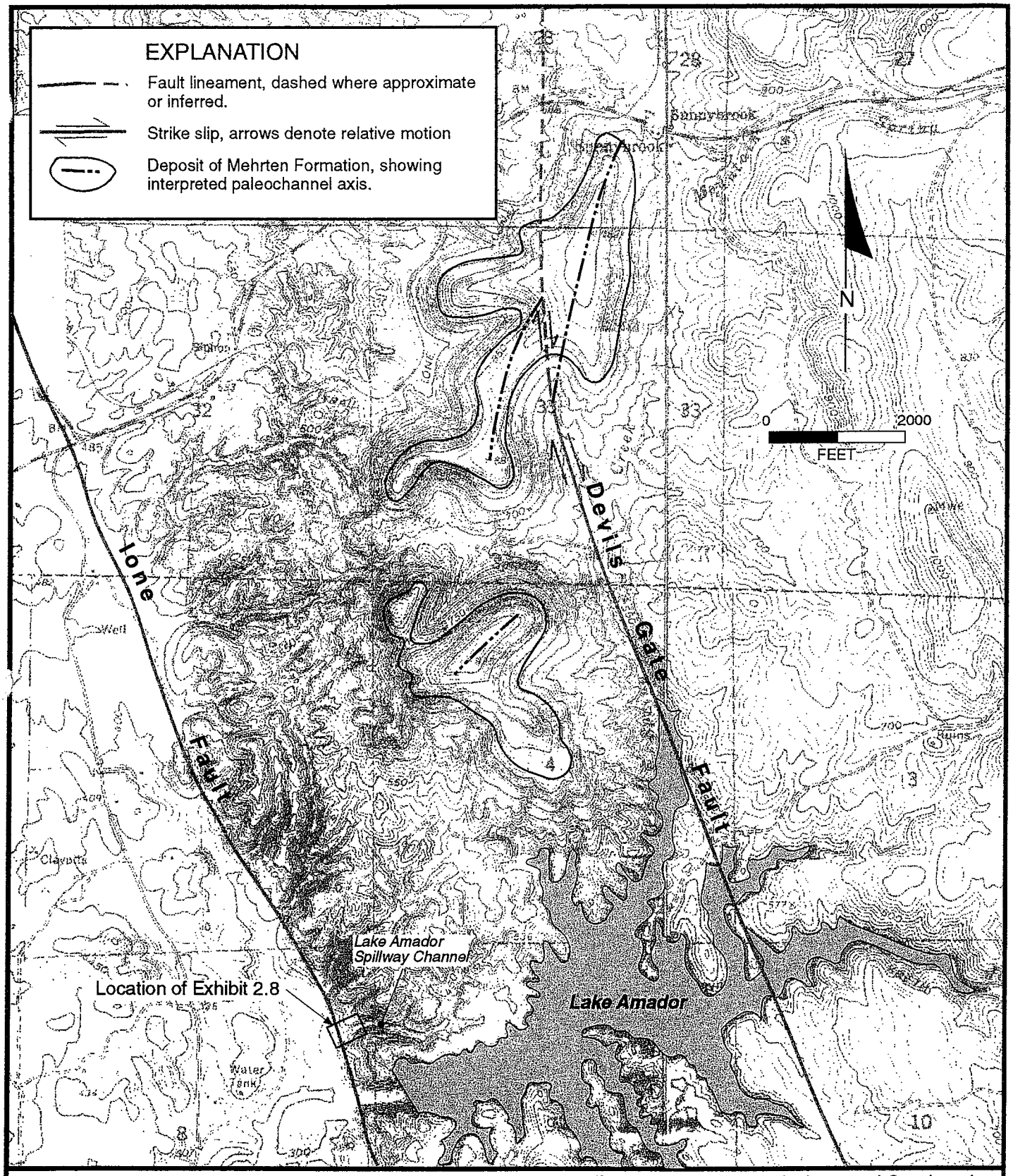

Base maps: Ione and Jackson 7.5' Quadrangles

HCG

Pardee Project Team

HDR Engineering Inc.
Christensen Associates Inc.
ΦGHI Consultants Inc.

Pardee Reservoir Enlargement Project

FAULT MAP OF LAKE AMADOR AREA

VOLUME	Exhibit 2.7	
SCALE		
DATE Dec. 1997		REV.

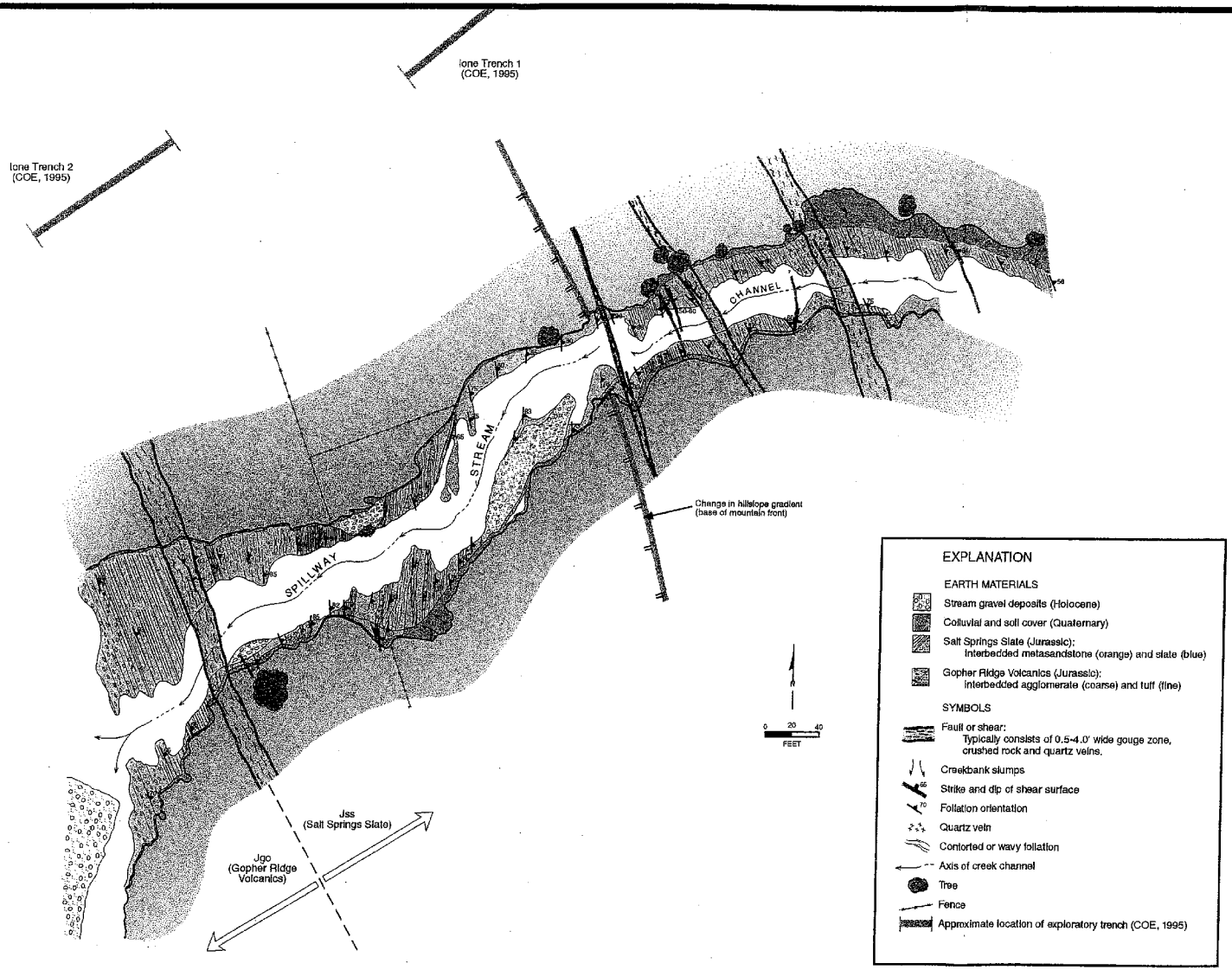

HCG

Pardee Project Team

HDR Engineering Inc.
Christensen Associates Inc.
GEI Consultants Inc.

Pardee Reservoir Enlargement Project

GEOLOGIC MAP OF
LAKE AMADOR SPILLWAY CHANNEL

VOLUME	Exhibit 2.8	
SCALE		REV.
DATE		

3. ESTIMATED GROUND MOTIONS

3.1 SUMMARY OF NEAR-FIELD SEISMIC SOURCES

Far-field seismic sources (e.g., San Andreas fault system, Coast Range thrust fault, and Sierra Nevada frontal fault zone) provide the most likely origins of earthquakes that will result in measurable ground motions at Pardee Dam and other proposed structures. However, faults of the Foothills fault are the seismic sources that will govern seismic dam design because they are much closer to the proposed structures. Ground motions for this study were estimated using the Youngs Creek, Devils Gate, Waters Peak, and Ione faults. General parameters of these faults are presented in Section 2 and summarized in Table 3-1.

Table 3-1
SUMMARY OF FAULT PARAMETERS

FAULT	ESTIMATED TIME SINCE MOST RECENT RUPTURING (years ago)	ESTIMATED QUATERNARY SLIP RATE(2) (mm/year)	ESTIMATED RUPTURE LENGTHS (km)	ESTIMATED MAXIMUM CREDIBLE EARTHQUAKE	LIKELY DISPLACEMENT TYPE	ESTIMATED LATERAL TO VERTICAL SLIP RATIO
Youngs Creek	14,000-60,000	0.002	22	6.4	Oblique-Slip	2:1
Devils Gate	Unknown	0.03	22	6.4	Oblique-Slip to Strike-Slip	5:1
Waters Peak	20,000-70,000	0.02	15	6.3(1)	Oblique-Slip	2:1
Ione	9,000-14,000	0.03	23	6.4	Oblique-Slip	2:1

(1) Increased to 6.4 for computation of design ground motion. See Section 3.2 for additional information.
(2) Based on average Cenozoic Slip Rate.

Distances from each fault to the various Pardee facilities are presented in Table 3-2.

Table 3-2
DISTANCES TO PARDEE FACILITIES
(kilometers)

FACILITIES	FAULTS			
	YOUNGS CREEK	DEVILS GATE	WATERS PEAK	IONE
Existing Pardee Dam	3.9	1.1	0.15	1.7
Jackson Creek Site	2.4	0.0	0.60	1.1
Downstream Dam Axis B-2	4.6	2.1	0.90	1.6
Downstream Dam Axis B-3	4.9	2.4	1.1	1.6
Existing Intake Tower	3.2	0.85	0.40	3.0

3.2 ATTENUATION RELATIONSHIPS

Vertical and horizontal ground motion components were estimated using recent attenuation relationships developed for rock sites. The average of three rock attenuation relationships, Boore, et al. (1994), Idriss (1991, 1994), and Sadigh, et al. (1993) were used to develop the horizontal component. Site class B is considered to be rock for the relationship of Boore, et al. (1994). These attenuation models were selected because they have been evaluated by Spudich, et al. (1996) for applicability to extensional regimes. Fewer attenuation relationships are available for the vertical components of ground motion, so the average of two rock attenuation relationships, those developed by Sadigh, et al. (1993) and Abrahamson and Silva (1997), were used.

The proposed Pardee structures are located in an extensional tectonic regime characterized by both oblique to dextral slip and normal dip-slip faulting. Based on recent studies of small to moderate earthquakes east of the Sierra Nevada in the extensional Basin and Range province, it appears that ground motions from normal-fault earthquakes are lower than ground motions resulting from pure strike-slip and reverse-slip earthquakes in transpressional regimes due to a lower stress drop for normal-fault events (Silva, 1994; Wong, et al., 1996).

Recently, Spudich, et al. (1996) completed an evaluation of strong motion recordings from earthquakes in extensional regimes as part of the seismic source characterization for the Yucca Mountain project, located in the Basin and Range province. Comparison of ground motions in extensional regimes to predictions using standard attenuation relationships based on earthquakes in California, which are primarily based on reverse-slip and strike-slip earthquakes in transpressional regimes, resulted in the development of extensional regime scale or correction factors (Spudich, et al., 1996). The scale factors apply to both strike-slip and normal faulting earthquakes in extensional regimes.

The extensional regime scale factors developed by Spudich, et al. (1996) were applied to all four local faults, including the Devils Gate fault, which may contain a significant strike-slip component of movement. Scale factors for the horizontal and vertical components of the attenuation relationships were based on the average for sites less than 20 km from the rupture plane. Spudich's scale factors for horizontal and vertical components are shown in Exhibits 3-1 and 3-2, respectively.

In addition to applying the extensional regime scale factors, directional effects are incorporated (for average directivity conditions) by increasing the component of motion oriented perpendicular to the strike of the fault plane based on Somerville, et al. (1997). At long periods, the fault-normal (fault-perpendicular) component is larger than the fault-parallel component. This ratio increases with increasing magnitude and decreasing source-to-site distance. These directivity ("fling") factors are based primarily on data from transpressional regimes, and for this study the fling factors were reduced to one-half of the values predicted by the Somerville, et al., model. The increase in the fault-normal component is about 35 percent at periods greater than 3 seconds for the Waters Peak fault at the existing Pardee Dam site.

3.3 DETERMINISTIC GROUND MOTIONS

The DSOD uses the maximum credible earthquake (MCE) for developing design ground motions. To compute ground motions, the MCE magnitude, distance from the source fault to the facility, and appropriate statistical level of shaking are required to estimate design ground motion. The MCE and distance to the Pardee facilities are presented in Tables 3-1 and 3-2, respectively. Traditionally, either the median (50th percentile) or 84th percentile ground motions from attenuation relations are used. The 84th percentile is one standard deviation above the median. If the MCE occurs, there is a 50 percent chance that the ground motion will be less than the median and an 84 percent chance that the ground motion will be less than the median plus one standard deviation.

The four faults considered in this evaluation, which are presented in Tables 3-1 and 3-2, have low slip rates (less than 0.1 mm/yr) with recurrence intervals of thousands of years. The median ground motion for the MCE is appropriate for developing the design spectra for the Youngs Creek, Waters Peak, Devils Gate, and Ione faults because of the long recurrence intervals.

Ground motions were evaluated with and without extensional regime scale factors for comparative purposes. Ground motions that include the extensional regime scale factors were used to develop the design ground motion, because this represents current science. Unscaled ground motions were developed for comparative purposes.

3.3.1 RESPONSE SPECTRA

Response spectra at the existing Pardee Dam site were developed based on the comparisons presented in the following sections. Response spectra for other project

facilities are based on the response spectra selected at the existing Pardee Dam site with adjustments only for source-to-site distance. The source-to-site scale factors are presented in Table 3-3.

Table 3-3
SOURCE-TO-SITE SCALE FACTORS

	Youngs Creek Fault	Devils Gate Fault	Waters Peak Fault	Ione Fault
Existing Pardee Dam	0.70	0.90	1.00	0.85
Jackson Creek Site	0.79	1.02	0.95	0.90
Downstream Dam Axis B-2	0.66	0.81	0.92	0.86
Downstream Dam Axis B-3	0.64	0.79	0.91	0.86
Existing Intake Tower	0.74	0.92	0.97	0.75

The horizontal and vertical response spectra, excluding scaling for extensional regimes, for the Waters Peak fault for each attenuation relationship are shown on Exhibits 3-3 and 3-4, respectively. The average horizontal and vertical response spectra for the attenuation relationships considered, are also shown on Exhibits 3-3 and 3-4, respectively. The average horizontal and vertical response spectra were used to develop the design ground motions.

For the Pardee facilities, the average horizontal spectrum is applied to the fault-parallel direction. This is a conservative assumption because the fault-parallel motion is expected to be lower than the average motion at long periods by the same ratio as the fault-normal to the average motion. The Somerville, et al. (1997) scale factors were applied for the fault-normal direction. The fault-parallel, fault-normal, and vertical response spectra, excluding scaling for extensional regimes, for the Waters Peak fault are shown in Exhibit 3-5. The fault-parallel, fault-normal, and vertical response spectra, based on the Spudich, et al. (1996) scale factors for earthquakes in extensional regimes, are shown in Exhibit 3-6.

Fault-parallel, fault-normal, and vertical spectral accelerations for damping values from 0.5 to 20 percent with and without scale factors for extensional regimes for the median ground motion for Waters Peak fault at the existing Pardee Dam are contained in Appendix A.

3.3.2 ACCELERATION TIME HISTORIES

Empirical recordings of earthquakes with appropriate characteristics were selected and then modified to be compatible with the target spectra (Exhibits 3-5 and 3-6) using a time domain spectral matching procedure. Three-component spectrum compatible time histories were developed using three sets of time histories recorded from actual earthquakes. It is preferable that the selected time histories be from earthquakes with similar focal mechanism, source-to-site distance, rupture direction, and site geology. In reality, all factors cannot be matched perfectly to actual recordings. The most important

factors are the magnitude, source-to-site distance, and directivity effects. The focal mechanism and site conditions are not as significant as long as the ground motion has a frequency content of sufficient bandwidth.

Three earthquake records were selected for this study:

1. Irpinia, Italy (M=6.8, rupture distance = 17 km, recorded at Sturno)

2. Imperial Valley, California (M=6.5, rupture distance = 1 km, recorded at El Centro Station 5)

3. Mammoth Lakes, California (M=6.2, rupture distance = 9 km, recorded at Convict Creek)

The Sturno and El Centro time histories show forward directivity effects ("fling pulse") that are often observed in near-fault ground motions. The Convict Creek time history does not have strong directivity effects, but has longer duration. The acceleration, velocity and displacement time histories for these three earthquakes are contained in Appendix B.

Each time history was modified to match the target spectrum, which is the median Waters Peak spectrum shown in Exhibit 3-6. The fault-normal, fault-parallel, and vertical spectral fit and modified time histories, scaled for extensional regimes and directional effects for each record are presented in Exhibits 3-7.1 through 3-7.6 (El Centro), 3-8.1 through 3-8.6 (Sturno), and 3-9.1 through 3-9.6 (Convict Creek).

3.3.3 COMPARISON TO PREVIOUS STUDIES

The main differences between this study and previous studies completed by Earth Sciences Associates (1992) and Dames and Moore (1992) are:

1. This study considered the Waters Peak fault, which is only 0.15 km from the existing Pardee Dam, as an active source. The previous studies considered the more distant Youngs Creek fault (4 km from Pardee Dam) as the closest active source.

2. This study is based on attenuation relationships for peak horizontal ground acceleration developed between 1991 and 1994, which reflect current science. Previous studies were based on attenuation relationships developed between 1985 and 1989.

3. Vertical components of ground acceleration for this study were based on two attenuation relationships developed between 1993 and 1997. Vertical components of ground acceleration in previous studies were based on a traditional fraction of the horizontal component.

4. This study incorporated recent information on differences in ground motion between extensional and compressional regimes. Previous studies did not consider this difference.
5. This study included near-fault directivity effects that result in larger long-period motion for the horizontal component that is oriented perpendicular to the fault strike.

These changes have resulted in ground motions that are different than those in previous studies. The fault-normal and fault-parallel peak horizontal ground acceleration (PGA) for the Waters Peak seismic source was estimated to be 0.40g. Previous estimates of horizontal PGA were 0.45g (Dames and Moore, 1992) and 0.50g (Earth Sciences Associates, 1992). The vertical PGA for the Waters Peak seismic source was estimated to be 0.52g. Although previous reports indicate that the vertical accelerations could approach or exceed the horizontal acceleration values, the vertical PGA for recommended design based on the traditional 2/3 fraction of the horizontal acceleration is 0.30g (Dames and Moore, 1992) and 0.33g (Earth Sciences Associates, 1992). The vertical PGA developed in this study is higher than the horizontal PGA because of the proximity of the sites to the faults and a smaller reduction for the vertical component than the horizontal component for extensional regimes, as shown in Exhibits 3-1 and 3-2.

The horizontal response spectra for the Waters Peak fault developed from the following procedures is presented as Exhibit 3-10:

1. Seed, Ugas, Lysmer (1976 84th Spectral Shape) with Seed and Idriss 1982 PGA.
2. Seed, Ugas, Lysmer (1976 Median Spectral Shape) with Seed and Idriss 1982 PGA.
3. Seed, Ugas, Lysmer (1976 Median Spectral Shape) with a peak acceleration updated based on the Sadigh, et al., Idriss, and Boore, et al., attenuation relations scaled for extensional regimes.
4. Fault-normal without scale factor for extensional regimes.
5. Fault-normal with scale factor for extensional regimes.
6. Dames and Moore, 1992.

The Seed, Ugas, Lysmer (Seed, et al. 1976) 84th percentile spectral shape scaled for magnitude using the method of Idriss (1985), and anchored to the peak acceleration predicted by the Seed and Idriss (1982) attenuation relationship, is generally accepted by DSOD. The main difference between the procedure generally accepted by DSOD and the spectra developed in this study is the use of an 84th percentile spectral shape versus use of the median spectral shape. The comparison with the median spectral shape is better. For this case, larger ground motions are due to the use of the Seed and Idriss (1982) attenuation relationship, because it was developed from a combination of strike-slip and reverse dip-slip faulting events, and does not account for extensional regime effects. The

resulting spectra is larger than the fault-normal spectrum (without scaling) at periods of 0.05 to 0.4 seconds and higher than the fault-normal spectrum with scaling at all periods.

3.4 PROBABILISTIC SEISMIC HAZARD ANALYSIS

A probabilistic seismic hazard analysis (PSHA) was performed to estimate the annual probability or recurrence interval of exceeding a specified level of ground motion. The PSHA follows the standard approach developed by Cornell (1968). The mathematical formulation for the hazard analysis used in this study is presented in Appendix C.

3.4.1 SOURCE PARAMETERS

The mean source parameters for the faults used in the hazard analysis are listed in Table 3-4. Source parameters for near-field faults (Waters Peak, Ione, Devils Gate, and Youngs Creek) were described in Section 3.3. Source parameters for far-field faults are based on the seismic hazard studies by the California Division of Mines and Geology (CDMG), in cooperation with U.S. Geological Survey (1996) and Geomatrix (1992). The background zone for the central valley is based on geometries of areal source zones from Thenhaus (1982) with seismicity rates updated through 1996.

Table 3-4
SOURCE PARAMETERS USED IN THE PROBABILISTIC SEISMIC HAZARD ANALYSIS

Fault or Source Zone[1]	Slip-Rate (mm/yr)	Number of Events (M>5)	Mean Maximum Magnitude	Closest Distance[2] (km)
Waters Peak	0.02	--	6.3	0.15
Ione	0.03	--	6.4	1.5
Devils Gate	0.03	--	6.4	1.0
Youngs Creek	0.002	--	6.4	3.9
Coast Range/Central Valley (CRCV)	1.5	--	6.8	82
Green Valley - Cedar Roughs	4.0	--	6.6	109
Calaveras North	6.0	--	6.7	112
Calaveras Southern	15.0	--	6.8	123
Hayward	9.0	--	7.0	124
Healdsburg - Rodgers Creek	8.0	--	7.0	139
San Andreas	24.0	--	7.8	154
Maacama - South	9.0	--	7.0	159
Hunting Creek - Lake Berry	6.0	--	7.0	162
Bartlett Springs	6.0	--	7.3	162
Maacama - Central	9.0	--	7.1	198
Background Zone 25	--	0.0085	6.25	
Background Zone 26	--	0.0153	6.25	

(1) A mean b-value of 0.9 is used for all sources.
(2) Distance is to existing Pardee Dam.

3.4.2 MAGNITUDE DENSITY FUNCTION

Two alternative magnitude density functions are considered for fault sources: 1) the characteristic model (Youngs and Coppersmith, 1985) was given a weight of 0.90, and 2) the truncated exponential model was given a weight of 0.1. This weighting was used because an exponential model for faults where the activity rate is computed from slip-rate leads to a large overprediction of the historical rate of moderate magnitude events. The truncated exponential model was given a weight of 1.0 for the background zones because these rates are based only on historical seismicity.

3.4.3 ATTENUATION RELATIONS

The three rock attenuation relations used for the deterministic analysis were also used for the probabilistic analysis: Sadigh et al. (1977); Idriss (1994); and Boore, Joyner, and Fumal (1994). For Boore, Joyner, Fumal, Class B was used for rock. The extensional regime scaling factor is not included in the attenuation relationships used for the

probabilistic hazard calculations. For all three relationships, the log-normal distribution was truncated at 3.0 standard deviations.

3.4.4 PROBABILISTIC SEISMIC HAZARD ANALYSES RESULTS

Results are presented as the annual probability of exceeding a given level of horizontal spectral acceleration at the existing Pardee Dam. The combined effect of the contributions from all magnitudes (greater than the minimum magnitude) and all distances are presented on the hazard curves, Exhibits 3-11 and 3-12. For short return periods (<500 years), the hazard is dominated by the Background Zone, Coast Range/Central Valley, and San Andreas. For long return periods (>3,000 years), the hazard is dominated by local faults.

The hazard can be broken down into contributions from various magnitude and distance ranges. This process is called deaggregation, and it provides useful insights into which events are controlling the hazard. The deaggregated hazard for peak acceleration and 1 second spectral acceleration for a return period of 3,000 years are shown in Exhibits 3-13 and 3-14, respectively. The heights of the bars in these exhibits indicate the fraction contribution to the hazard. As presented on these exhibits, the peak acceleration hazard is dominated by events of magnitude 5.5 to 6.5 at distances of 0 to 5 km. For a 1 second period, the larger magnitude and slightly more distant sources have a larger contribution to the hazard than for peak acceleration, but the local sources are still the dominant hazard.

An equal hazard spectrum was developed by computing the spectral acceleration at each period that has a specified annual probability of being exceeded. The computed equal hazard spectra for return periods of 3,000, 5,000, and 10,000 years and the unscaled median spectra computed from the deterministic analyses are shown in Exhibit 3-15 for comparison. The unscaled deterministic spectrum is used for comparison to be consistent with the attenuation relationships used in the probabilistic hazard analysis.

The Board of Consultants recommended using the larger of the equal hazard spectrum with a return period of 3,000 years or the median deterministic spectrum. For the existing Pardee Dam, the deterministic spectrum is significantly greater than the 3,000 year return period equal hazard spectrum. The median deterministic spectrum has a return period of about 10,000 years. Therefore, the deterministic spectrum was used to specify the target spectra. The long return period of 10,000 years for the deterministic spectra supports the decision to use the median ground motion for design of the Pardee facilities.

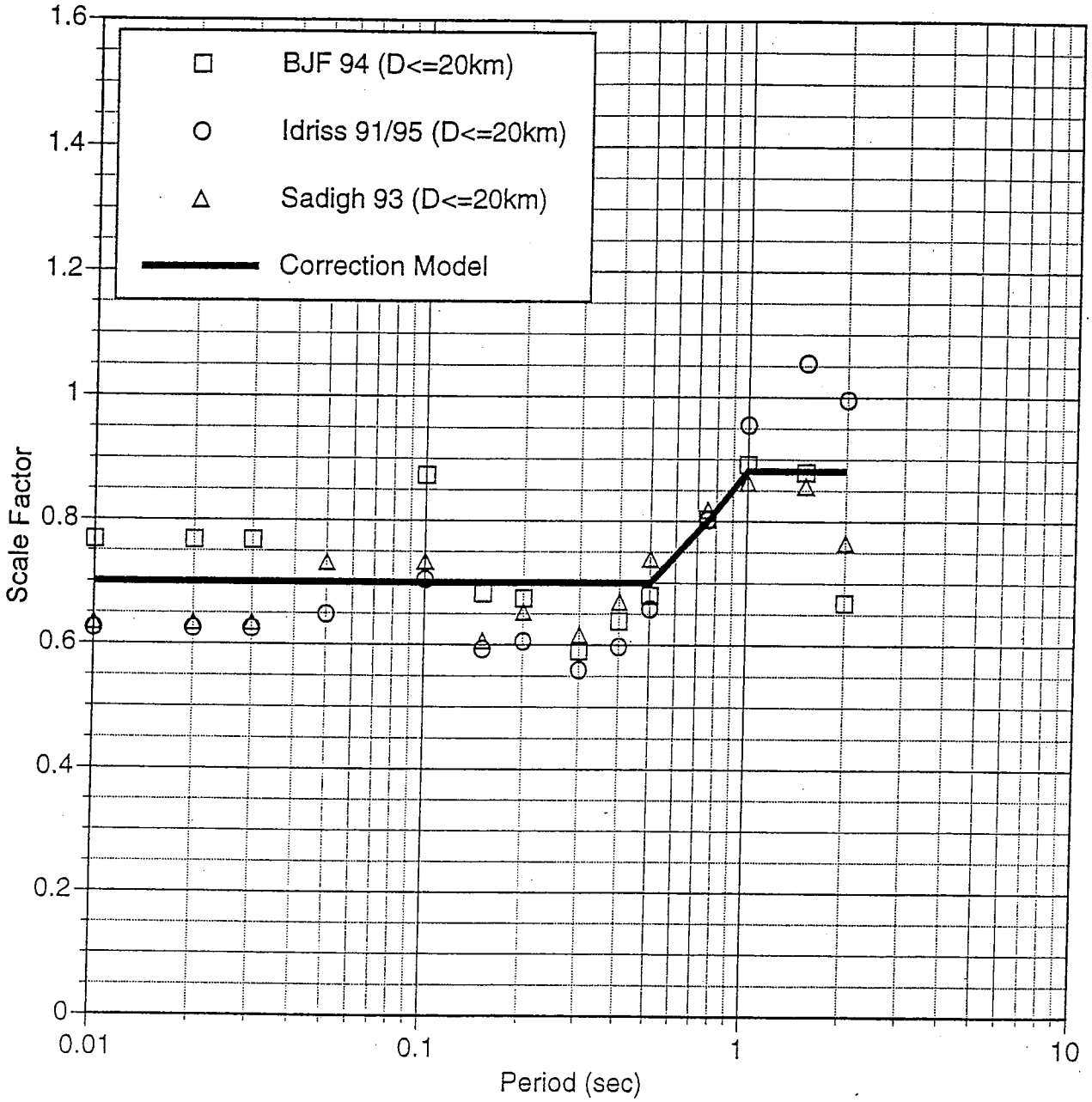

HCG
Pardee Project Team
HDR Engineering Inc.
Christensen Associates Inc.
GEI Consultants Inc.

Pardee Reservoir Enlargement Project

NORMAL-FAULT HORIZONTAL SCALE FACTOR

VOLUME		Exhibit 3-1	
SCALE			
DATE	Dec. 1997		REV.

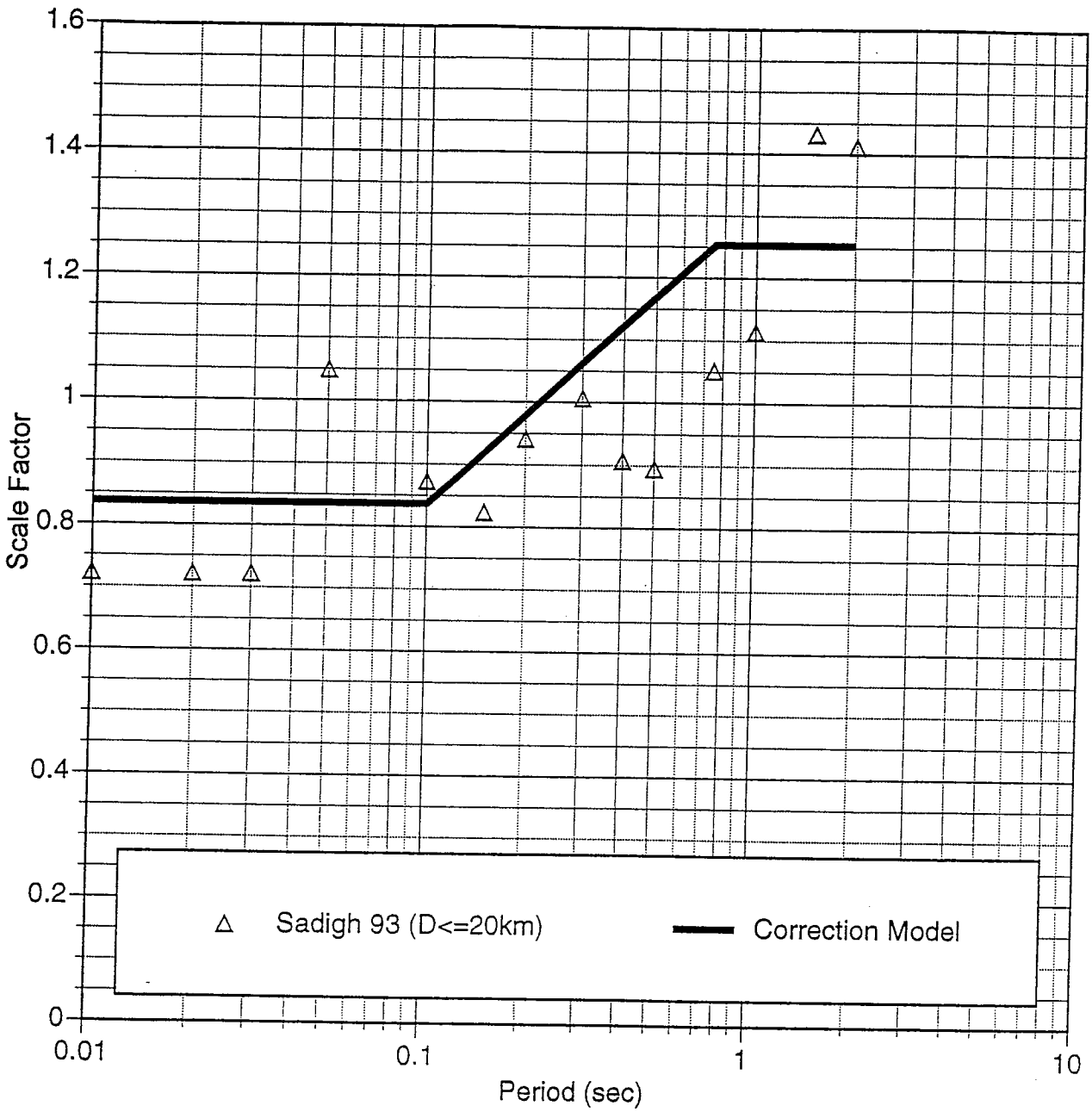

HCG

Pardee Project Team

HDR Engineering Inc.
Christensen Associates Inc.
GEI Consultants Inc.

Pardee Reservoir Enlargement Project

NORMAL-FAULT VERTICAL SCALE FACTOR

VOLUME			
SCALE		Exhibit 3-2	
DATE	Dec. 1997		REV.

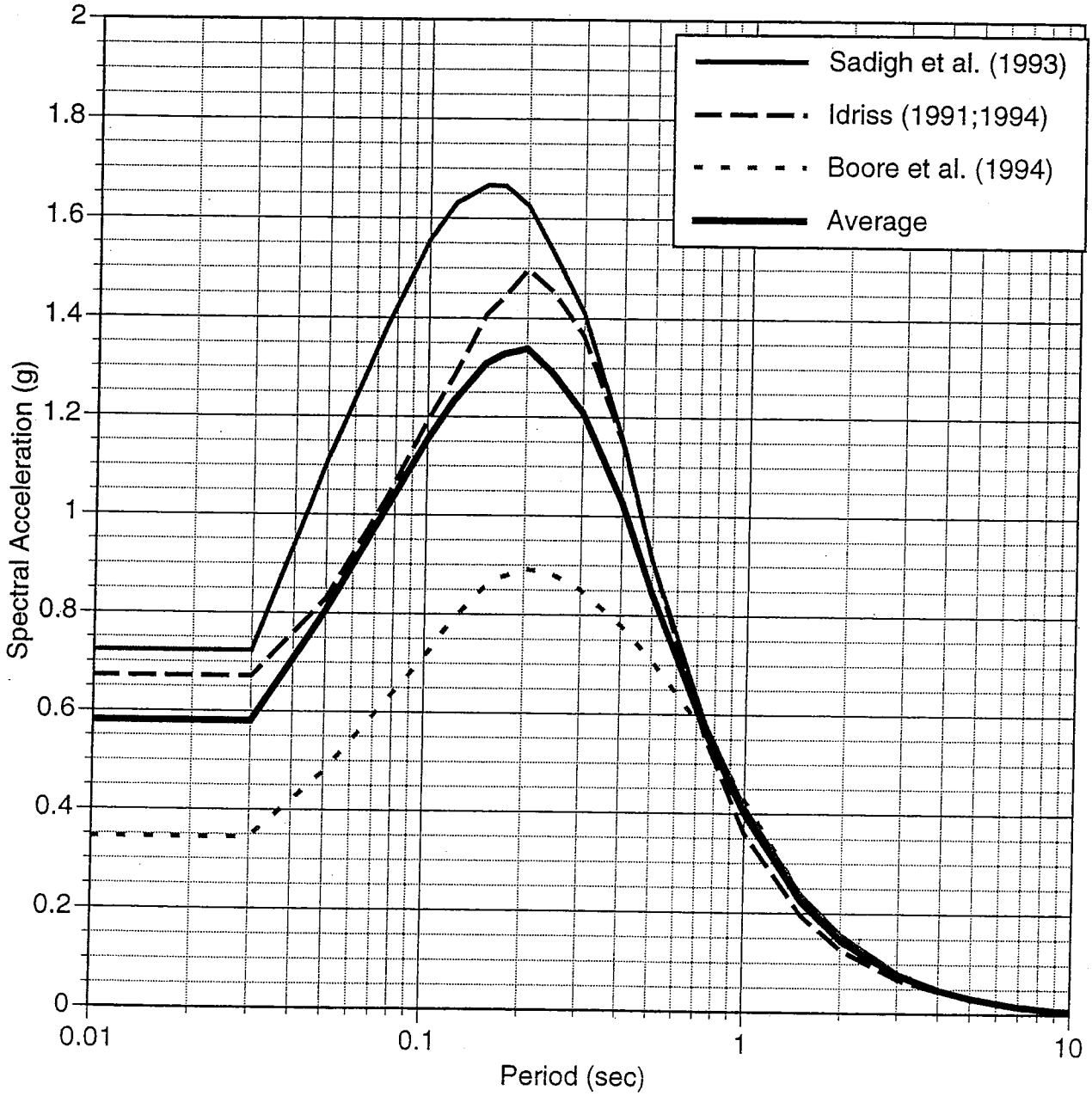

NOTE: Does Not Include Scale Factor for Extensional Regimes.

HCG
Pardee Project Team
EDR Engineering Inc.
Christensen Associates Inc.
HGH Consultants Inc.

Pardee Reservoir Enlargement Project
COMPARATIVE RESPONSE SPECTRA
HORIZONTAL COMPONENT
WATERS PEAK

VOLUME		
SCALE		Exhibit 3-3
DATE	Dec. 1997	REV.

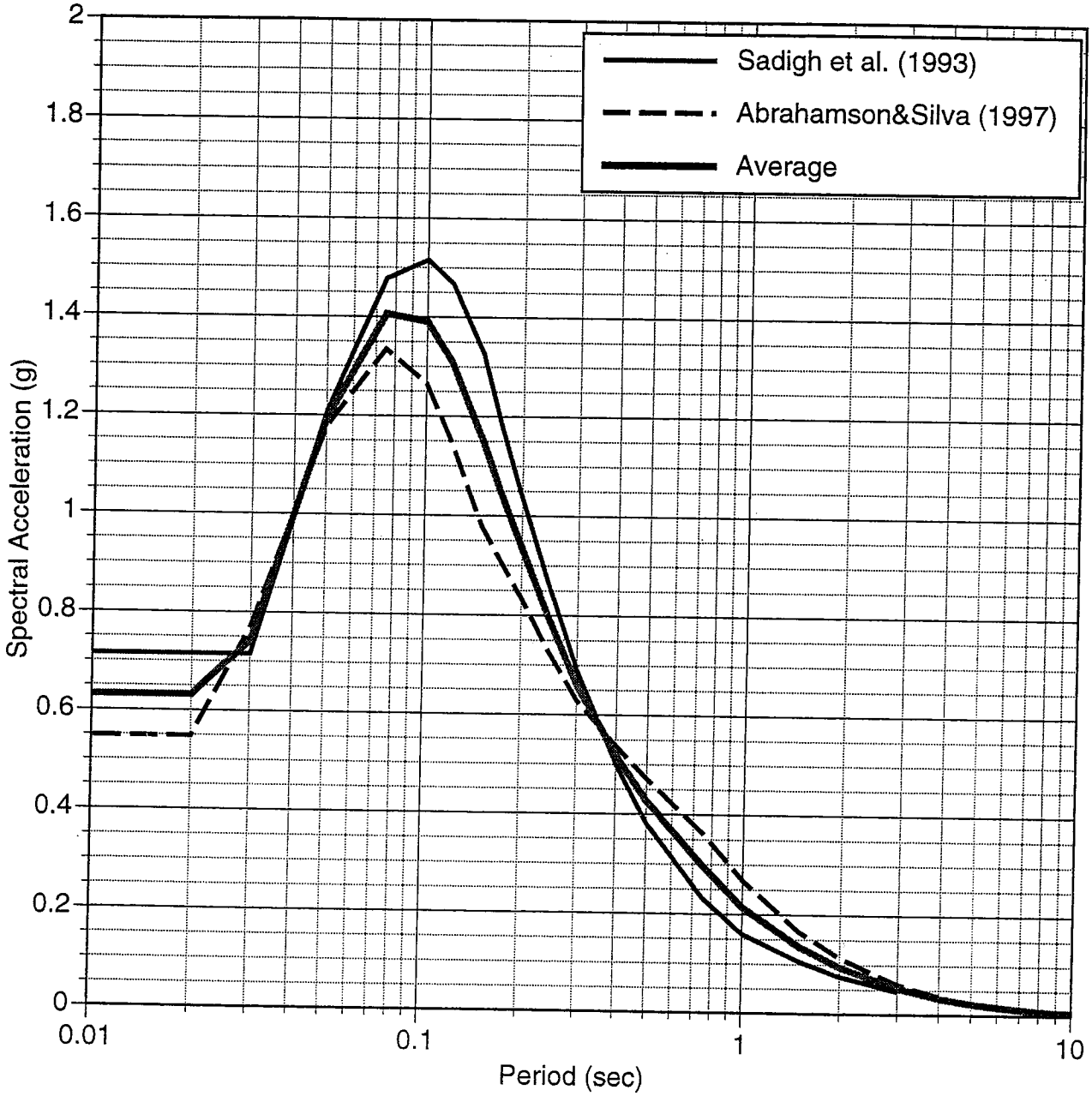

NOTE: Does Not Include Scale Factor for Extensional Regimes.

HCG
Pardee Project Team
HDR Engineering Inc.
Christensen Associates Inc.
HGM Consultants Inc.

Pardee Reservoir Enlargement Project
COMPARATIVE RESPONSE SPECTRA
VERTICAL COMPONENT
WATERS PEAK

VOLUME		
SCALE	Exhibit 3-4	
DATE Dec. 1997		REV.

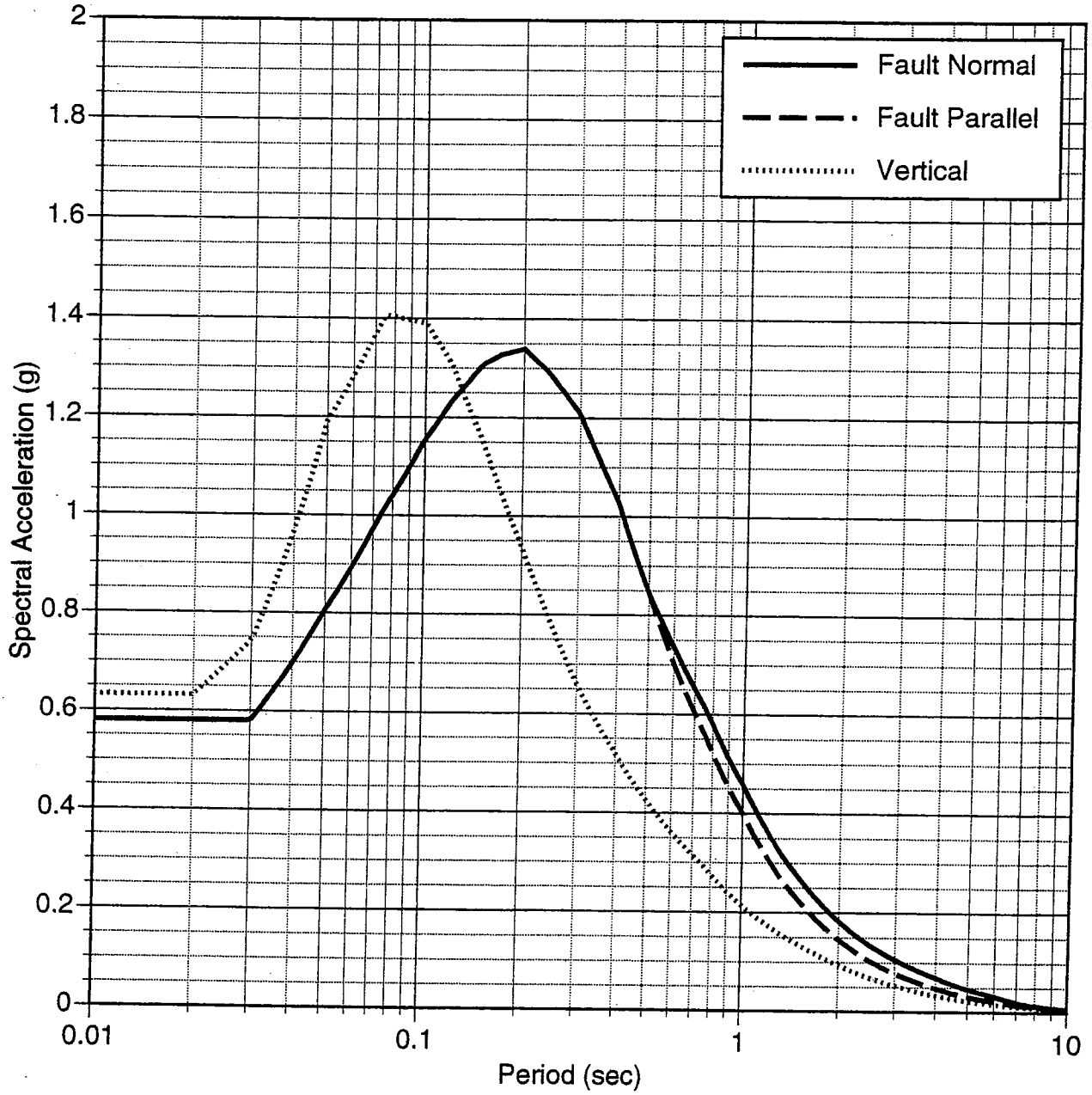

NOTE: Does Not Include Scale Factor for Extensional Regimes.

HCG
Pardee Project Team

Pardee Reservoir Enlargement Project
COMPARATIVE RESPONSE SPECTRA
HORIZONTAL AND VERTICAL
COMPONENTS WATERS PEAK

VOLUME		
SCALE	Exhibit 3-5	
DATE Dec. 1997		REV.

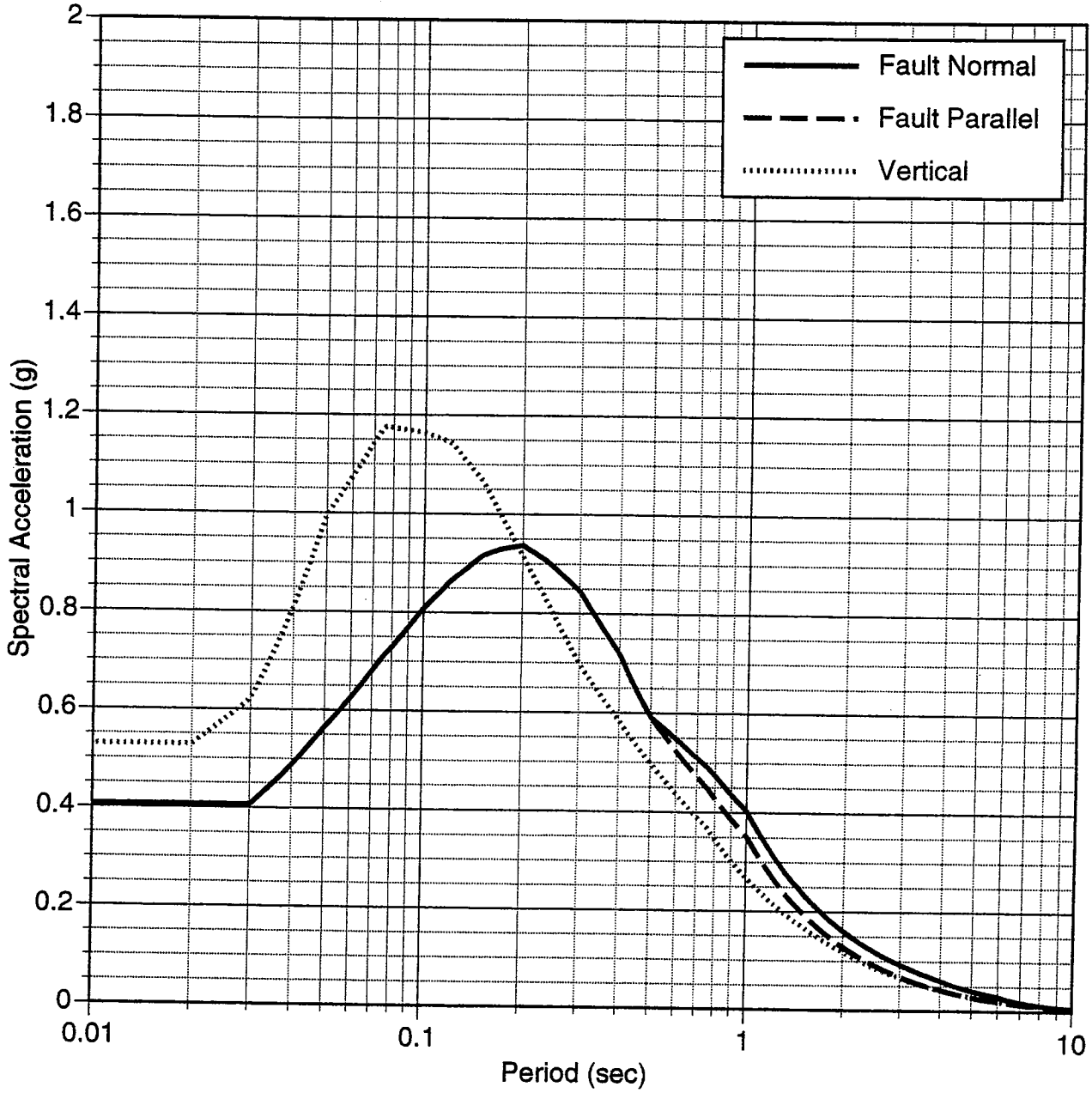

NOTE: Includes Scale Factor for Extensional Regimes.

HCG
Pardee Project Team

Pardee Reservoir Enlargement Project
SCALED RESPONSE SPECTRA,
HORIZONTAL AND VERTICAL,
WATERS PEAK

DRAWING		
SCALE		Exhibit 3-6
DATE	Dec. 1997	REV.

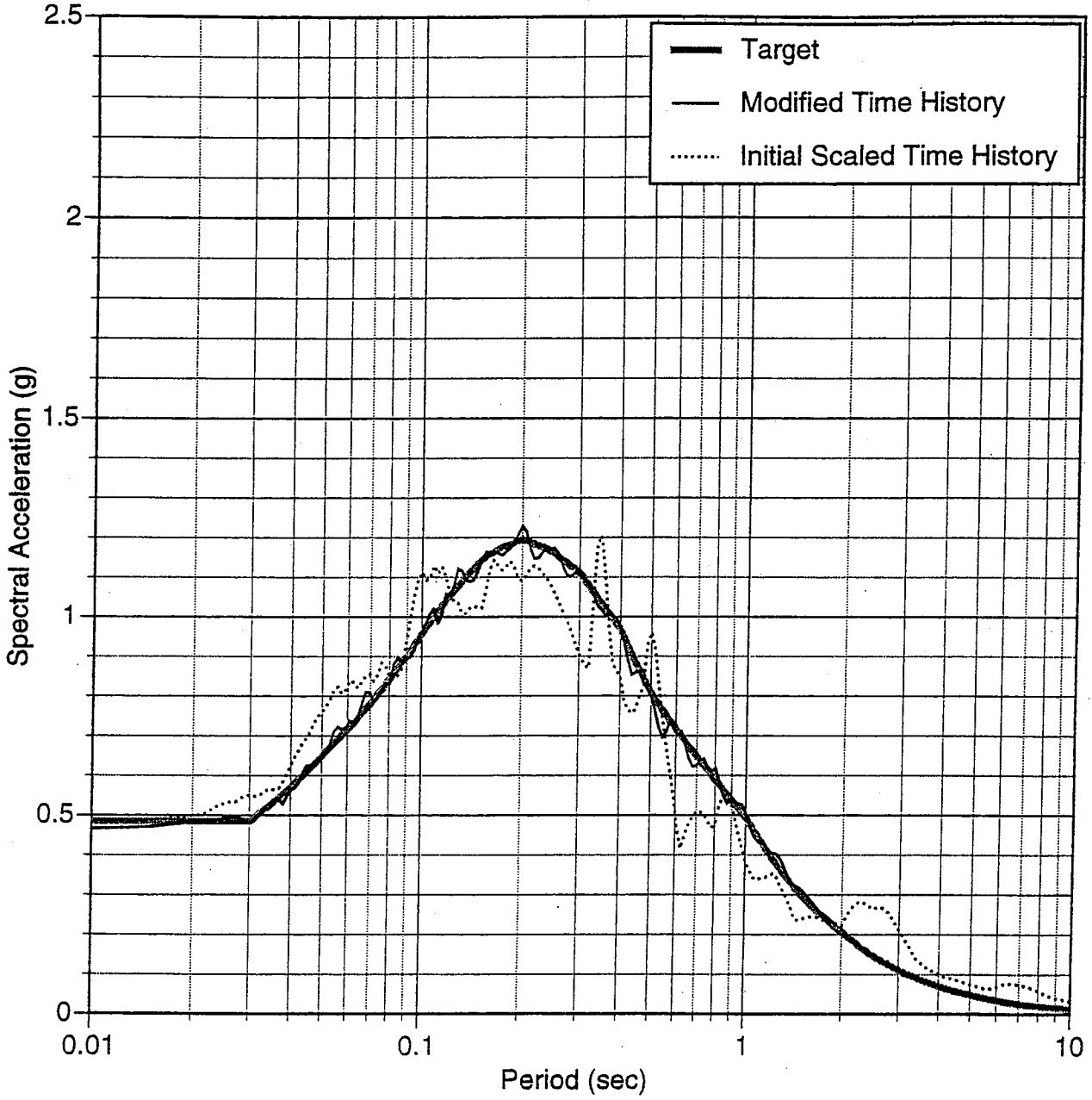

NOTE: Includes Scale Factor for Extensional Regimes.
Time History Modified to Match Target Spectrum,
Which is Median Waters Peak Spectrum
Shown on Exhibit 3-6

HCG
Pardee Project Team
HDR Engineering Inc.
Christopoulos Associates Inc.
GKI Consultants Inc.

Pardee Reservoir Enlargement Project
RESPONSE SPECTRA,
FAULT PARALLEL COMPONENT,
EL CENTRO RECORD

VOLUME		
SCALE	**Exhibit 3-7.1**	
DATE Dec. 1997		REV.

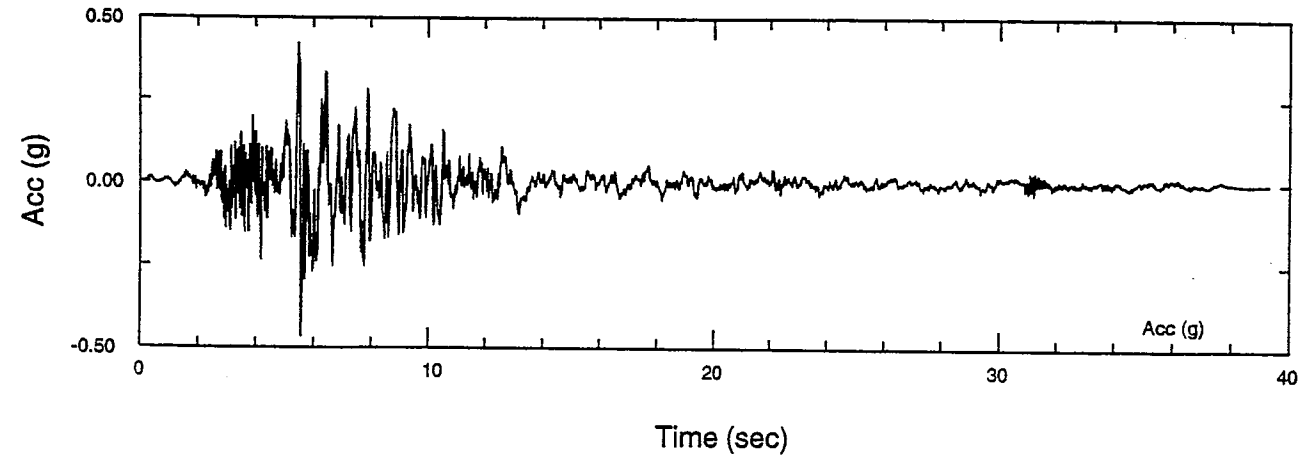

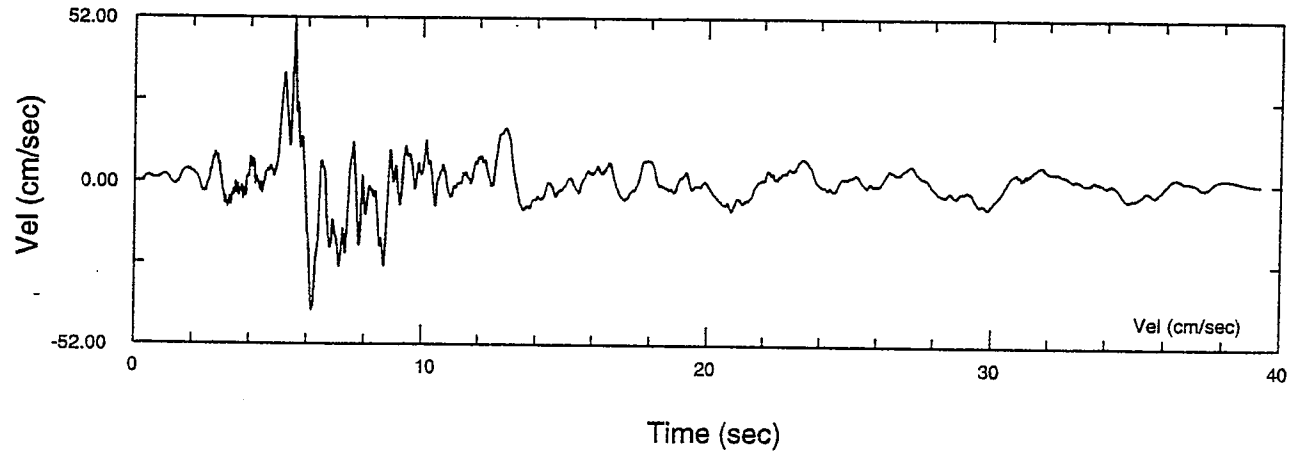

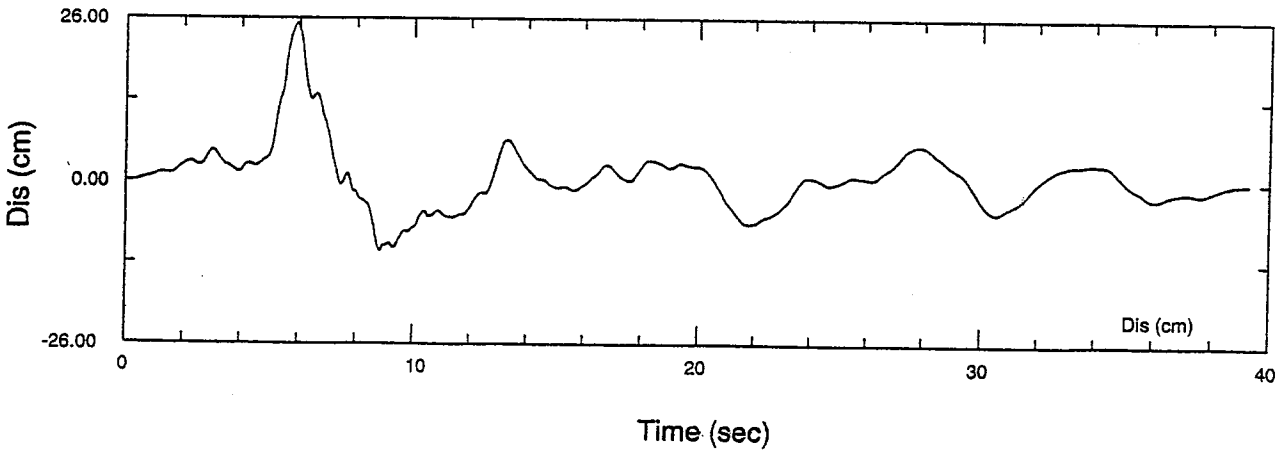

NOTE: Includes Scale Factor for Extensional Regimes.
Time History Modified to Match Target Spectrum,
Which is Median Waters Peak Spectrum
Shown on Exhibit 3-6

HCG
Pardee Project Team
HDR Engineering Inc.
Christiansen Associates Inc.
GEI Consultants Inc.

Pardee Reservoir Enlargement Project
MODIFIED TIME HISTORIES,
FAULT PARALLEL COMPONENT,
EL CENTRO RECORD

VOLUME			
SCALE		**Exhibit 3-7.2**	
DATE	Dec. 1997		REV.

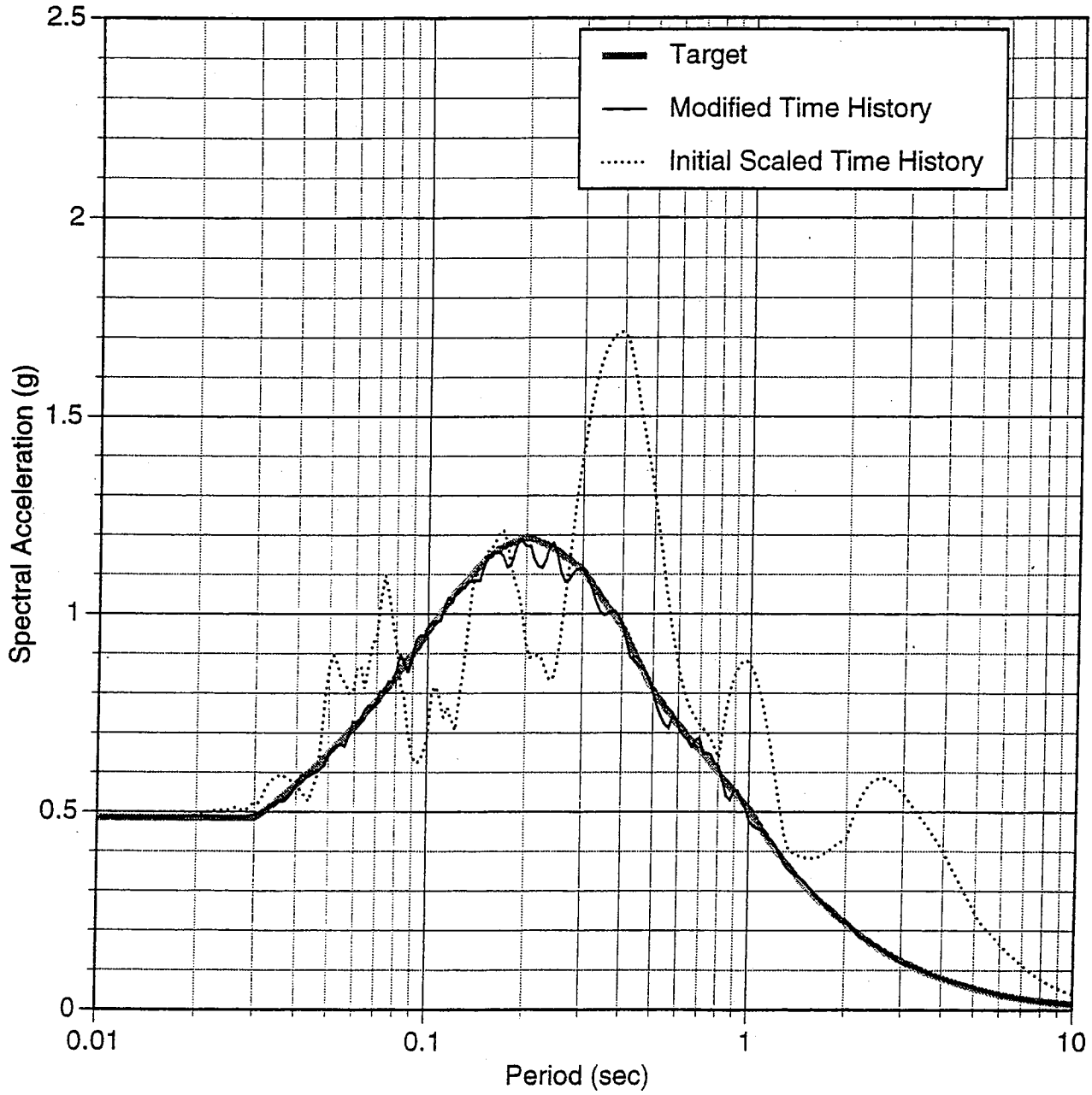

NOTE: Includes Scale Factor for Extensional Regimes.
Time History Modified to Match Target Spectrum,
Which is Median Waters Peak Spectrum
Shown on Exhibit 3-6

HCG
Pardee Project Team
HDR Engineering Inc.
Christenson Associates Inc.
[illegible] Consultants Inc.

Pardee Reservoir Enlargement Project
RESPONSE SPECTRA,
FAULT-NORMAL COMPONENT,
EL CENTRO RECORD

VOLUME		
SCALE	Exhibit 3-7.3	
DATE Dec. 1997		REV.

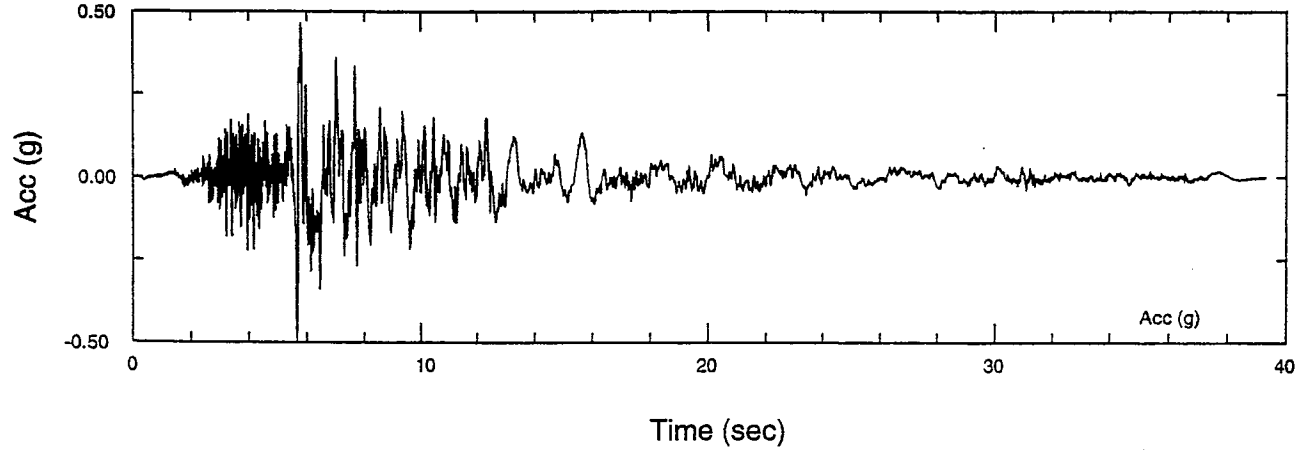

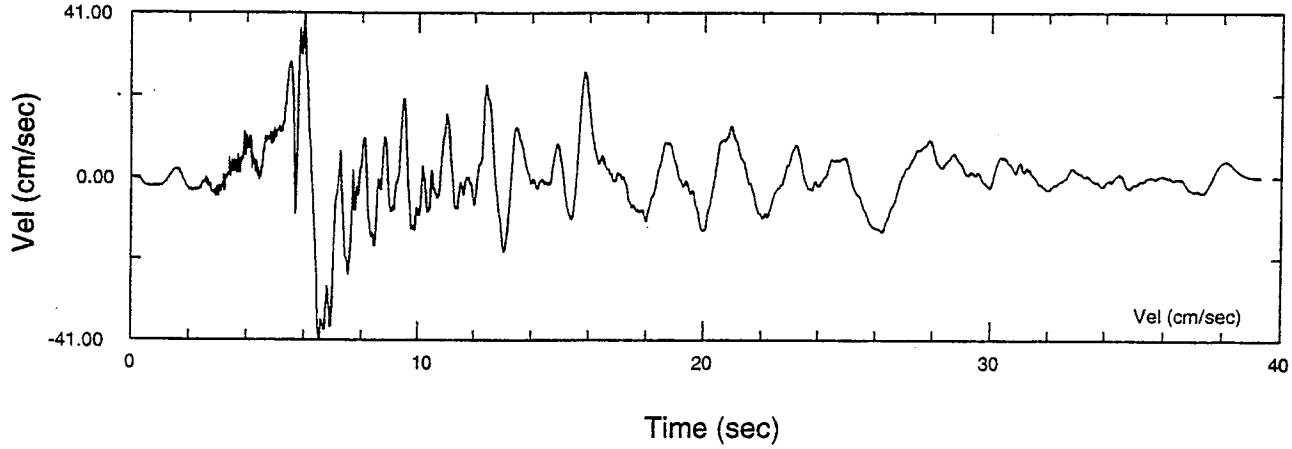

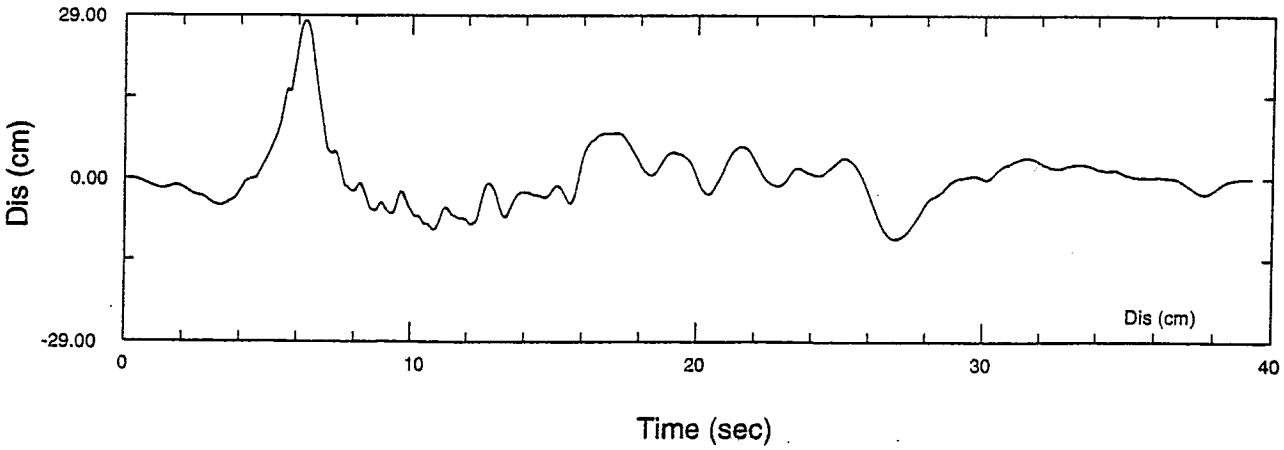

NOTE: Includes Scale Factor for Extensional Regimes.
Time History Modified to Match Target Spectrum,
Which is Median Waters Peak Spectrum
Shown on Exhibit 3-6

Pardee Reservoir Enlargement Project
MODIFIED TIME HISTORIES,
FAULT-NORMAL COMPONENT,
EL CENTRO RECORD

HCG
Pardee Project Team
HDR Engineering Inc.
Christensen Associates Inc.
GKI Consultants Inc.

VOLUME		Exhibit 3-7.4	
SCALE			
DATE	Dec. 1997		REV.

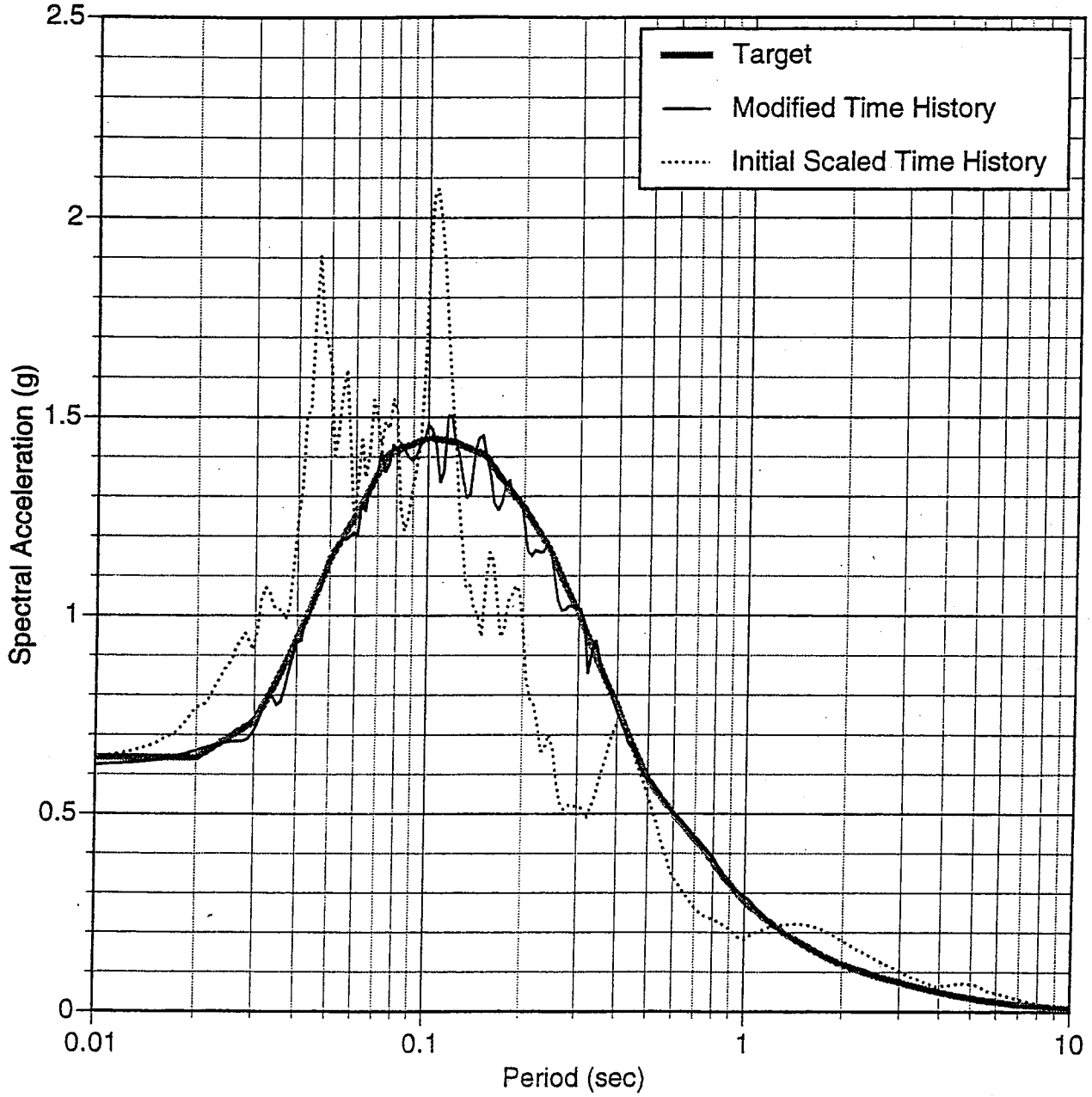

NOTE: Includes Scale Factor for Extensional Regimes.
Time History Modified to Match Target Spectrum,
Which is Median Waters Peak Spectrum
Shown on Exhibit 3-6

HCG
Pardee Project Team
BDR Engineering Inc.
Christensen Associates Inc.
GEI Consultants Inc.

Pardee Reservoir Enlargement Project
RESPONSE SPECTRA,
VERTICAL COMPONENT,
EL CENTRO RECORD

VOLUME		Exhibit 3-7.5
SCALE		
DATE	Dec. 1997	REV.

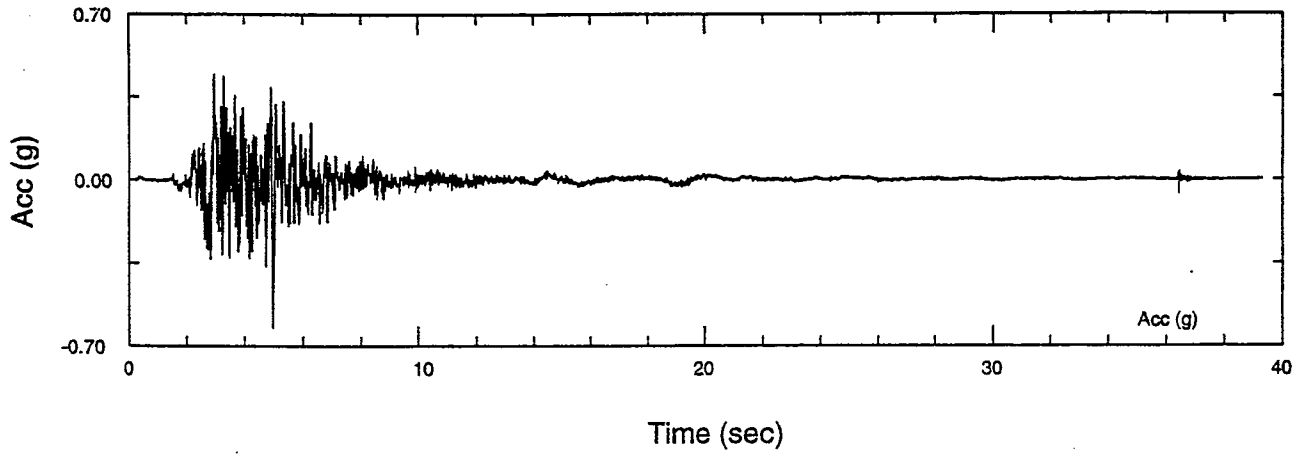

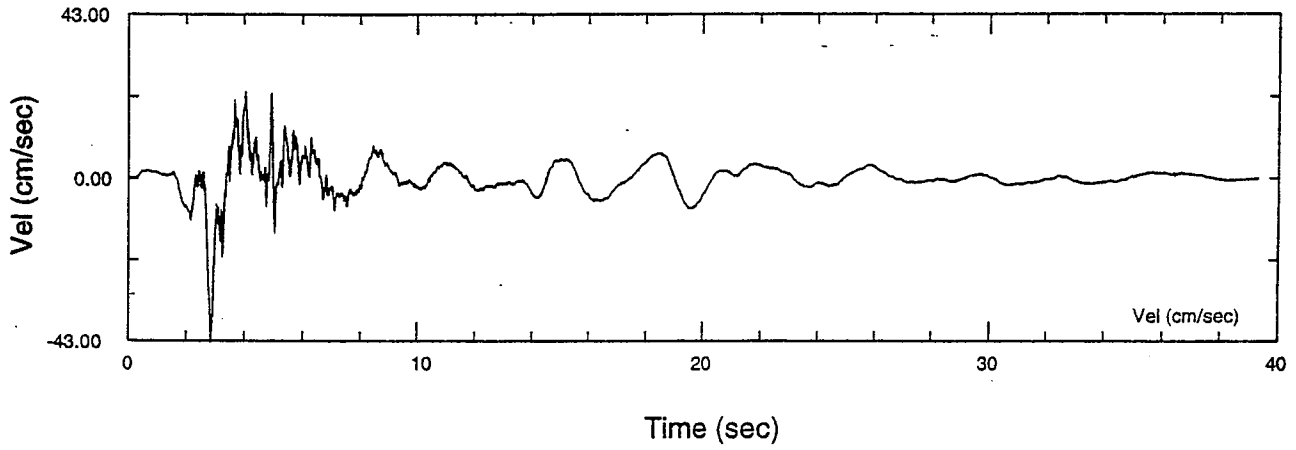

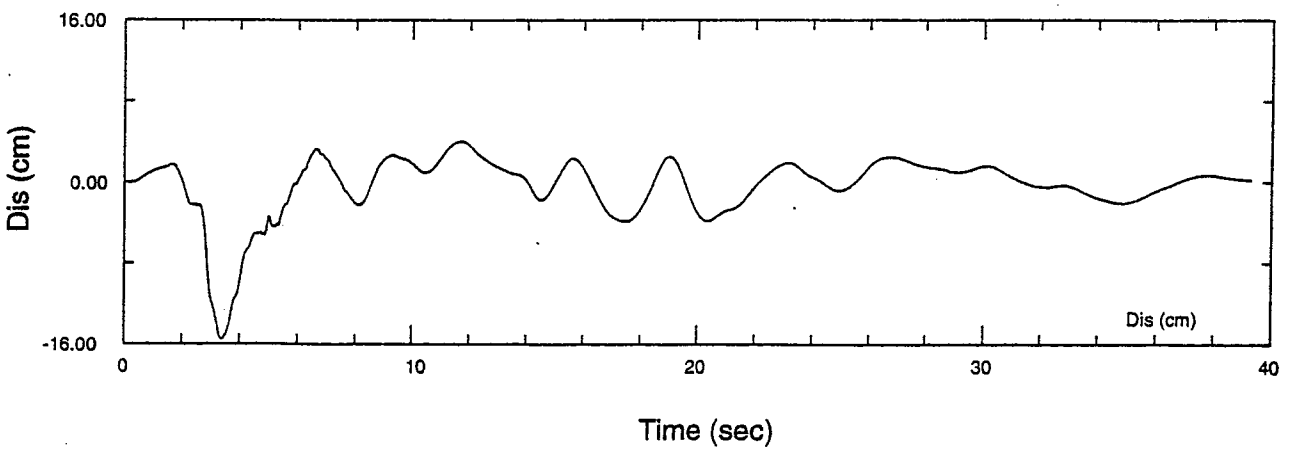

NOTE: Includes Scale Factor for Extensional Regimes.
Time History Modified to Match Target Spectrum,
Which is Median Waters Peak Spectrum
Shown on Exhibit 3-6

HCG
Pardee Project Team
HDR Engineering Inc.
Christensen Associates Inc.
GEI Consultants Inc.

Pardee Reservoir Enlargement Project
MODIFIED TIME HISTORIES, VERTICAL COMPONENT, EL CENTRO RECORD

VOLUME		Exhibit 3-7.6	
SCALE			REV.
DATE	Dec. 1997		

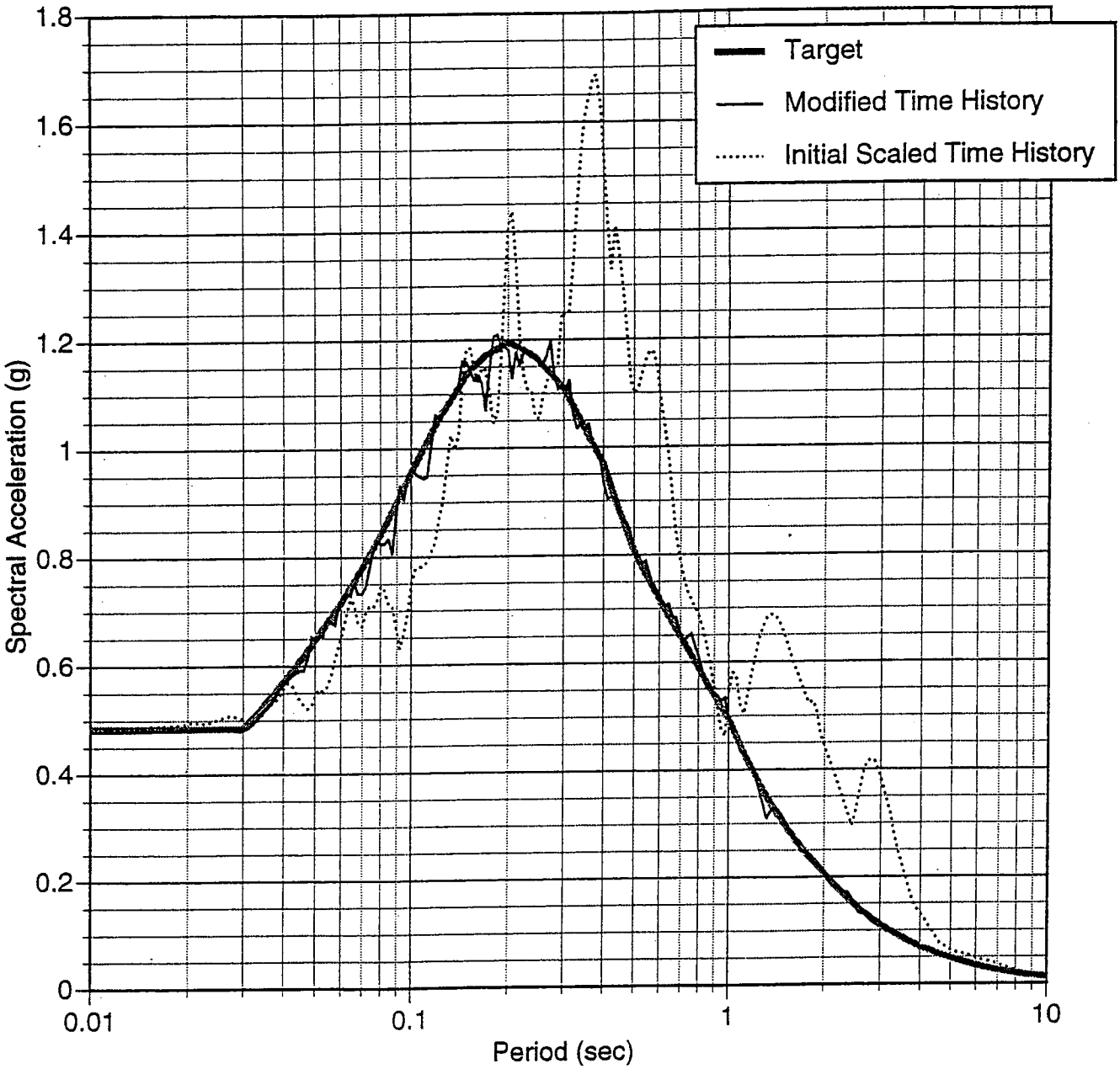

NOTE: Includes Scale Factor for Extensional Regimes.
Time History Modified to Match Target Spectrum,
Which is Median Waters Peak Spectrum
Shown on Exhibit 3-6

HCG
Pardee Project Team
HDR Engineering Inc.
Christensen Associates Inc.
EI Consultants Inc.

Pardee Reservoir Enlargement Project
RESPONSE SPECTRA,
FAULT PARALLEL COMPONENT,
STURNO RECORD

VOLUME		Exhibit 3-8.1	
SCALE			
DATE	Dec. 1997		REV.

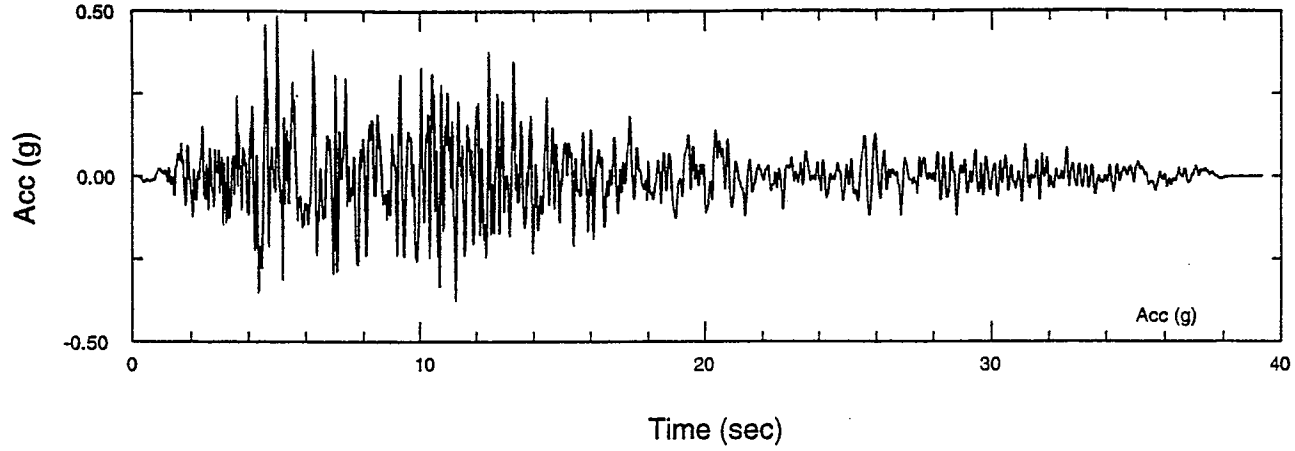

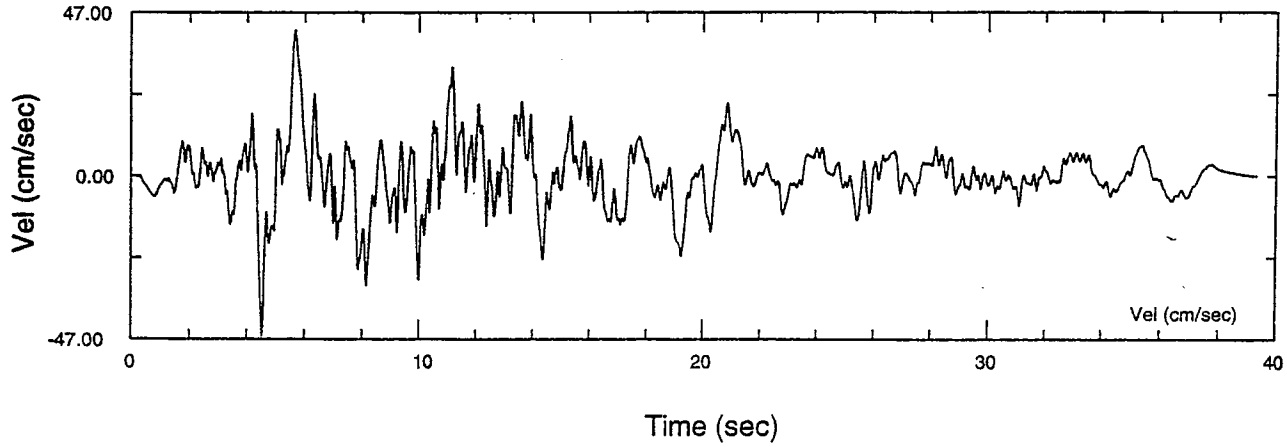

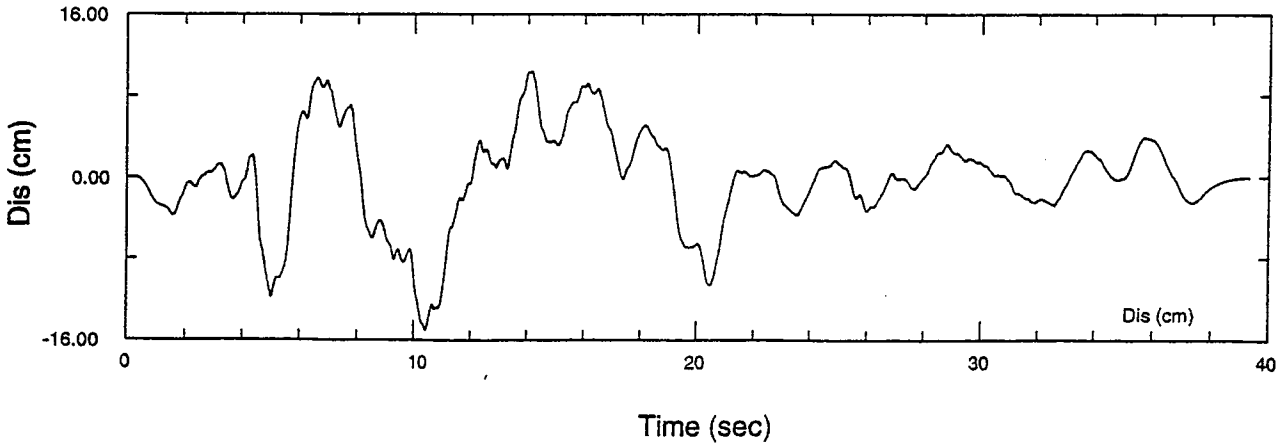

NOTE: Includes Scale Factor for Extensional Regimes.
Time History Modified to Match Target Spectrum,
Which is Median Waters Peak Spectrum
Shown on Exhibit 3-6

HCG
Pardee Project Team
HDR Engineering Inc.
Christenson Associates Inc.
GOEI Consultants Inc.

Pardee Reservoir Enlargement Project
MODIFIED TIME HISTORIES,
FAULT PARALLEL COMPONENT,
STURNO RECORD

VOLUME		
SCALE		Exhibit 3-8.2
DATE	Dec. 1997	REV.

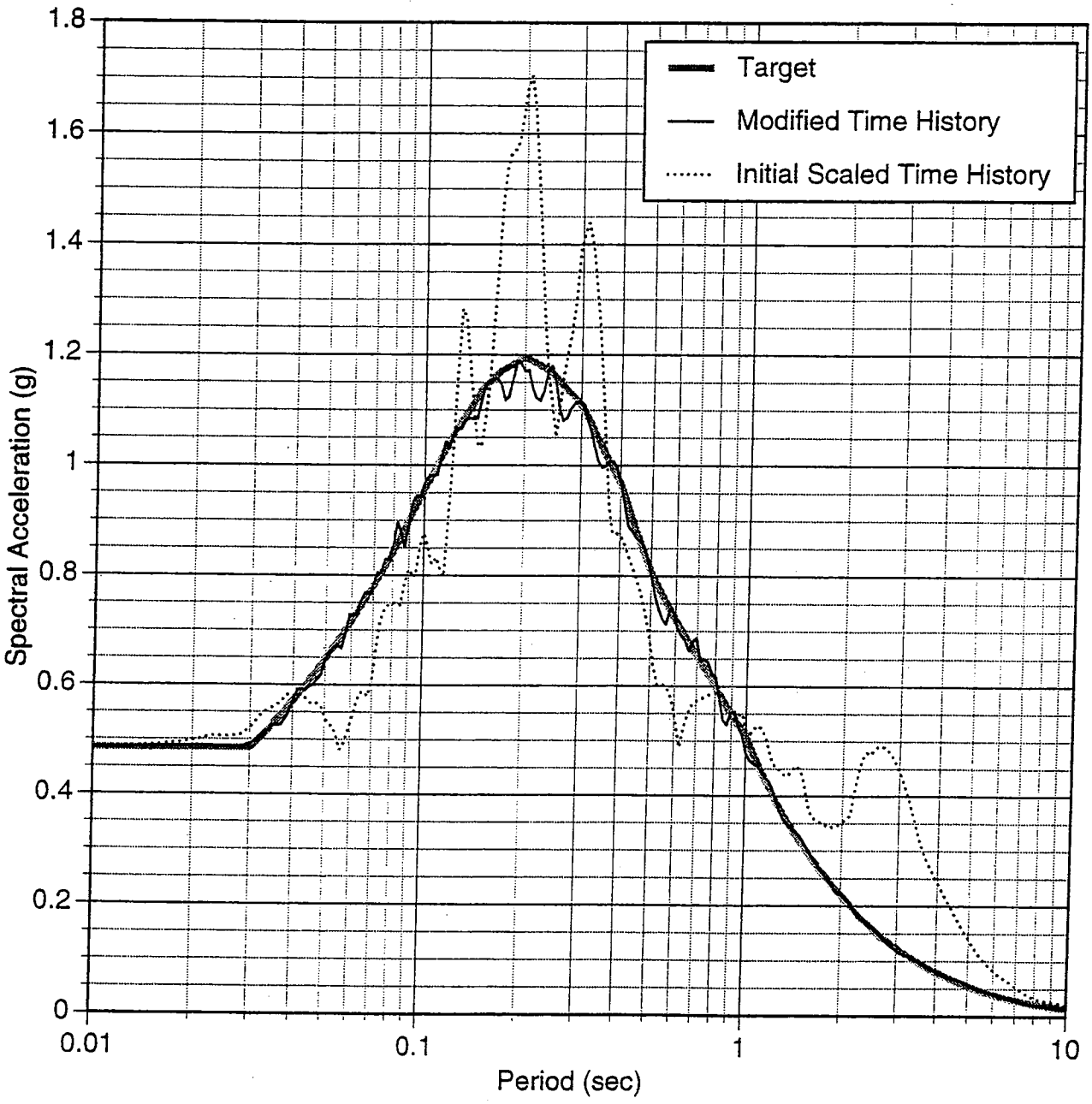

NOTE: Includes Scale Factor for Extensional Regimes.
Time History Modified to Match Target Spectrum,
Which is Median Waters Peak Spectrum
Shown on Exhibit 3-6

HCG
Pardee Project Team
HDR Engineering Inc.
Christensen Associates Inc.
GEI Consultants Inc.

Pardee Reservoir Enlargement Project
RESPONSE SPECTRA,
FAULT-NORMAL COMPONENT,
STURNO RECORD

VOLUME		
SCALE		Exhibit 3-8.3
DATE	Dec. 1997	REV.

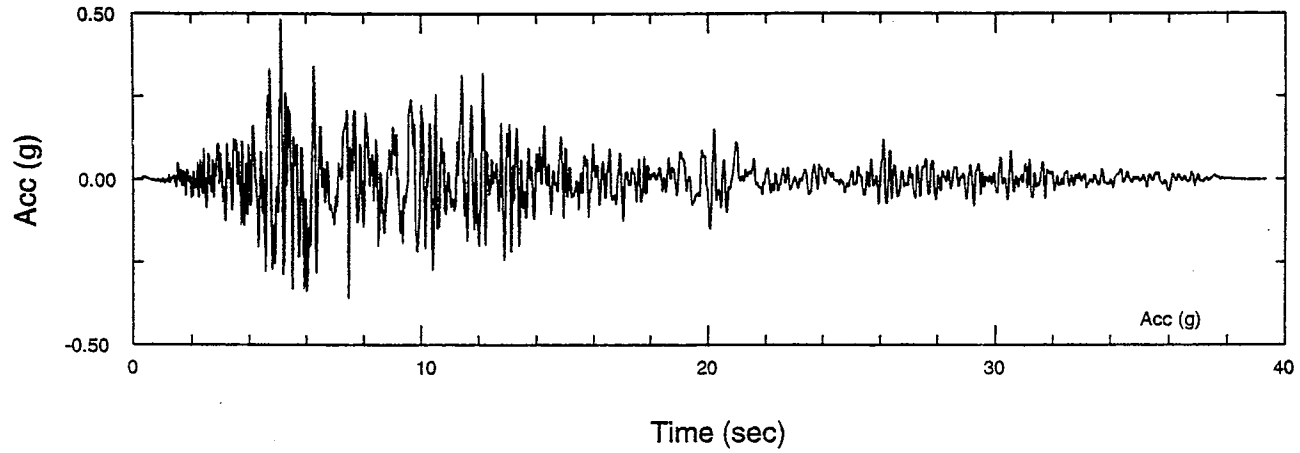

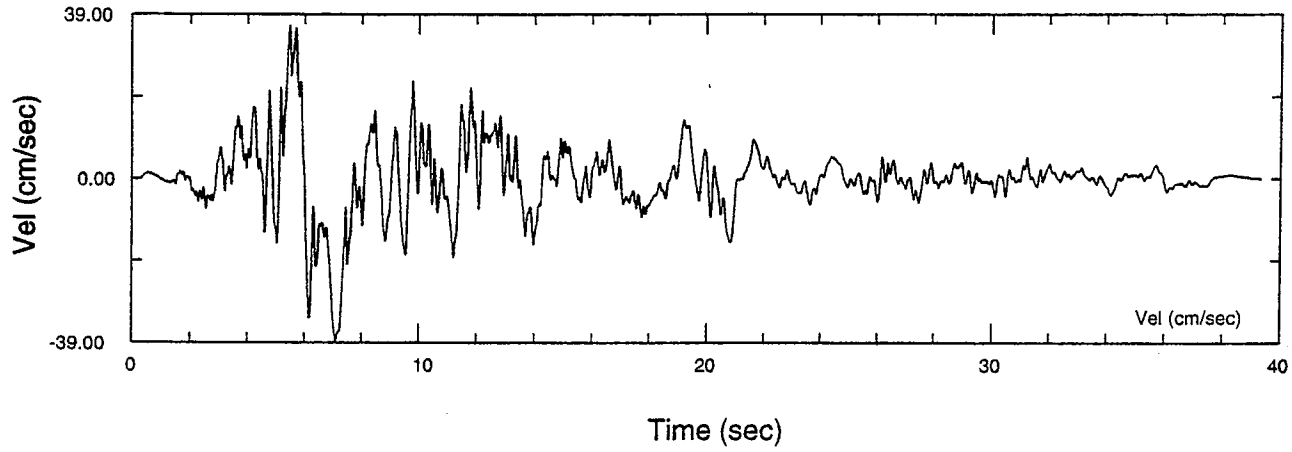

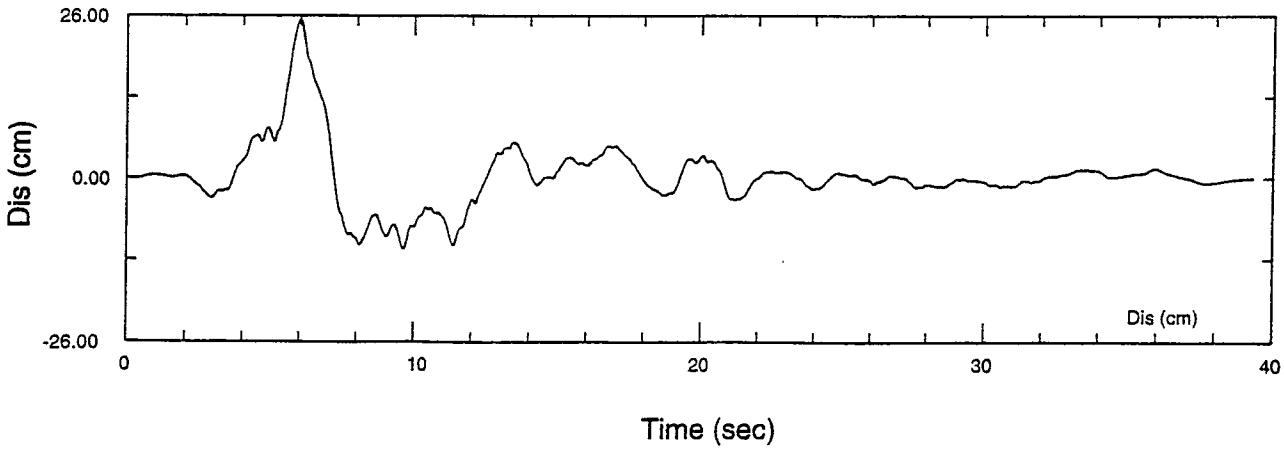

NOTE: Includes Scale Factor for Extensional Regimes.
Time History Modified to Match Target Spectrum,
Which is Median Waters Peak Spectrum
Shown on Exhibit 3-6

HCG
Pardee Project Team
HDR Engineering Inc.
Christensen Associates Inc.
GOEI Consultants Inc.

Pardee Reservoir Enlargement Project
MODIFIED TIME HISTORIES,
FAULT-NORMAL COMPONENT,
STURNO RECORD

VOLUME		
SCALE		Exhibit 3-8.4
DATE	Dec. 1997	REV.

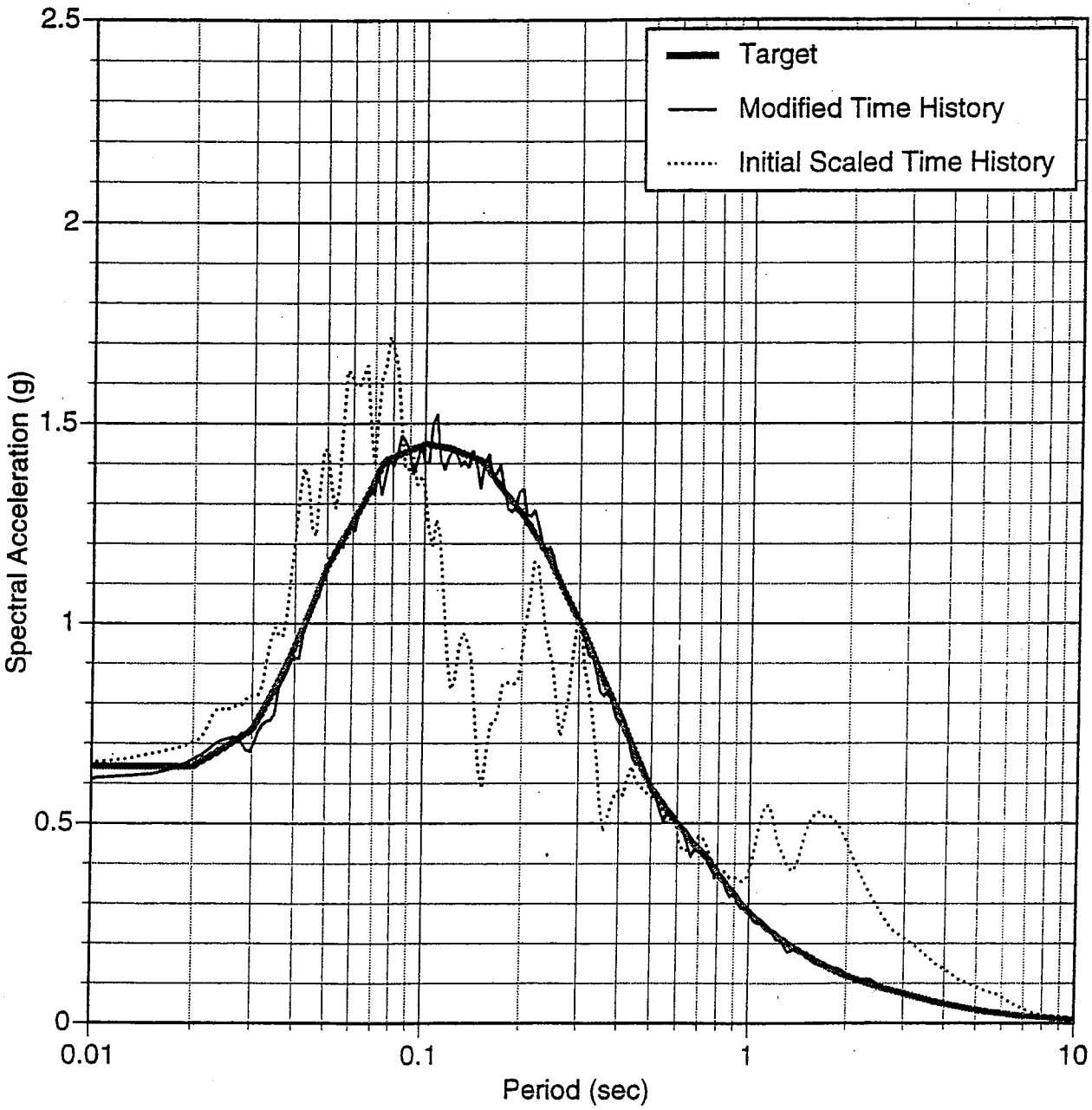

NOTE: Includes Scale Factor for Extensional Regimes.
Time History Modified to Match Target Spectrum,
Which is Median Waters Peak Spectrum
Shown on Exhibit 3-6

HCG
Pardee Project Team
HDR Engineering Inc.
Christensen Associates Inc.
GEI Consultants Inc.

Pardee Reservoir Enlargement Project
RESPONSE SPECTRA, VERTICAL COMPONENT, STURNO RECORD

VOLUME		
SCALE		Exhibit 3-8.5
DATE	Dec. 1997	REV.

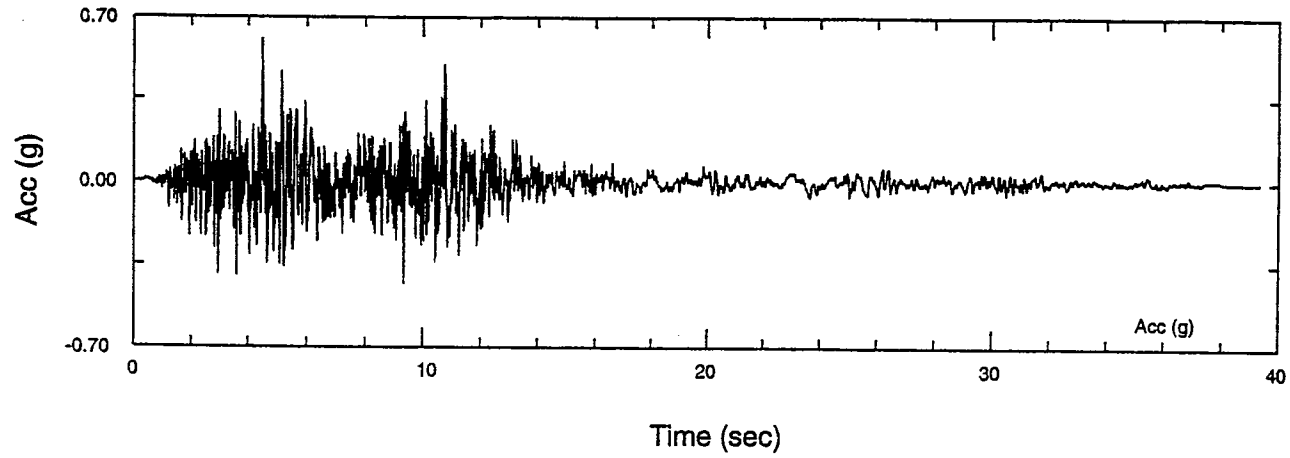

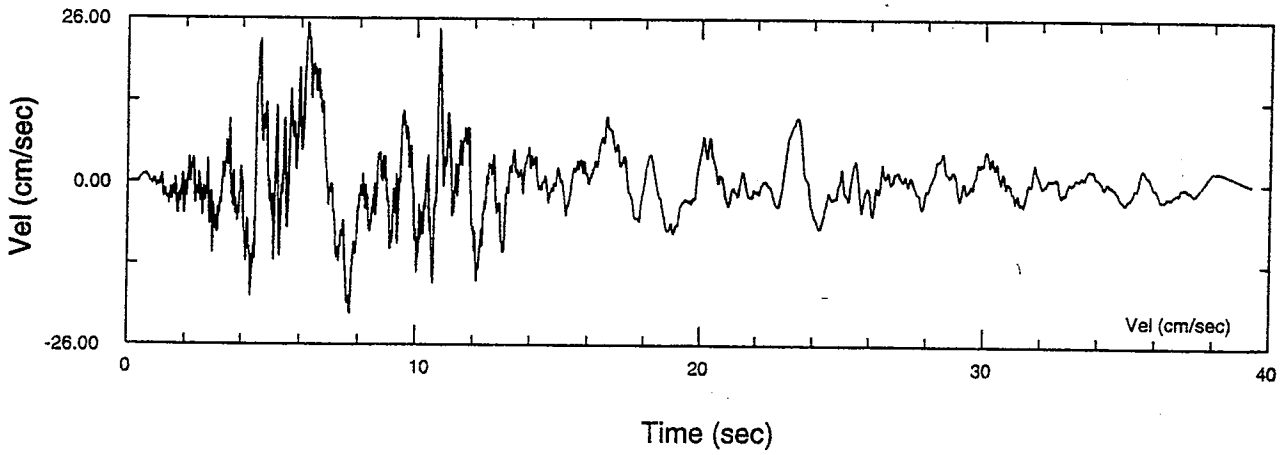

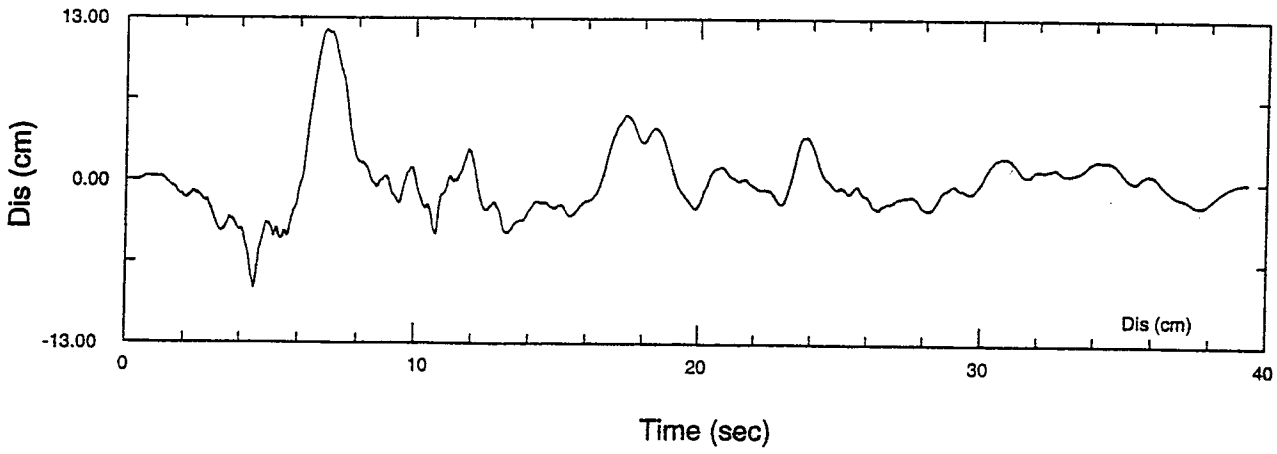

NOTE: Includes Scale Factor for Extensional Regimes.
Time History Modified to Match Target Spectrum,
Which is Median Waters Peak Spectrum
Shown on Exhibit 3-6

HCG
Pardee Project Team
HDR Engineering Inc.
Christensen Associates Inc.
GKI Consultants Inc.

Pardee Reservoir Enlargement Project
MODIFIED TIME HISTORIES, VERTICAL COMPONENT, STURNO RECORD

VOLUME
SCALE
DATE Dec. 1997

Exhibit 3-8.6

REV.

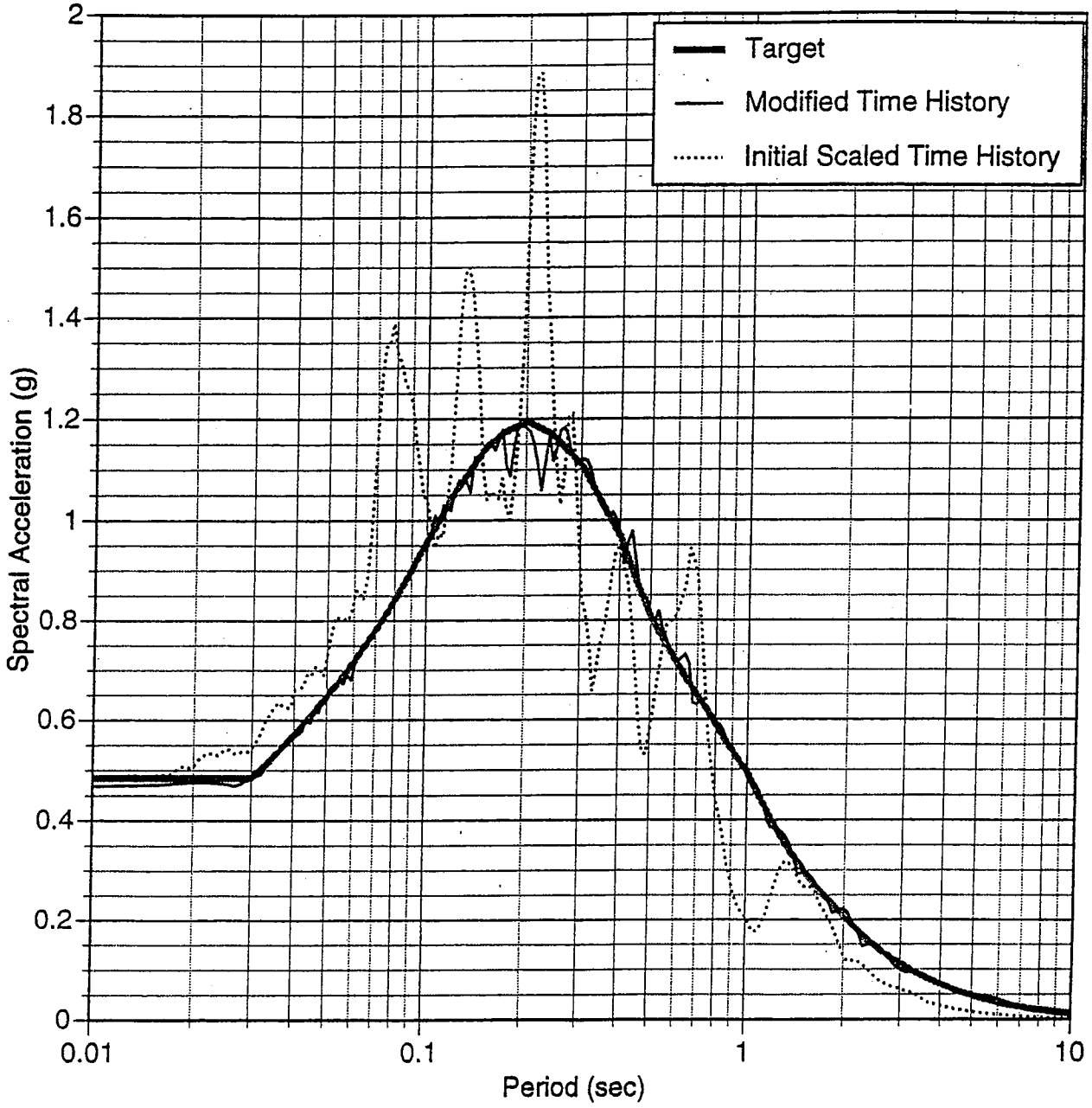

NOTE: Includes Scale Factor for Extensional Regimes.
Time History Modified to Match Target Spectrum,
Which is Median Waters Peak Spectrum
Shown on Exhibit 3-6

HCG
Pardee Project Team
EDR Engineering Inc.
Christenson Associates Inc.
GEI Consultants Inc.

Pardee Reservoir Enlargement Project
RESPONSE SPECTRA,
FAULT PARALLEL COMPONENT,
CONVICT CREEK

VOLUME		
SCALE	**Exhibit 3-9.1**	
DATE Dec. 1997		REV.

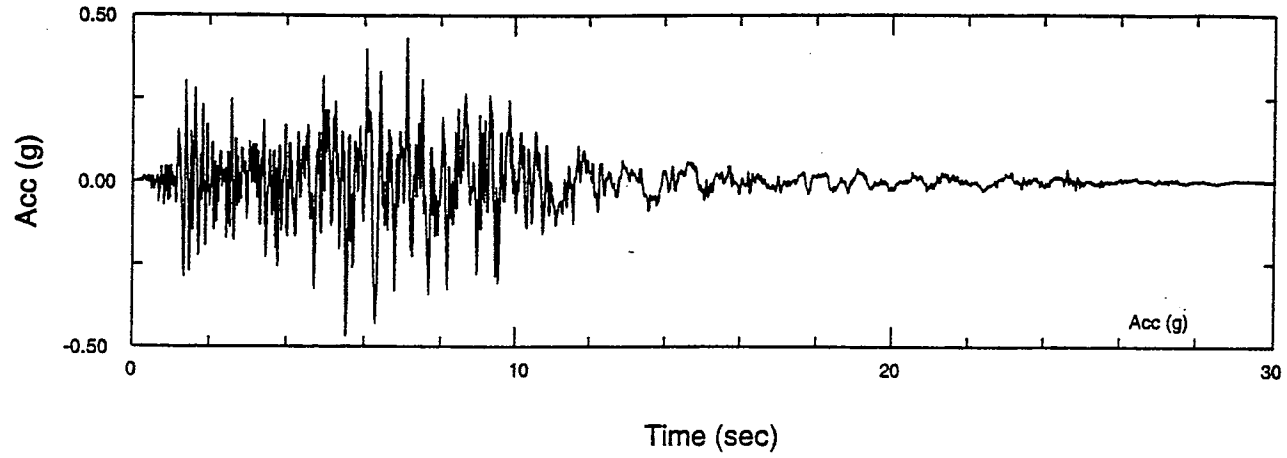

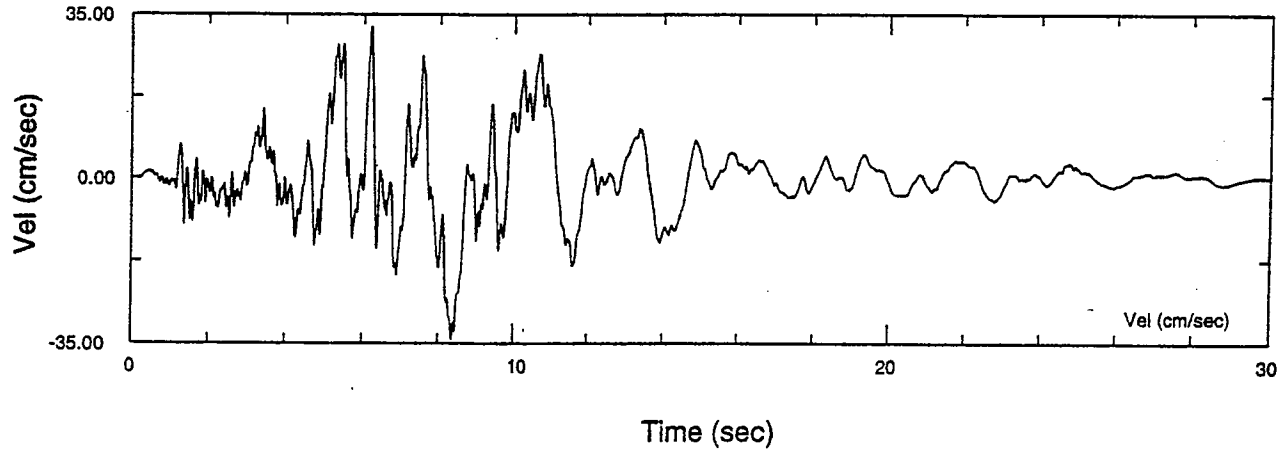

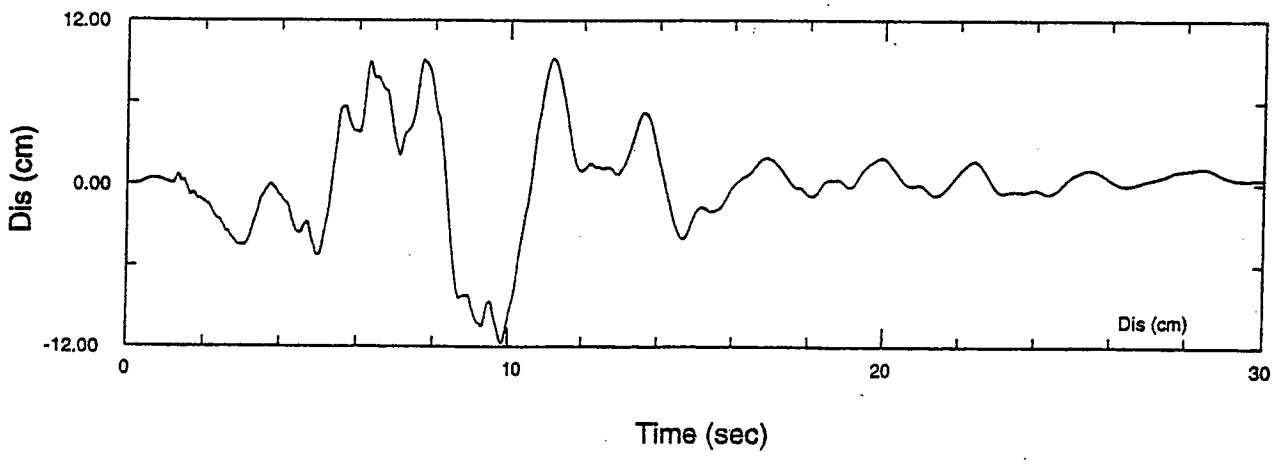

NOTE: Includes Scale Factor for Extensional Regimes.
Time History Modified to Match Target Spectrum,
Which is Median Waters Peak Spectrum
Shown on Exhibit 3-6

HCG
Pardee Project Team
HDR Engineering Inc.
Christensen Associates Inc.
GEI Consultants Inc.

Pardee Reservoir Enlargement Project
MODIFIED TIME HISTORIES,
FAULT PARALLEL COMPONENT,
CONVICT CREEK

VOLUME		
SCALE	Exhibit 3-9.2.	
DATE Dec. 1997		REV.

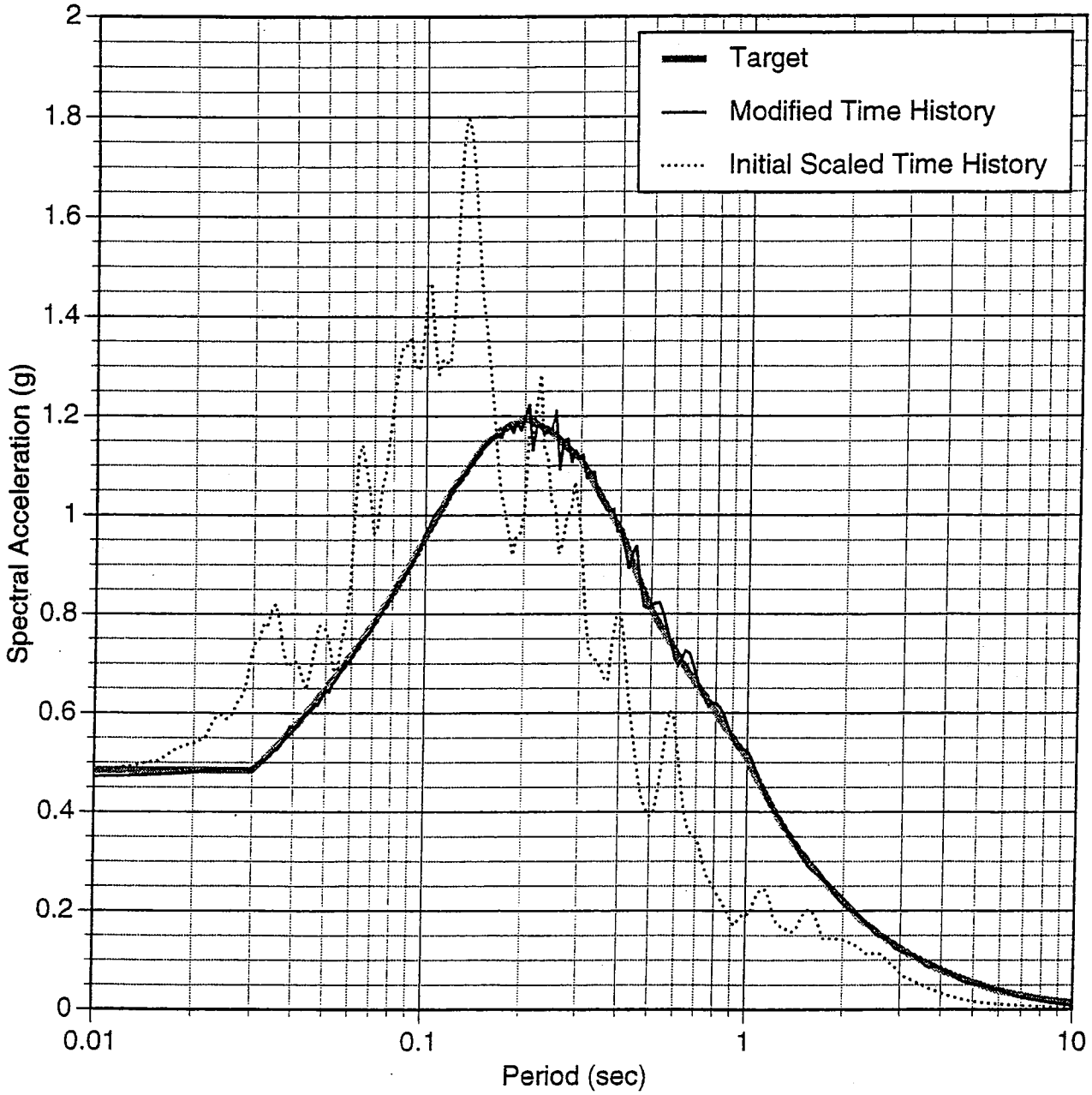

NOTE: Includes Scale Factor for Extensional Regimes.
Time History Modified to Match Target Spectrum,
Which is Median Waters Peak Spectrum
Shown on Exhibit 3-6

HCG
Pardee Project Team
HDR Engineering Inc.
Christensen Associates Inc.
GOE Consultants Inc.

Pardee Reservoir Enlargement Project
RESPONSE SPECTRA,
FAULT-NORMAL COMPONENT,
CONVICT CREEK

VOLUME		
SCALE		Exhibit 3-9.3
DATE	Dec. 1997	REV.

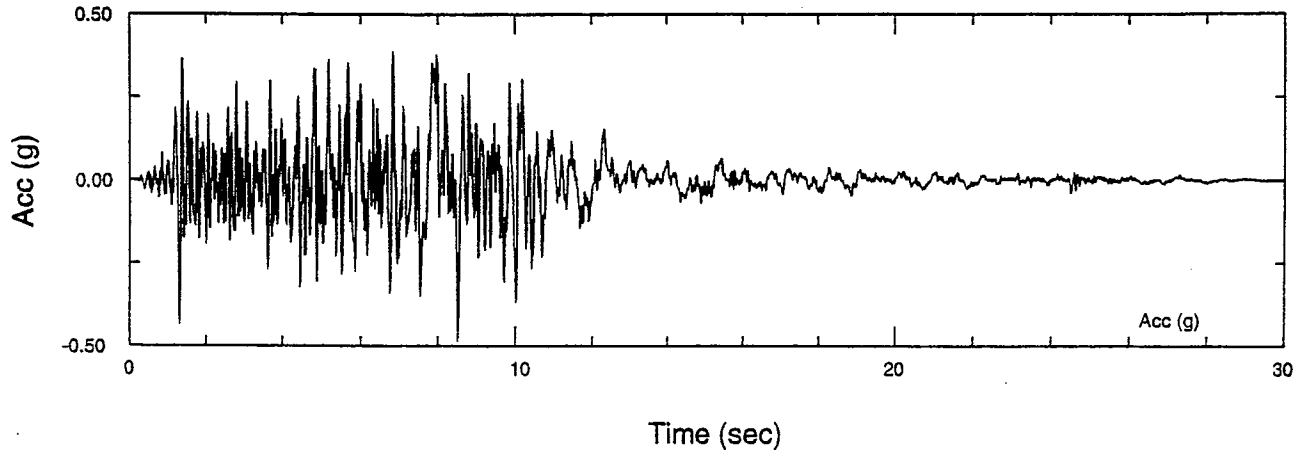

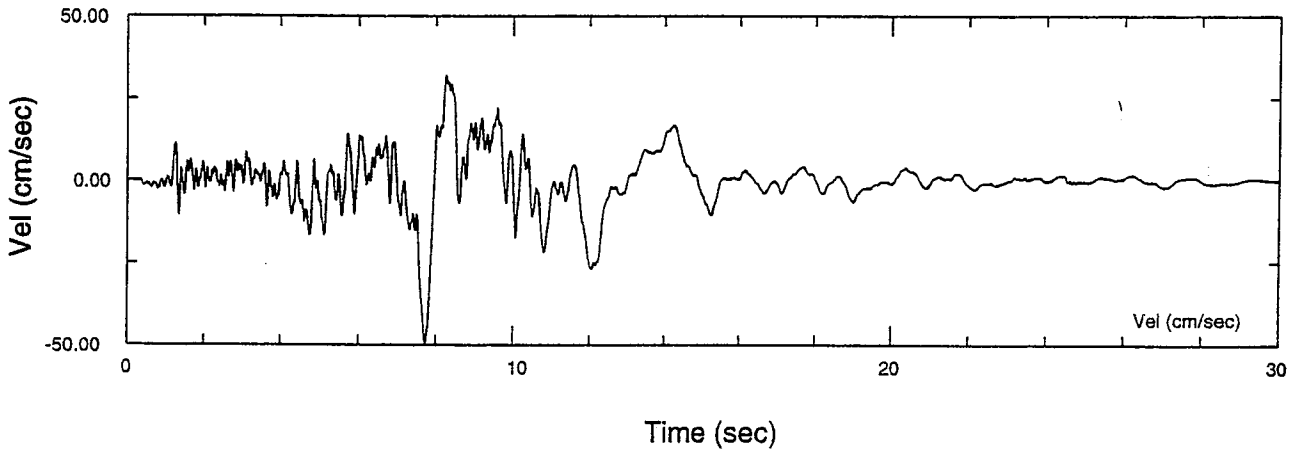

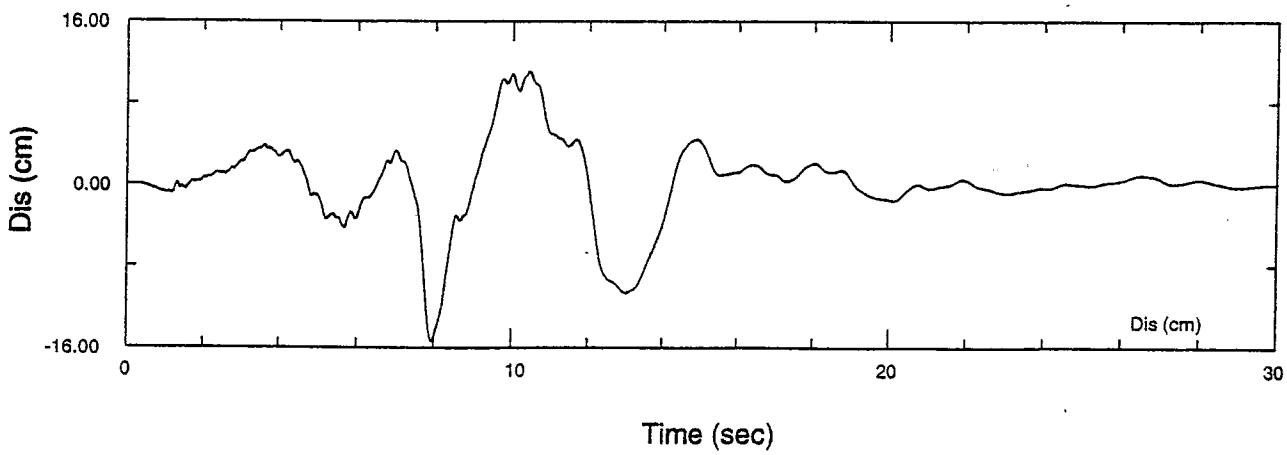

NOTE: Includes Scale Factor for Extensional Regimes.
Time History Modified to Match Target Spectrum,
Which is Median Waters Peak Spectrum
Shown on Exhibit 3-6

HCG
Pardee Project Team
HDR Engineering Inc.
Christensen Associates Inc.
GEI Consultants Inc.

Pardee Reservoir Enlargement Project
MODIFIED TIME HISTORIES,
FAULT-NORMAL COMPONENT,
CONVICT CREEK

VOLUME		
SCALE		**Exhibit 3-9.4**
DATE	Dec. 1997	REV.

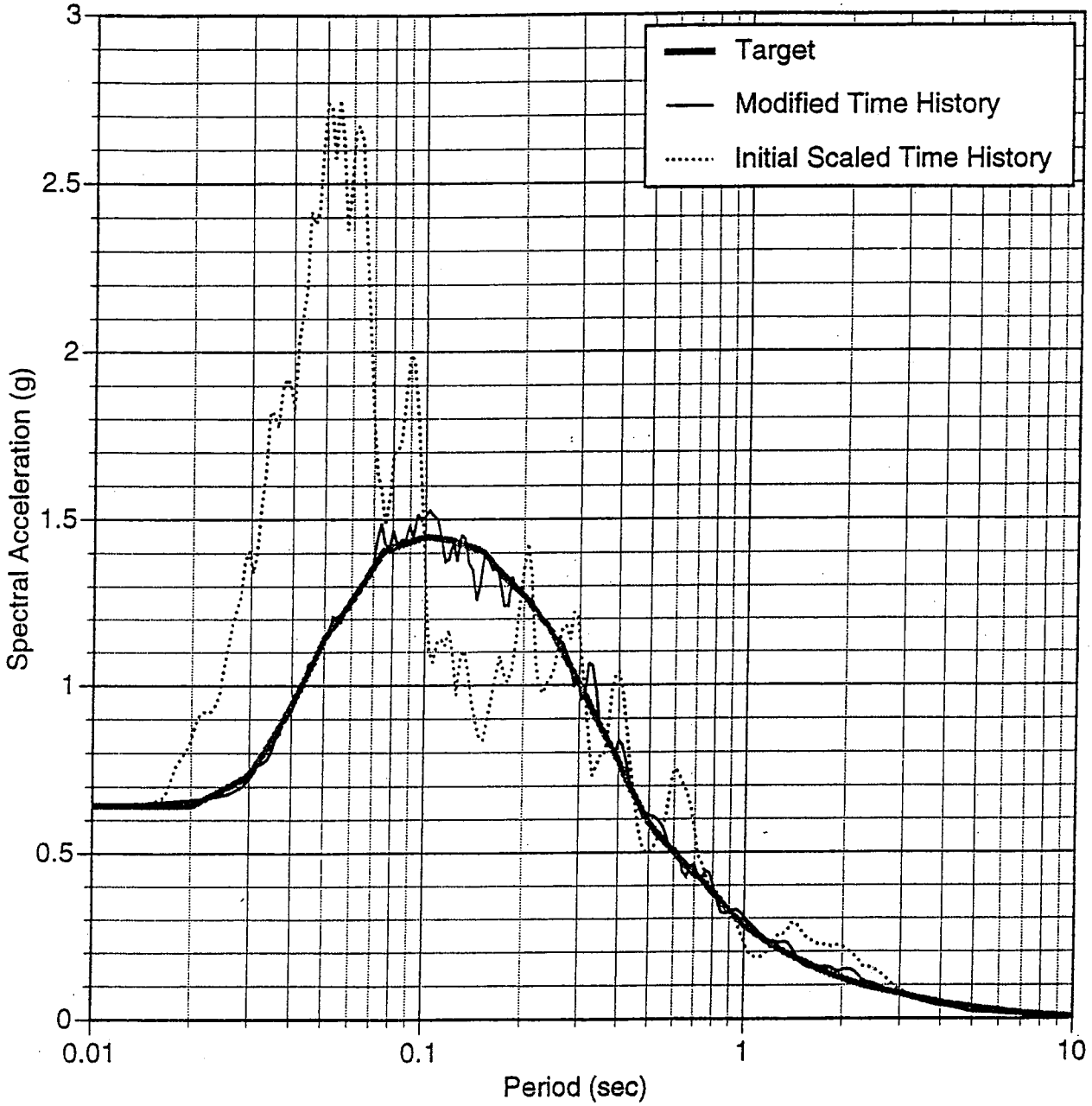

NOTE: Includes Scale Factor for Extensional Regimes.
Time History Modified to Match Target Spectrum,
Which is Median Waters Peak Spectrum
Shown on Exhibit 3-6

Pardee Reservoir Enlargement Project
RESPONSE SPECTRA,
VERTICAL COMPONENT,
CONVICT CREEK

HCG
Pardee Project Team
HDR Engineering Inc.
Christensen Associates Inc.
GKI Consultants Inc.

VOLUME		
SCALE		Exhibit 3-9.5
DATE	Dec. 1997	REV.

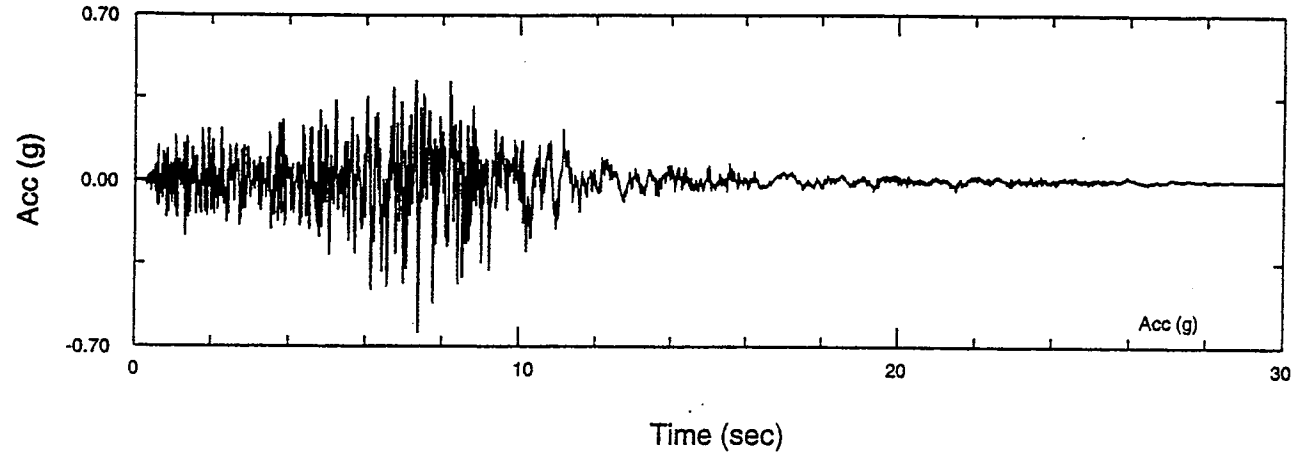

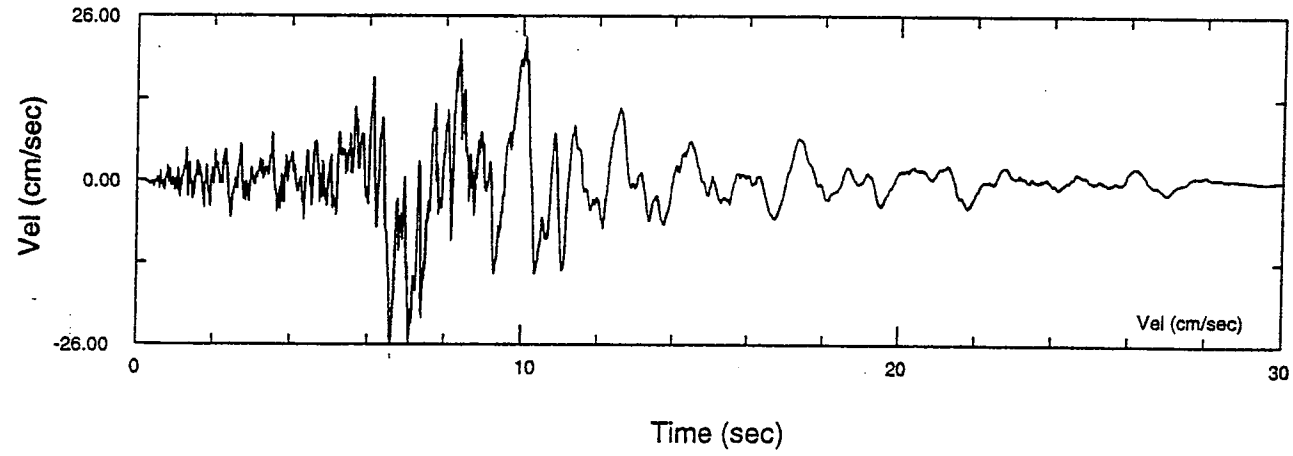

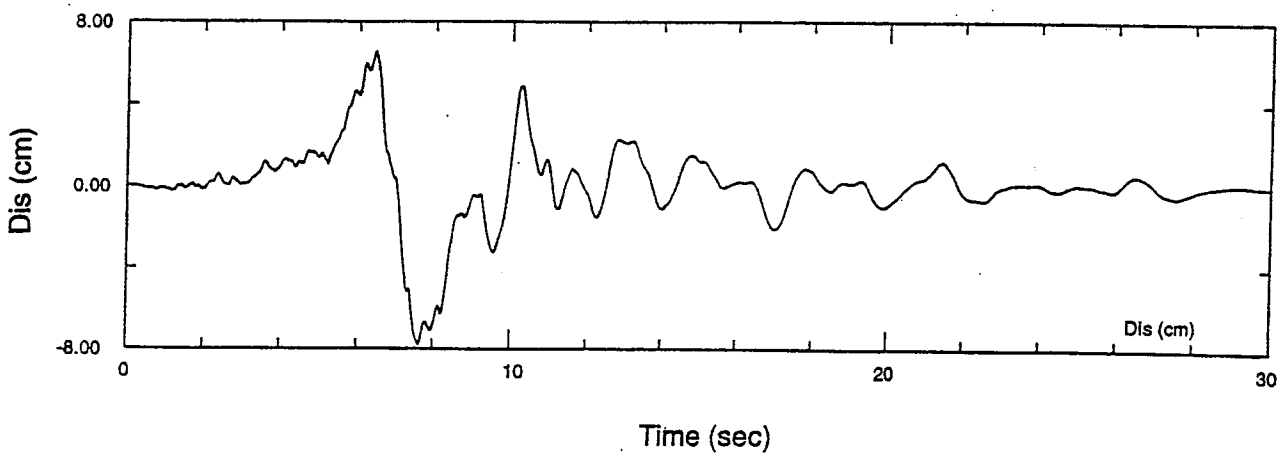

NOTE: Includes Scale Factor for Extensional Regimes.
Time History Modified to Match Target Spectrum,
Which is Median Waters Peak Spectrum
Shown on Exhibit 3-6

Pardee Reservoir Enlargement Project
MODIFIED TIME HISTORIES,
VERTICAL COMPONENT,
CONVICT CREEK

HCG
Pardee Project Team
HSR Engineering Inc.
Christensen Associates Inc.
SGI Consultants Inc.

VOLUME		
SCALE		Exhibit 3-9.6
DATE	Dec. 1997	REV.

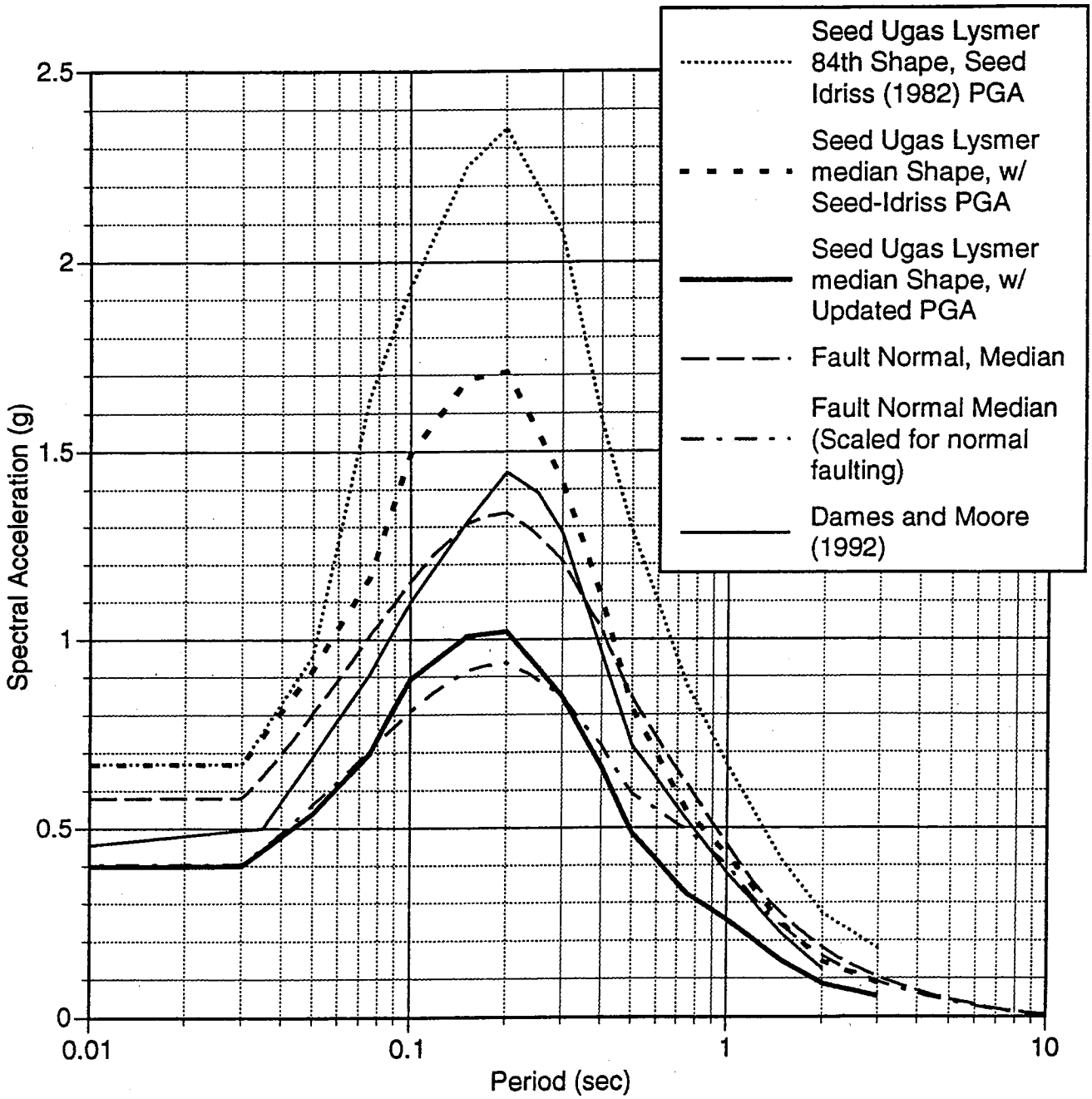

NOTE: Horizontal Acceleration Response Spectra with 5 Percent Damping.

HCG
Pardee Project Team

Pardee Reservoir Enlargement Project
HORIZONTAL RESPONSE SPECTRA COMPARISON
WATERS CREEK

VOLUME		
SCALE	Exhibit 3-10	
DATE Dec. 1997		REV.

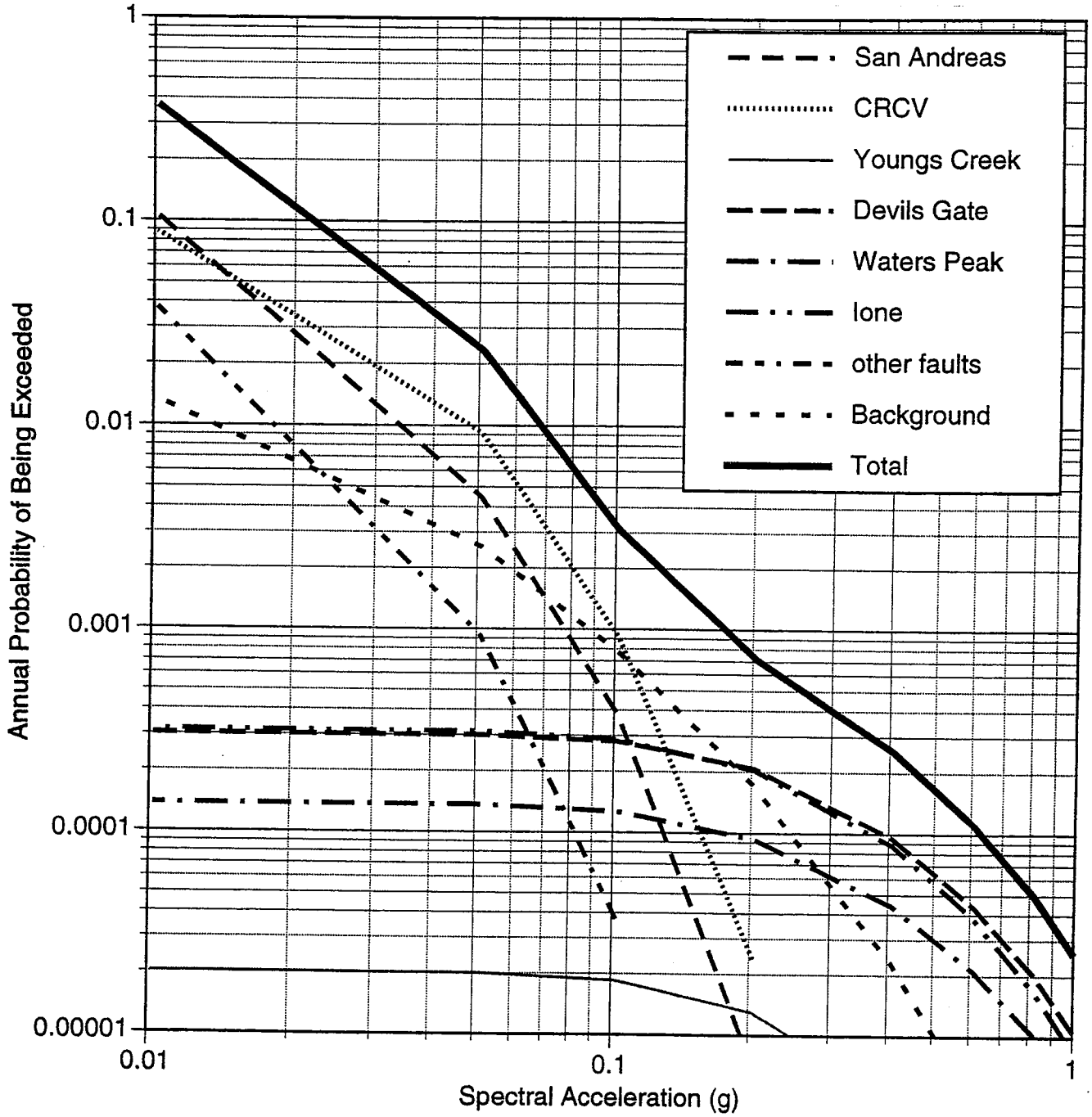

HCG

Pardee Project Team

Pardee Reservoir Enlargement Project

PROBABILISTIC HAZARD
FOR PEAK
HORIZONTAL ACCELERATION

DRAWING		
SCALE		Exhibit 3-11
DATE	Dec. 1997	REV.

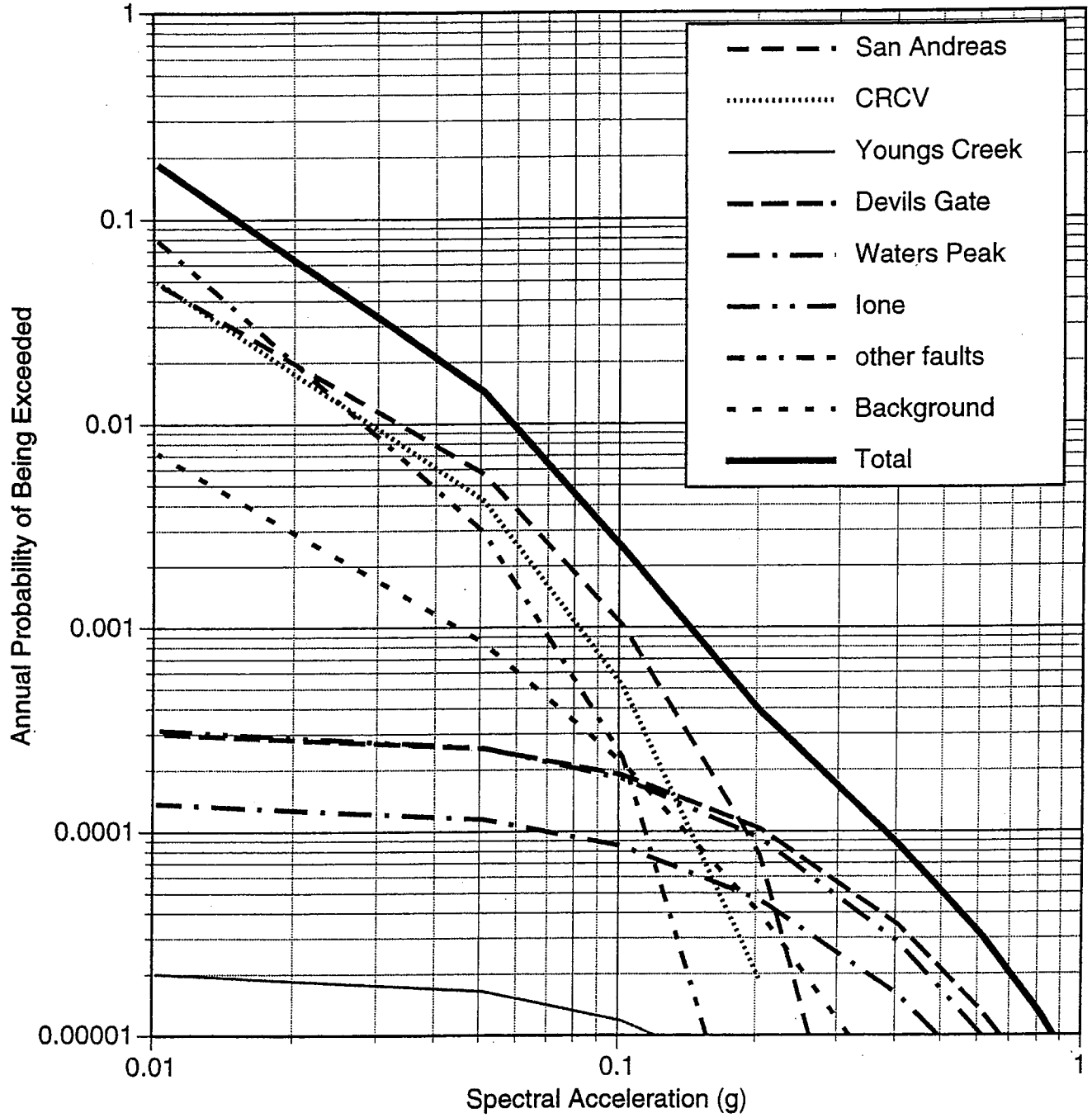

HCG
Pardee Project Team

Pardee Reservoir Enlargement Project

PROBABILISTIC HAZARD FOR 5 PERCENT DAMPED HORIZONTAL ACCELERATION AT A PERIOD OF 1 SECOND

TOLERANCE		
SCALE		Exhibit 3-12
DATE	Dec. 1997	REV.

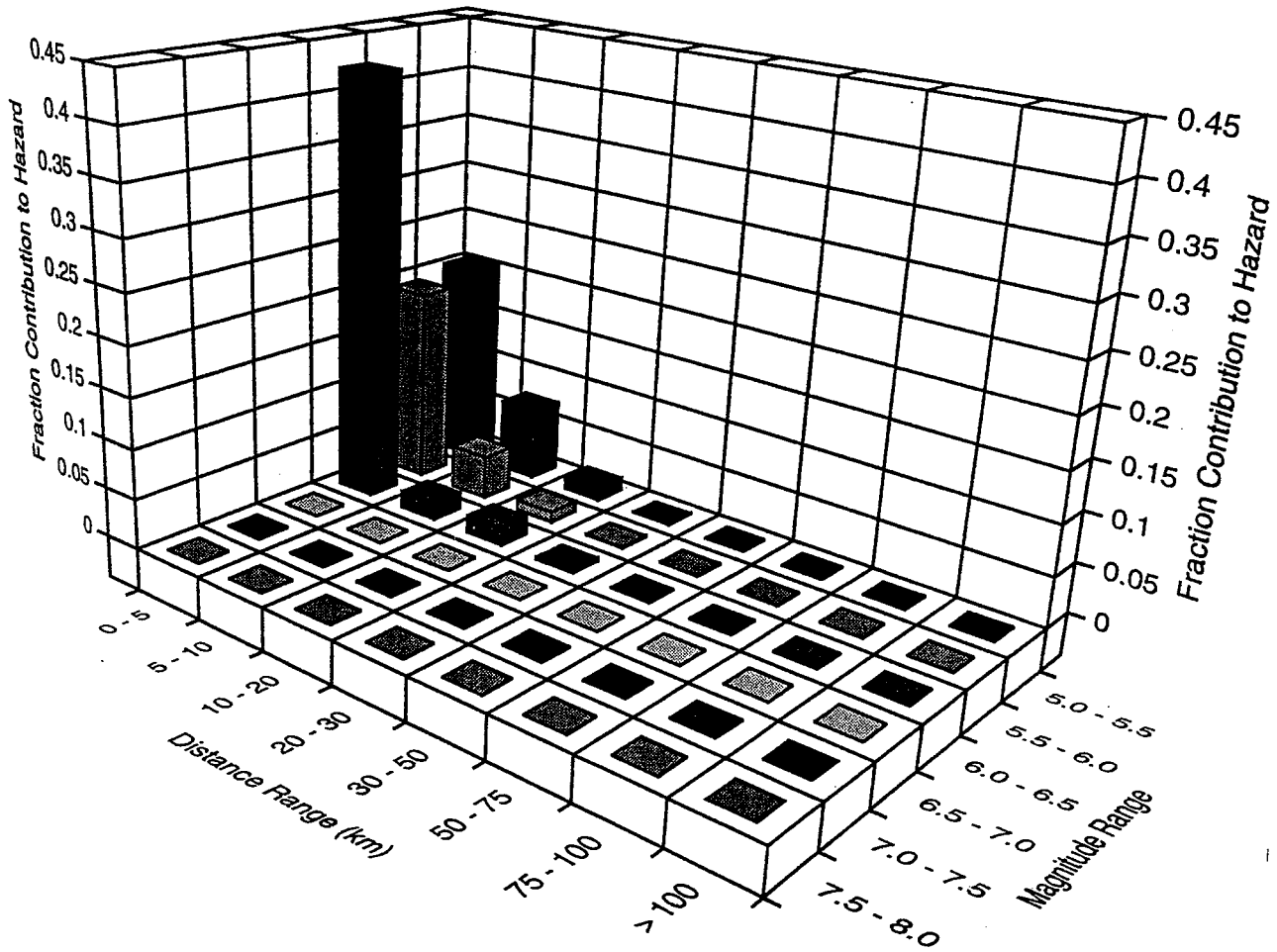

Pardee Reservoir Enlargement Project

DEAGGREGATED HAZARD FOR PEAK ACCELERATION, RETURN PERIOD OF 3000 YEARS

VOLUME		
SCALE		Exhibit 3-13
DATE	Dec. 1997	REV.

HCG

Pardee Project Team

HBE Engineering Inc.
Christensen Associates Inc.
HGE Consultants Inc.

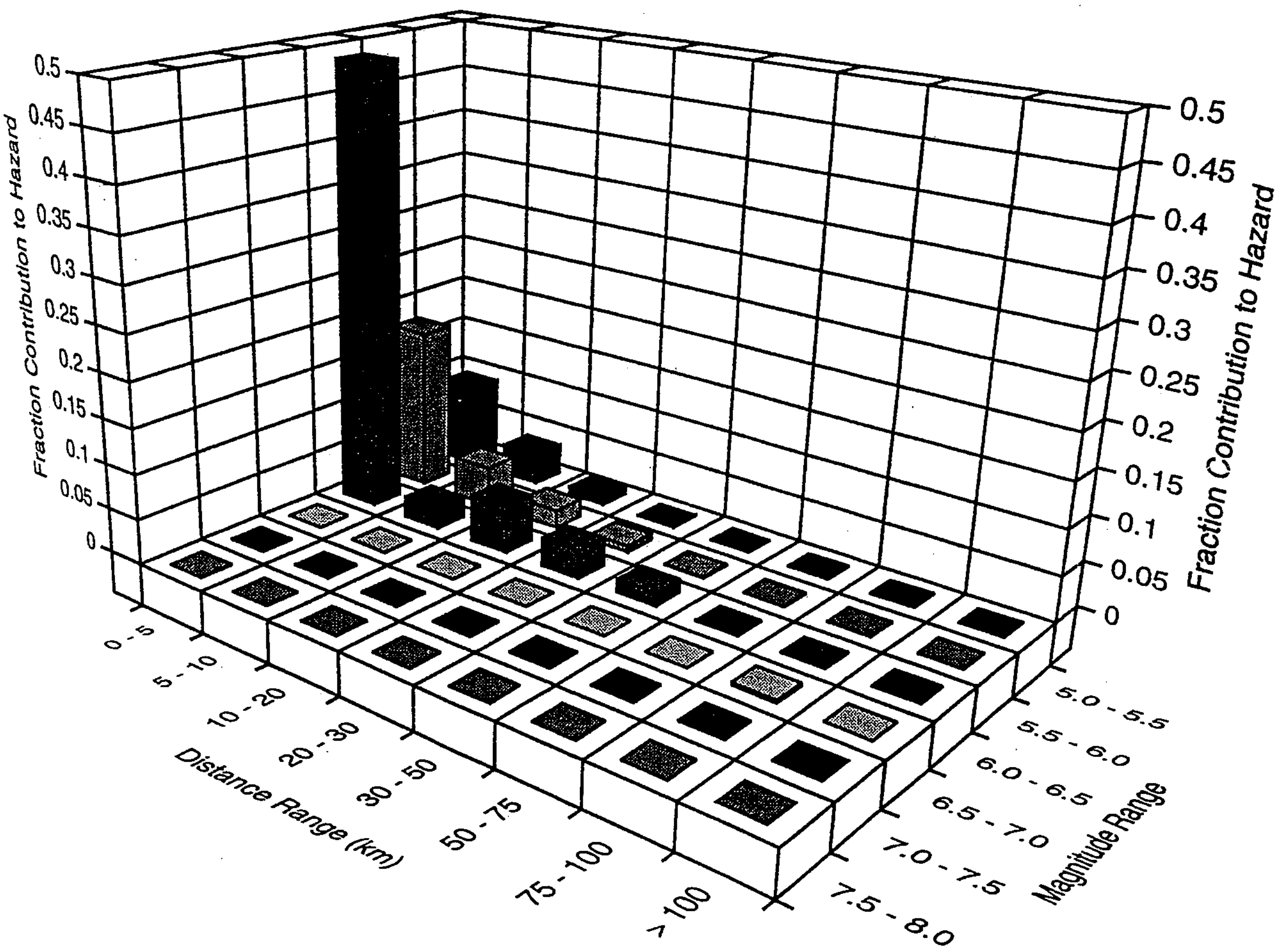

HCG

Pardee Project Team

EBR Engineering Inc.
Christensen Associates Inc.
(KEI Consultants Inc.

Pardee Reservoir Enlargement Project

DEAGGREGATED HAZARD T=1.0 SECOND, ACCELERATION RETURN PERIOD OF 3000 YEARS

VOLUME
SCALE
DATE Dec. 1997

Exhibit 3-14

REV.

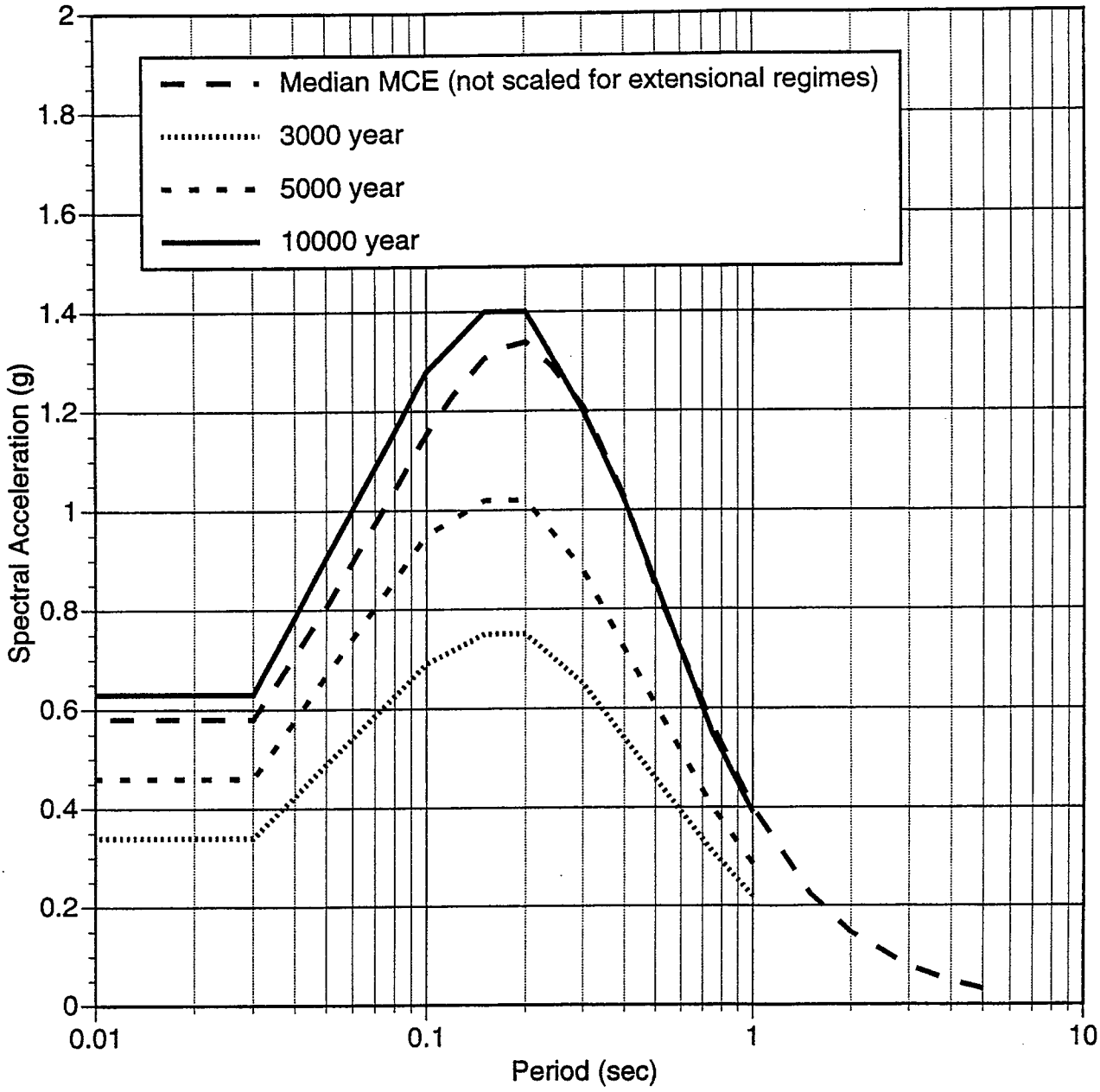

Pardee Reservoir Enlargement Project

COMPARISON OF MEDIAN DETERMINISTIC AND PROBABILISTIC SPECTRA

HCG

Pardee Project Team

VOLUME	
SCALE	
DATE	Dec. 1997

Exhibit 3-15

REV.

4. RECOMMENDATIONS

4.1 DESIGN RECOMMENDATIONS

Preliminary design of a raised or replacement dam at the existing Pardee Dam site should be based on the median percentile deterministic ground motion for the Waters Peak fault adjusted for extensional regime effects. Modified records for the fault-normal, fault-parallel, and vertical components of movement for three earthquake records: El Centro, Sturno, and Convict Creek, presented in Exhibits 3-7.1 through 3-7.6, 3-8.1 through 3-8.6, and 3-9.1 through 3-9.6, should be used for design. Designs for the other facilities should be based on records developed by scaling records developed for the existing Pardee Dam site based on differences in source-to-site distance. The source-to-site scale factors are presented in Table 3-3.

Geomorphic lineaments crossing the Jackson Creek Dam site should be assumed to be secondary faults that could experience surface fault rupture during a nearby earthquake. Structures crossing these lineaments should be designed to accommodate displacements of 10 to 40 cm.

4.2 ADDITIONAL STUDIES

Faults in the Pardee Reservoir area are classified as "conditionally active seismic sources" based on the State of California Division of Safety of Dams criteria. For the purpose of seismic design, the Youngs Creek, Devils Gate, Waters Peak, and Ione faults were considered as active seismic sources. However, supplemental geologic and seismologic data could be developed to better define the activity, deformation style, recurrence interval, and displacement potential of these faults. Surface mapping of geomorphic lineaments alone will not result in data sufficient to reassess fault activity. A strategy for successful assessment of fault capability and potential earthquake magnitude would be to use the paleoseismic technique of trenching and to evaluate instrumental seismicity, which should aid in defining the style of deformation in the Pardee Reservoir region. Supplemental seismotectonic studies could involve all or some of the following tasks:

1. Compilation and analysis of instrumental seismicity for the western Sierra Nevada. Based on available data, it is concluded that the style of deformation in the western portion of the Foothills fault system is oblique slip with a strong dextral strike slip component. Earthquake focal mechanisms could be used to quantify the relative components of dip-slip and strike-slip, which could lead to a revised interpretation of deformation style and estimated ground motions.

2. Detailed mapping of geomorphic lineaments in the Campo Seco area, south of the Mokelumne River, could be performed during the next level of design for the downstream dam. The purpose of this mapping would be to acquire data to evaluate if these lineaments are the result of faulting. Supplemental work, including trenching, could be performed if faulting is confirmed or suspected to evaluate late Cenozoic activity and deformation style.

3. Supplemental mapping and trenching of geomorphic lineaments in the Jackson Creek area could be performed before the next level of design for the proposed Jackson Creek Saddle Dam. The purpose of this work would be to acquire data to evaluate the presence of faulting, style of faulting, and displacement potential of these lineaments.

4. Supplemental mapping and trenching of the Devils Gate fault zone could be performed before the next level of design for the proposed Jackson Creek Dam. The purpose of this work would be to acquire data to evaluate the presence of faulting, dominant style of faulting, probable age of past rupture events, Quaternary slip rate, and displacement estimates. The fault exposure along the east side of Pardee Reservoir south of Jackson Creek Spillway could be logged in detail to further evaluate the style of faulting. The Mehrten-capped ridges south of State Highway 88 could be mapped in detail to examine the potential for faulting in this area.

5. The Waters Peak fault appears to be the controlling seismic source for the existing Pardee Dam and South Spillway, the existing intake tower, and the downstream damsites. Detailed logging of fault exposures and trenching of the Waters Peak fault could be performed to acquire data for the evaluation of the dominant style of faulting, probable age of past rupture events, and Quaternary slip rate.

6. Supplemental mapping and trenching of the Ione fault could be performed to acquire data for the evaluation of the presence of faulting, dominant style of faulting, probable age of past rupture events, and Quaternary slip rate. Trenching at the southern terminus of the Ione fault could be considered to evaluate the extent and style of faulting.

7. The Youngs Creek fault does not appear to be a controlling seismic source for proposed structures. If the fault is suspected of being a potentially controlling seismic source in the future, geologic mapping and trenching could be performed to acquire supplemental data for the evaluation of dominant style of faulting, probable age of past rupture events, and Quaternary slip rate. Lineaments in the vicinity of the mapped fault trace could also be investigated to determine activity potential and relationship to the main fault trace.

Ground motions and response spectra recommended for preliminary design are based on the median ground motion from a deterministic analysis. Based on the results of our probabilistic analysis, the deterministic spectrum recommended has a return period of about 10,000 years. Ground motions based on a return period less than 10,000 years may be appropriate for the Pardee structures and should be evaluated in subsequent phases of

design. Ground motions based on the results of a probabilistic analyses were not recommended for preliminary design because the California DSOD does not currently accept probabilistic analyses. Both the deterministic and probabilistic ground motions should be updated in the next phase of design based on accepted regulatory procedures and current science.

5. REFERENCES

Abrahamson, N. A., and Silva, W. J., 1997. Empirical Response Spectral Attenuation Relations for Shallow Crustal Earthquakes, Seismological Research Letters, Vol. 68, No. 1, p. 94.

Bartow, J. A., and Marchand, D. E., 1979. Preliminary Geologic Maps of Cenozoic Deposits of The Sutter Creek and Valley Springs Quadrangles, California: U. S. Geological Survey Open-File Report 79-436, Scale 1:62,500.

Bechtel Corporation, 1966. Pardee Dam Stability Study: Unpublished Report to East Bay Municipal Utility District.

Bolt, B. A., 1977. Seismicity and Seismic Intensity Study, Pardee and Camanche Dams: Unpublished Report East Bay Municipal Utility District, Oakland, California.

Boore, D. M., Joyner, W. B., and Fumal, T. E., 1997. Equations for Estimating Horizontal Response Spectra and Peak Acceleration from Western North American Earthquakes: A Summary of Recent Work, Seismological Research Letters, Vol. 68, No. 1, p. 128.

California Division of Mines and Geology, in cooperation with U.S. Geological Survey, 1996. Probabilistic Seismic Hazard Assessment for the State of California: Open-File Report 96-08.

Clark, L. D., 1964. Stratigraphy and Structure of Part of the Western Sierra Nevada Metamorphic Belt, California: U. S. Geological Survey Professional Paper 410, 70 p., 11 plates.

Cornell, C. A., 1968. Engineering Seismic Risk Analysis, Seismological Society of America Bulletin, v. 58, 1583-1606.

Dames and Moore, 1992. Pardee Dam Stability Evaluation: Unpublished Report to East Bay Municipal Utility District, Oakland, California.

Dames and Moore, 1993. Photogeologic and Imagery Analysis for the Geologic and Seismologic Investigation, New Hogan Dam, Calaveras County, California: Unpublished Report to the U. S. Army Corps of Engineers, Sacramento District, 51 pages.

Earth Sciences Associates, 1992. Raised Pardee Dam, Additional Storage Alternative, Geotechnical Investigation: Unpublished Report to East Bay Municipal Utility District, Oakland, California.

Geomatrix, 1992. Seismic Ground Motion Study for West San Francisco Bay Bridge, Report to Caltrans, Project No. 2016G.

Graymer, R. W., and Jones, D. L., 1994. Tectonic Implications of Radiolarian Cherts from the Placerville Belt, Sierra Nevada Foothills, California: Nevadan-age Continental Growth by Accretion of Multiple Terranes: Geological Society of America Bulletin, v. 106, pp. 531-540.

Hart, E. W., and Rapp, J. S., 1975. Ground Rupture Along the Cleveland Hill Fault: Oroville, California Earthquake, 1 August 1975, California Division of Mines and Geology Special Report 124, pp. 61-72.

Hill, D. P., Jr., Eaton, J. P., Ellsworth, E. L., Cockerham, R. S., Lester,, F. W., and Corbett, E. J., 1991. The Seismotectonic Fabric of Central California, in Neotectonics of North America, D. B. Slemmons, E. R. Engdahl, M. D. Zoback, and D. D. Blackwell (editors), Geological Society of America, pp. 107-132.

Idriss, I. M., 1985. "Evaluating Seismic Risk in Engineering Practice," Proceedings of International Conference on Soil Mechanics and Foundation Engineering, Vol. I., San Francisco.

Idriss, I. M., 1991. Selection of Earthquake Ground Motions at Rock Sites, Report prepared for the Structures Division, Building and Fire Research Lab., NIST.

Idriss, I. M., 1994a. Updated Standard Errors, Personal Communication, April 17, 1994.

Idriss, I. M., 1994b. Attenuation Relations for Peak Horizontal Acceleration at Rock Sites, Personal Communication, September 1, 1994.

Louderback, G. W., 1928. Geological Report on Pardee Dam Site: Unpublished Report to East Bay Municipal Utility District, Oakland, California.

Marchand, D. E., and Allwardt, A., 1981. Late Cenozoic Stratigraphic Units, Northeastern San Joaquin Valley, California: U. S. Geological Survey Bulletin 1470, 70 p., 2 plates.

Pacific Gas and Electric Company (unpublished data). Geomorphic and Geologic Profiles Across the Foothills Fault System, Central Sierra Nevada.

Pacific Gas and Electric Company (in progress). Late Cenozoic Faulting Within the Northern and Central Sierra Nevada, California: Report to State of California Division of Safety of Dams, Sacramento, California.

Page, W. D., 1994. Review of Fault Trenches, New Hogan Dam, Calaveras County: Unpublished Report for the U. S. Army Corps of Engineers, Sacramento District, 11 p.

Page, W. D., 1997. Personal conversation with William Cole.

Sadigh, K., Chang, C.-Y., Egan, J. A., Makdisi, F., and Youngs, R. R., 1997. Attenuation Relationships for Shallow Crustal Earthquakes Based on California Strong Motion Data, Seismological Research Letters, Vol. 68, No. 1, p. 180.

Schwartz, D., 1997. Personal conversation with William Cole.

Seed, H. B., Ugas, C., and Lysmer, J., 1976. Site-Dependent Spectra for Earthquake-Resistant Design, Bulletin of the Seismological Society of America, Vol. 66, No. 1, p. 221.

Somerville, P. G., Smith, N. F., Graves, R. W., and Abrahamson, N. A., 1997. Modification of Empirical Strong Ground Motion Attenuation Relations to Include the Amplitude and Duration Effects of Rupture Directivity, Seismological Research Letters, Vol. 68, No. 1, p. 199.

Spudich, P., Fletcher, J. B., Hellweg, M., Boatwright, J., Sullivan, C., Joyner, W. B., Hanks, T. C., Boore, D. M., McGarr, A., Baker, L. M., and Lindh, A. G., 1997. SEA96 - A New Predictive Relation for Earthquake Ground Motions in Extensional Regimes, Seismological Research Letters, Vol. 68, pp. 190-198.

Stark, C. L., Silva, W. J., Wong, I. J., and Jackson, S. M., 1992. Assessment of Stress Drops of Normal Faulting Earthquakes in the Basin and Range Province, Seismological Research Letters, Vol. 63, p. 39.

Taliaferro, N. L., and Solari, A. J., 1948. Geologic Map of the Copperopolis Quadrangle, California: California Division of Mines Bulletin 145.

Thenhaus, P. C., Perkins, D. M., Ziony, J. I., and Algermissen, S. T., 1980. Probabilistic Estimates of Maximum Seismic Horizontal Ground Motion on Rock in Coastal California and the Adjacent Outer Continental Shelf, U. S. Geological Survey, Open File Report, pp. 80-924.

U. S. Army Corps of Engineers, 1995. Geologic and Seismologic Investigation (Fault Study), New Hogan Dam and Reservoir, Calaveras River, California 50 p.

Unruh, J. R., 1991. The Uplift of the Sierra Nevada and Implications for Late Cenozoic Epeirogeny in the Western Cordillera: Geological Society of America Bulletin, v. 103, pp. 1395-1404.

Urhammer, R. A., 1991. Northern California Seismicity: In Neotectonics of North America, D. B. Slemmons, E. R. Engdahl, M. D. Zoback, and D. D. Blackwell (editors), Geological Society of America, pp. 99-106.

Wallace, R. E., 1990. The San Andreas Fault System, California, U. S. Geological Survey Professional Paper 1515, 283 p.

Wells, D. L., and Coppersmith, K. J., 1994. Updated Empirical Relationships Among Magnitude, Rupture Length, Rupture Area, and Surface Displacement: Seismological Society of America Bulletin, v. 84, pp. 974-1002.

William Lettis and Associates, Inc., 1994. Seismotectonic Evaluation, New Hogan Dam, Calaveras County: Unpublished Report Prepared for U. S. Army Corps of Engineers, Sacramento District, 19 p.

Wong, et al., 1996.

Wong, I. G., 1996. Site-specific Probabilistic Seismic Hazard Analyses for the Idaho National Engineering Laboratory, Woodward-Clyde Report to Lockheed, May 1996, INEL-95/0536.

Wong, I. G., and Savage, W. U., 1983. Deep Intraplate Seismicity in the Western Sierra Nevada, Central California: Bulletin of the Seismological Society of America, Volume 73, No. 3, pp. 797-812.

Woodward-Clyde Consultants, 1977. Earthquake Evaluation Studies of the Auburn Dam Area; Report to U. S. Bureau of Reclamation, Contract No. 6/07/DS/72090, Auburn-Folsom South Unit, Central Valley Project, California, 8 Volumes.

Woodward-Clyde Consultants, 1978. Foothills Fault System Study, Volume 6, Stanislaus Nuclear Project, Site Suitability - Site Safety Report: Report to Pacific Gas and Electric Company, San Francisco, 166 p.

Woodward-Clyde Consultants, 1994. Seismic Evaluation of Southern California Bridges, Final Report to Caltrans, 59N771.

Youngs, R. R., and K. Coppersmith, 1985. Implications of Fault Slip Rates and Earthquake Recurrence Models to Probabilistic Seismic Hazard Estimates, Seismological Society of America Bulletin, v. 75, 939-964.

Stereoscopic Aerial Photography

Date	Scale	Flight/Frame	Source
6/16/71	1:20,000	2942-27/105-107	University of California, Berkeley
6/17/87	1:34,000	NAPP 461/90-93	U. S. Geological Survey
7/2/87	1:34,000	NAPP 476/49-51	U. S. Geological Survey
7/3/87	1:34,000	NAPP 478/171-174	U. S. Geological Survey
12/31/87	1:32,400	AV-3216-01/1-4	Pacific Aerial Surveys

9/14/95	1:40,000	#314-CIR4928-1/5-6	East Bay Municipal Water District
9/12/91	1:63,360	AV-4130-21/27-32	Pacific Aerial Surveys
7/22/92	1:63,360	AV-4130-22/27-30	Pacific Aerial Surveys
9/14/95	1:40,000	#314-CIR4928-1/5-6	East Bay Municipal Water District
4/4/96	1:7,200	AV 5125-1/1-6	East Bay Municipal Water District
4/4/96	1:7,200	AV 5125-2/1-12	East Bay Municipal Water District
4/4/96	1:7,200	AV 5125-3/1-8	East Bay Municipal Water District

APPENDIX A

Table A-1
SPECTRAL ACCELERATION(g) [1]
50TH PERCENTILE MCE
FAULT PARALLEL COMPONENT

Period (sec)	0.5%	1.0%	2.0%	3.0%	5.0%	7.0%	10.0%	15.0%	20.0%
0.01	0.580	0.580	0.580	0.580	0.580	0.580	0.580	0.580	0.580
0.02	0.580	0.580	0.580	0.580	0.580	0.580	0.580	0.580	0.580
0.03	0.637	0.624	0.607	0.597	0.580	0.568	0.555	0.538	0.526
0.05	1.005	0.958	0.899	0.860	0.806	0.768	0.725	0.675	0.638
0.075	1.388	1.294	1.181	1.108	1.009	0.940	0.866	0.781	0.721
0.10	1.701	1.563	1.398	1.293	1.154	1.059	0.959	0.845	0.766
0.12	1.898	1.727	1.525	1.397	1.232	1.120	1.002	0.871	0.780
0.15	2.073	1.875	1.642	1.496	1.306	1.181	1.049	0.902	0.803
0.17	2.146	1.933	1.683	1.528	1.327	1.194	1.055	0.903	0.799
0.2	2.164	1.949	1.697	1.541	1.339	1.204	1.064	0.910	0.806
0.24	2.086	1.878	1.637	1.485	1.290	1.160	1.025	0.878	0.777
0.3	1.952	1.758	1.532	1.390	1.207	1.086	0.960	0.821	0.727
0.4	1.660	1.494	1.301	1.181	1.026	0.923	0.816	0.698	0.618
0.5	1.365	1.229	1.071	0.972	0.844	0.759	0.671	0.574	0.509
0.75	0.913	0.823	0.716	0.650	0.565	0.508	0.449	0.384	0.340
1.0	0.637	0.576	0.504	0.459	0.400	0.361	0.321	0.276	0.245
1.5	0.347	0.315	0.278	0.254	0.224	0.204	0.182	0.158	0.142
2.0	0.219	0.201	0.178	0.164	0.146	0.133	0.120	0.105	0.095
3.0	0.112	0.103	0.092	0.086	0.078	0.071	0.065	0.058	0.053
4.0	0.066	0.062	0.056	0.053	0.048	0.045	0.041	0.037	0.034
5.0	0.041	0.039	0.036	0.034	0.031	0.029	0.027	0.025	0.023

(1) Does not include scale factor for extensional regimes.

Table A-2
SPECTRAL ACCELERATION(g) [1]
50TH PERCENTILE MCE
FAULT NORMAL COMPONENT

Period (sec)	0.5%	1.0%	2.0%	3.0%	5.0%	7.0%	10.0%	15.0%	20.0%
0.01	0.580	0.580	0.580	0.580	0.580	0.580	0.580	0.580	0.580
0.02	0.580	0.580	0.580	0.580	0.580	0.580	0.580	0.580	0.580
0.03	0.637	0.624	0.607	0.597	0.580	0.568	0.555	0.538	0.526
0.05	1.005	0.958	0.899	0.860	0.806	0.768	0.725	0.675	0.638
0.075	1.388	1.294	1.181	1.108	1.009	0.940	0.866	0.781	0.721
0.10	1.701	1.563	1.398	1.293	1.154	1.059	0.959	0.845	0.766
0.12	1.898	1.727	1.525	1.397	1.232	1.120	1.002	0.871	0.780
0.15	2.073	1.875	1.642	1.496	1.306	1.181	1.049	0.902	0.803
0.17	2.146	1.933	1.683	1.528	1.327	1.194	1.055	0.903	0.799
0.2	2.164	1.949	1.697	1.541	1.339	1.204	1.064	0.910	0.806
0.24	2.086	1.878	1.637	1.485	1.290	1.160	1.025	0.878	0.777
0.3	1.952	1.758	1.532	1.390	1.207	1.086	0.960	0.821	0.727
0.4	1.660	1.494	1.301	1.181	1.026	0.923	0.816	0.698	0.618
0.5	1.365	1.229	1.071	0.972	0.844	0.759	0.671	0.574	0.509
0.75	0.999	0.900	0.783	0.711	0.618	0.556	0.491	0.420	0.372
1.0	0.728	0.658	0.576	0.525	0.457	0.413	0.367	0.315	0.280
1.5	0.417	0.379	0.335	0.306	0.270	0.245	0.219	0.190	0.171
2.0	0.275	0.251	0.224	0.206	0.182	0.167	0.150	0.131	0.119
3.0	0.151	0.140	0.125	0.117	0.105	0.097	0.088	0.078	0.071
4.0	0.095	0.089	0.081	0.076	0.069	0.064	0.059	0.053	0.049
5.0	0.061	0.058	0.053	0.050	0.046	0.043	0.040	0.037	0.034

(1) Does not include scale factor for extensional regimes.

Table A-3
SPECTRAL ACCELERATION(g) [1]
50TH PERCENTILE MCE
VERTICAL COMPONENT

Period (sec)	0.5%	1.0%	2.0%	3.0%	5.0%	7.0%	10.0%	15.0%	20.0%
0.01	0.631	0.631	0.631	0.631	0.631	0.631	0.631	0.631	0.631
0.02	0.631	0.631	0.631	0.631	0.631	0.631	0.631	0.631	0.631
0.03	0.811	0.768	0.714	0.679	0.631	0.598	0.563	0.523	0.493
0.05	1.816	1.656	1.465	1.345	1.191	1.090	0.984	0.867	0.787
0.075	2.323	2.080	1.796	1.622	1.401	1.258	1.113	0.957	0.852
0.10	2.467	2.176	1.844	1.642	1.391	1.232	1.073	0.903	0.792
0.12	2.354	2.069	1.746	1.550	1.307	1.155	1.001	0.840	0.733
0.15	2.096	1.840	1.548	1.372	1.154	1.018	0.881	0.737	0.643
0.17	1.908	1.676	1.412	1.253	1.055	0.932	0.808	0.676	0.590
0.2	1.666	1.468	1.242	1.105	0.935	0.828	0.720	0.605	0.530
0.24	1.399	1.239	1.056	0.944	0.804	0.715	0.625	0.529	0.466
0.3	1.164	1.029	0.873	0.779	0.662	0.587	0.512	0.432	0.380
0.4	0.904	0.800	0.682	0.609	0.519	0.462	0.404	0.342	0.300
0.5	0.743	0.658	0.561	0.501	0.426	0.380	0.332	0.281	0.248
0.75	0.518	0.458	0.391	0.349	0.297	0.265	0.231	0.196	0.173
1.0	0.366	0.325	0.278	0.250	0.214	0.191	0.168	0.143	0.126
1.5	0.223	0.200	0.173	0.156	0.135	0.121	0.108	0.093	0.083
2.0	0.150	0.136	0.118	0.108	0.094	0.085	0.077	0.067	0.060
3.0	0.080	0.074	0.066	0.060	0.053	0.049	0.044	0.039	0.036
4.0	0.047	0.043	0.039	0.036	0.033	0.030	0.028	0.025	0.023
5.0	0.030	0.028	0.026	0.024	0.022	0.020	0.019	0.018	0.016

(1) Does not include scale factor for extensional regimes.

Table A-4
SPECTRAL ACCELERATION(g) [1]
50TH PERCENTILE MCE
FAULT PARALLEL COMPONENT

Period (sec)	0.5%	1.0%	2.0%	3.0%	5.0%	7.0%	10.0%	15.0%	20.0%
0.01	0.406	0.406	0.406	0.406	0.406	0.406	0.406	0.406	0.406
0.02	0.406	0.406	0.406	0.406	0.406	0.406	0.406	0.406	0.406
0.03	0.446	0.437	0.425	0.418	0.406	0.398	0.388	0.377	0.368
0.05	0.704	0.671	0.629	0.602	0.564	0.537	0.508	0.473	0.447
0.075	0.972	0.906	0.827	0.776	0.706	0.658	0.606	0.547	0.505
0.10	1.191	1.094	0.979	0.905	0.808	0.741	0.671	0.592	0.536
0.12	1.328	1.209	1.068	0.978	0.862	0.784	0.701	0.609	0.546
0.15	1.451	1.312	1.149	1.047	0.914	0.826	0.734	0.631	0.562
0.17	1.502	1.353	1.178	1.069	0.929	0.836	0.739	0.632	0.559
0.2	1.515	1.364	1.188	1.078	0.937	0.843	0.745	0.637	0.564
0.24	1.460	1.314	1.146	1.039	0.903	0.812	0.718	0.614	0.544
0.3	1.367	1.231	1.072	0.973	0.845	0.760	0.672	0.575	0.509
0.4	1.162	1.046	0.911	0.827	0.718	0.646	0.571	0.489	0.433
0.5	0.956	0.860	0.750	0.680	0.591	0.531	0.470	0.402	0.356
0.75	0.730	0.657	0.572	0.520	0.452	0.406	0.359	0.307	0.272
1.0	0.561	0.507	0.444	0.404	0.352	0.318	0.282	0.243	0.216
1.5	0.305	0.277	0.245	0.224	0.197	0.179	0.160	0.139	0.125
2.0	0.193	0.177	0.157	0.145	0.128	0.117	0.105	0.092	0.084
3.0	0.098	0.091	0.081	0.076	0.068	0.063	0.057	0.051	0.046
4.0	0.058	0.054	0.050	0.046	0.042	0.039	0.036	0.033	0.030
5.0	0.036	0.034	0.031	0.030	0.027	0.026	0.024	0.022	0.020

(1) Includes scale factor for extensional regimes.

Table A-5
SPECTRAL ACCELERATION(g) [1]
50TH PERCENTILE MCE
FAULT NORMAL COMPONENT

Period (sec)	0.5%	1.0%	2.0%	3.0%	5.0%	7.0%	10.0%	15.0%	20.0%
0.01	0.406	0.406	0.406	0.406	0.406	0.406	0.406	0.406	0.406
0.02	0.406	0.406	0.406	0.406	0.406	0.406	0.406	0.406	0.406
0.03	0.446	0.437	0.425	0.418	0.406	0.398	0.388	0.377	0.368
0.05	0.704	0.671	0.629	0.602	0.564	0.537	0.508	0.473	0.447
0.075	0.972	0.906	0.827	0.776	0.706	0.658	0.606	0.547	0.505
0.10	1.191	1.094	0.979	0.905	0.808	0.741	0.671	0.592	0.536
0.12	1.328	1.209	1.068	0.978	0.862	0.784	0.701	0.609	0.546
0.15	1.451	1.312	1.149	1.047	0.914	0.826	0.734	0.631	0.562
0.17	1.502	1.353	1.178	1.069	0.929	0.836	0.739	0.632	0.559
0.2	1.515	1.364	1.188	1.078	0.937	0.843	0.745	0.637	0.564
0.24	1.460	1.314	1.146	1.039	0.903	0.812	0.718	0.614	0.544
0.3	1.367	1.231	1.072	0.973	0.845	0.760	0.672	0.575	0.509
0.4	1.162	1.046	0.911	0.827	0.718	0.646	0.571	0.489	0.433
0.5	0.956	0.860	0.750	0.680	0.591	0.531	0.470	0.402	0.356
0.75	0.798	0.719	0.626	0.568	0.494	0.444	0.392	0.336	0.297
1.0	0.642	0.580	0.508	0.462	0.403	0.364	0.323	0.278	0.247
1.5	0.368	0.334	0.295	0.270	0.238	0.216	0.193	0.168	0.150
2.0	0.242	0.222	0.197	0.181	0.161	0.147	0.132	0.116	0.105
3.0	0.133	0.123	0.110	0.103	0.093	0.085	0.078	0.069	0.063
4.0	0.083	0.078	0.071	0.067	0.061	0.057	0.052	0.047	0.043
5.0	0.054	0.051	0.046	0.044	0.040	0.038	0.035	0.032	0.030

(1) Includes scale factor for extensional regimes.

Table A-6
SPECTRAL ACCELERATION(g) [1]
50TH PERCENTILE MCE
VERTICAL COMPONENT

Period (sec)	0.5%	1.0%	2.0%	3.0%	5.0%	7.0%	10.0%	15.0%	20.0%
0.01	0.528	0.528	0.528	0.528	0.528	0.528	0.528	0.528	0.528
0.02	0.528	0.528	0.528	0.528	0.528	0.528	0.528	0.528	0.528
0.03	0.679	0.642	0.597	0.568	0.528	0.501	0.471	0.438	0.413
0.05	1.519	1.385	1.226	1.126	0.997	0.912	0.823	0.725	0.658
0.075	1.944	1.740	1.502	1.357	1.172	1.053	0.931	0.800	0.713
0.10	2.064	1.821	1.542	1.374	1.163	1.031	0.898	0.755	0.663
0.12	2.058	1.810	1.527	1.355	1.143	1.010	0.876	0.734	0.641
0.15	1.937	1.700	1.430	1.268	1.067	0.941	0.815	0.681	0.594
0.17	1.811	1.591	1.340	1.189	1.002	0.885	0.767	0.642	0.560
0.2	1.633	1.438	1.217	1.083	0.916	0.811	0.705	0.593	0.520
0.24	1.460	1.314	1.146	1.039	0.903	0.812	0.718	0.614	0.544
0.3	1.233	1.090	0.925	0.826	0.701	0.622	0.543	0.458	0.403
0.4	1.017	0.900	0.767	0.686	0.584	0.520	0.454	0.385	0.338
0.5	0.869	0.769	0.656	0.586	0.499	0.444	0.388	0.328	0.290
0.75	0.649	0.573	0.489	0.437	0.372	0.331	0.289	0.245	0.216
1.0	0.458	0.407	0.349	0.313	0.268	0.239	0.210	0.179	0.158
1.5	0.280	0.251	0.217	0.195	0.170	0.152	0.135	0.116	0.104
2.0	0.188	0.171	0.148	0.136	0.118	0.107	0.096	0.083	0.075
3.0	0.100	0.092	0.082	0.075	0.066	0.061	0.055	0.048	0.045
4.0	0.059	0.054	0.049	0.046	0.041	0.038	0.035	0.032	0.029
5.0	0.038	0.035	0.032	0.030	0.028	0.025	0.024	0.022	0.020

(1) Includes scale factor for extensional regimes.

APPENDIX B

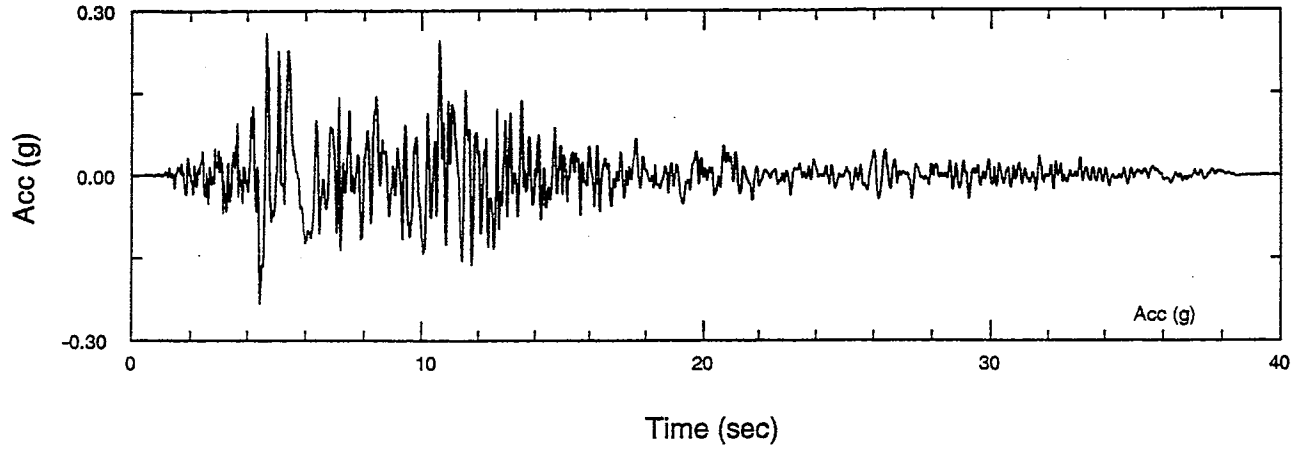

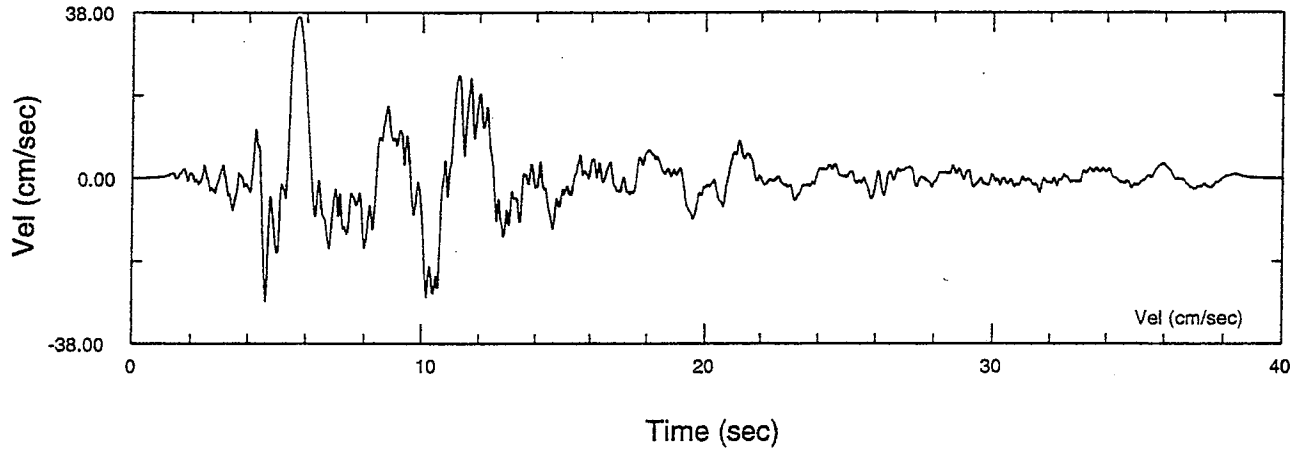

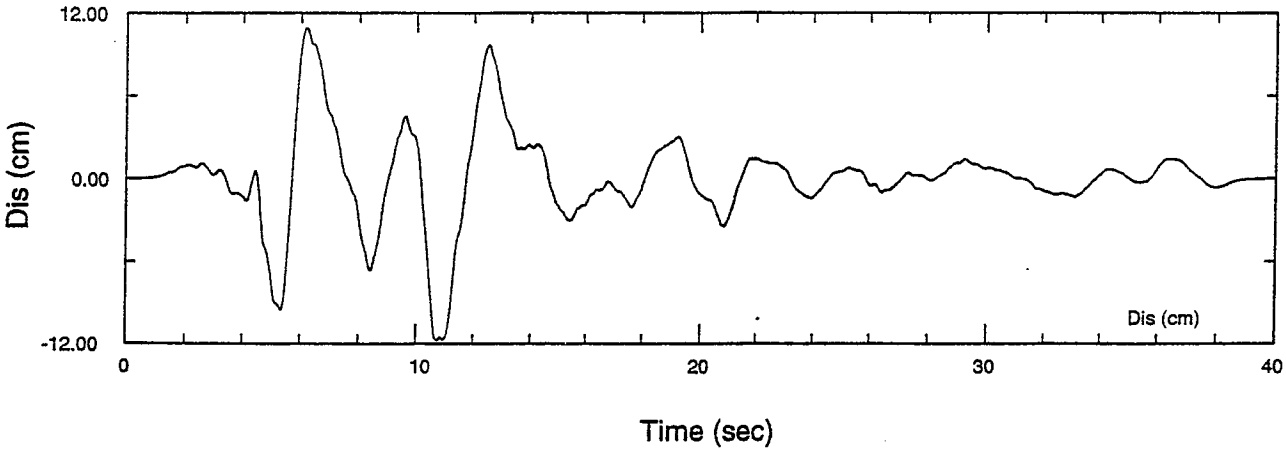

HCG

Pardee Project Team

HDR Engineering Inc.
Christensen Associates Inc.
GEI Consultants Inc.

Pardee Reservoir Enlargement Project

TIME HISTORY, HORIZONTAL COMPONENT 000, STURNO RECORD

VOLUME		**Exhibit B-1.1**	
SCALE			
DATE	Dec. 1997		REV.

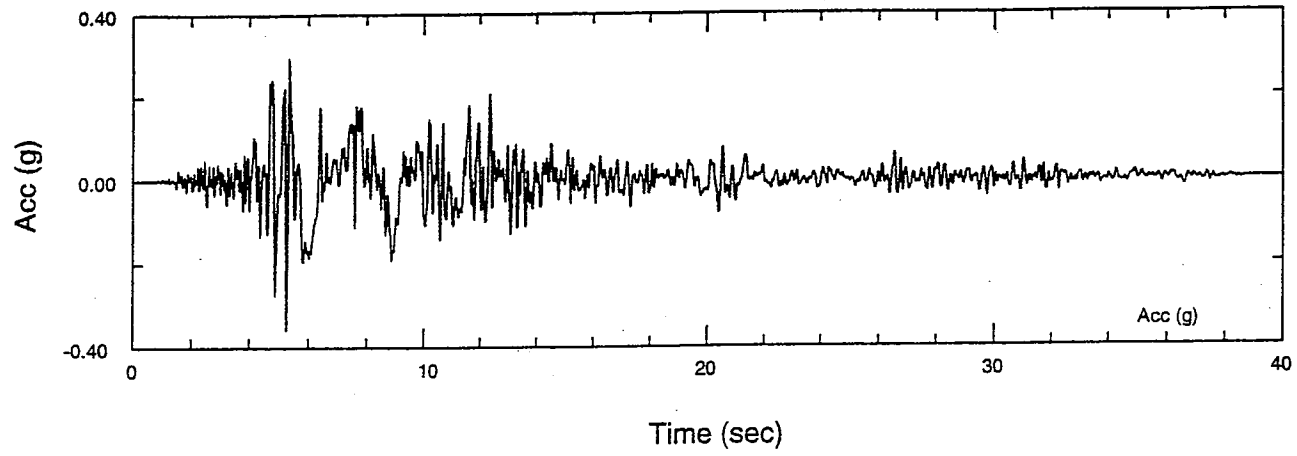

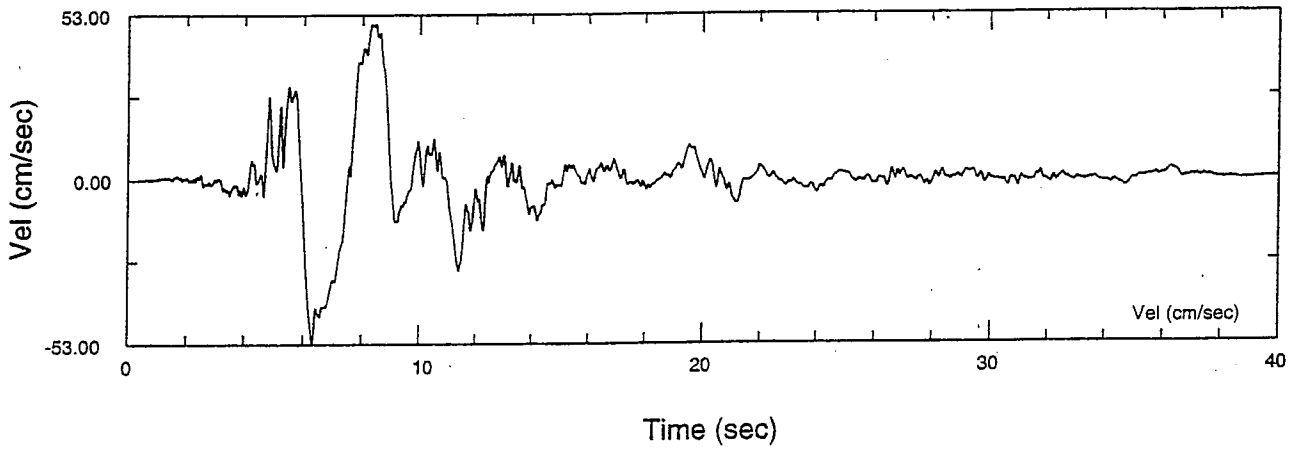

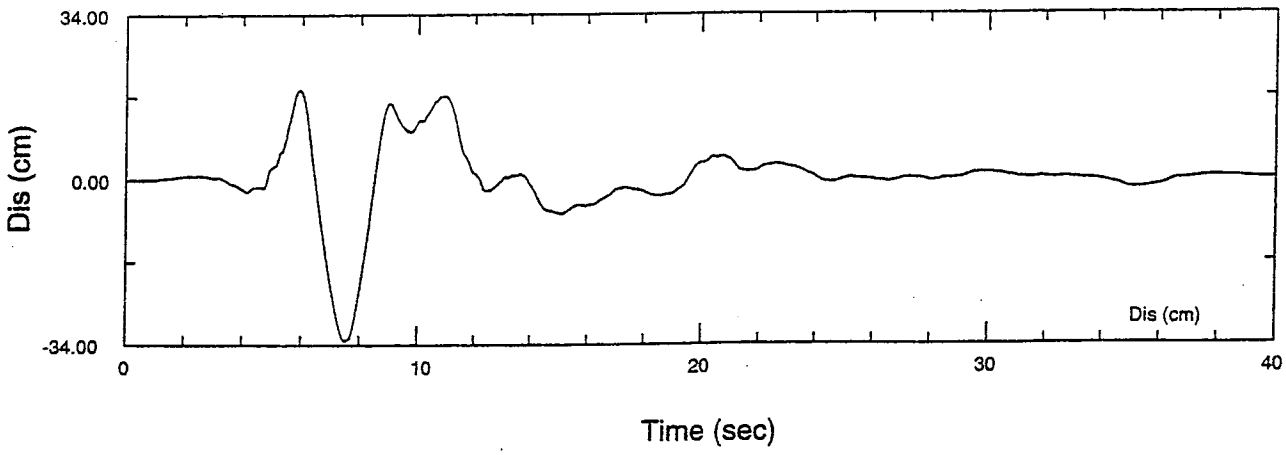

HCG
Pardee Project Team
HDR Engineering Inc.
Christensen Associates Inc.
[OZ] Consultants Inc.

Pardee Reservoir Enlargement Project
TIME HISTORY,
HORIZONTAL COMPONENT 270,
STURNO RECORD

VOLUME		
SCALE	Exhibit B-1.2	
DATE Dec. 1997		REV.

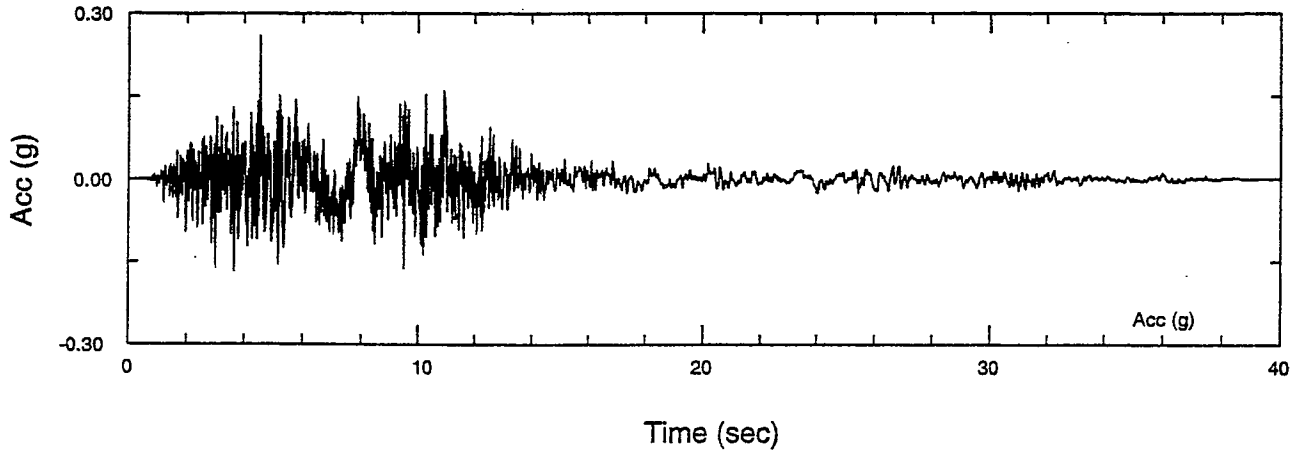

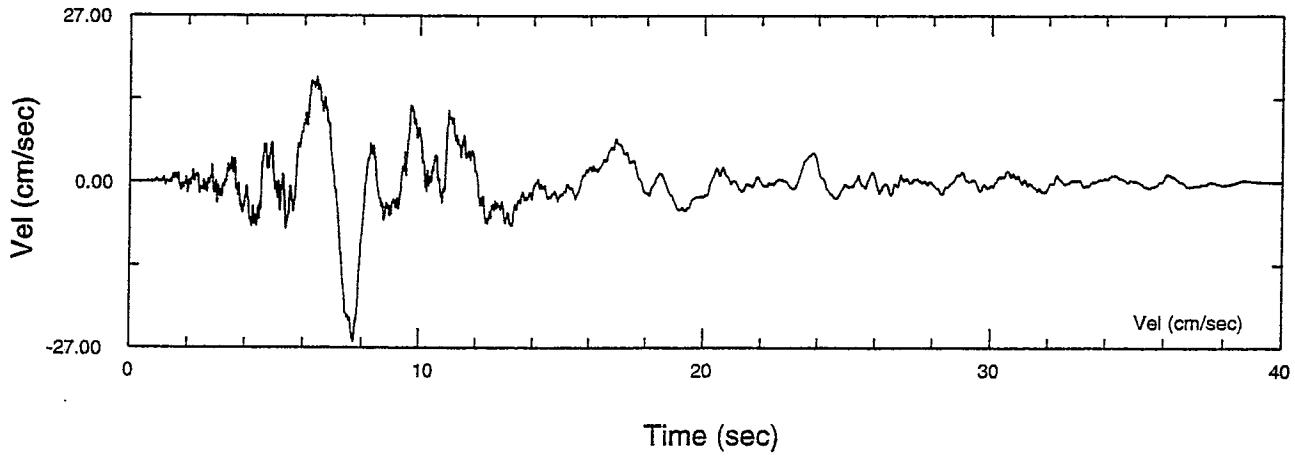

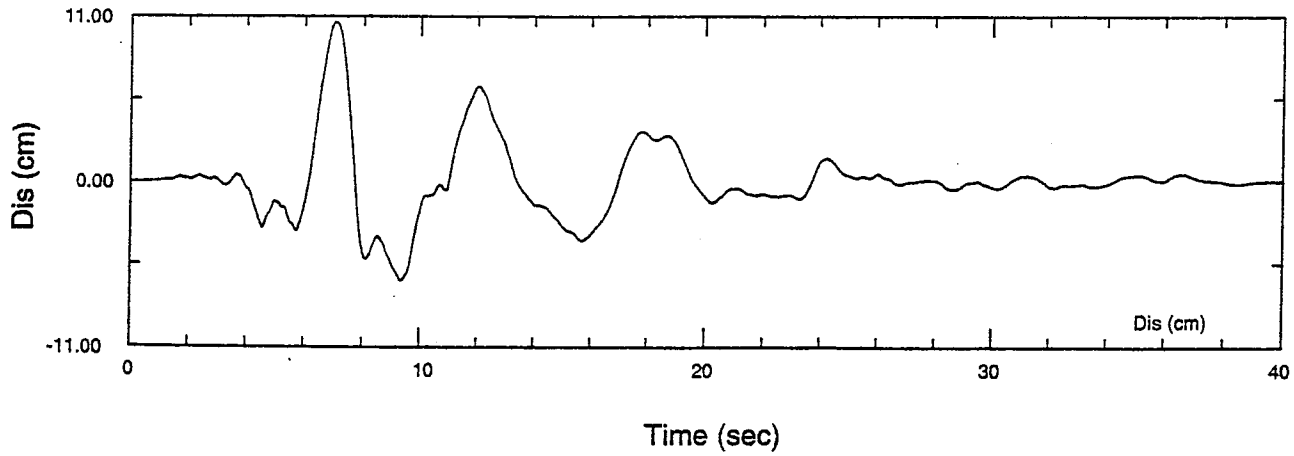

HCG
Pardee Project Team
HDR Engineering Inc.
Christiansen Associates Inc.
GEI Consultants Inc.

Pardee Reservoir Enlargement Project
TIME HISTORY,
VERTICAL,
STURNO RECORD

VOLUME		
SCALE		**Exhibit B-1.3**
DATE	Dec. 1997	REV.

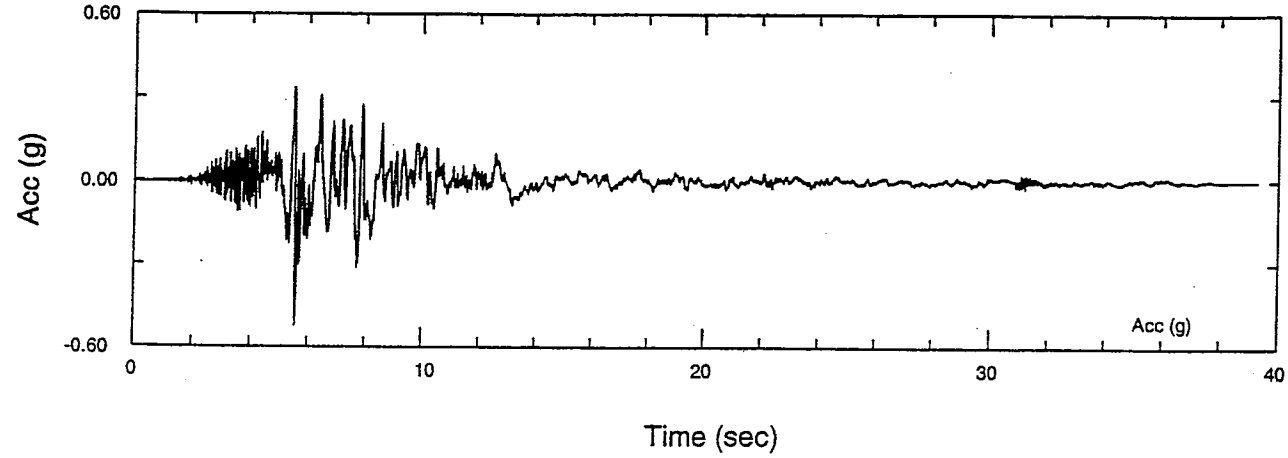

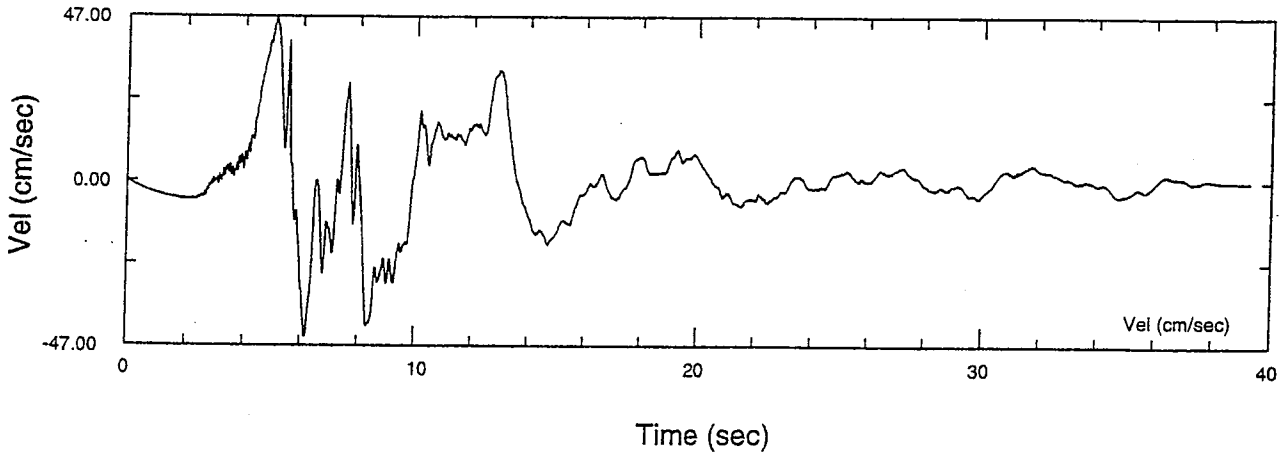

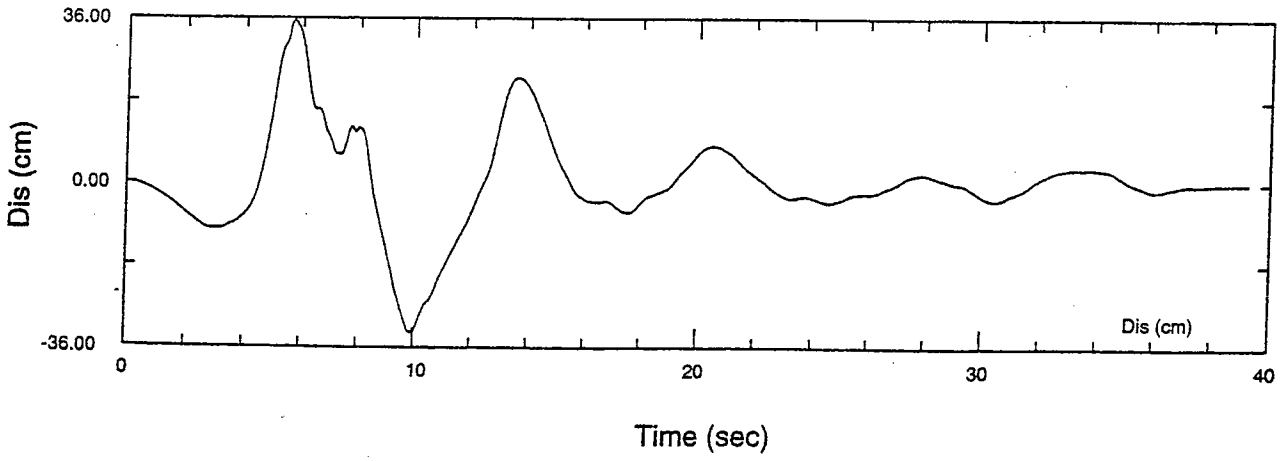

HCG

Pardee Project Team

HDR Engineering Inc.
Christensen Associates Inc.
GEI Consultants Inc.

Pardee Reservoir Enlargement Project
TIME HISTORY,
HORIZONTAL COMPONENT 140,
EL CENTRO RECORD

VOLUME		
SCALE		Exhibit B-2.1
DATE	Dec. 1997	REV.

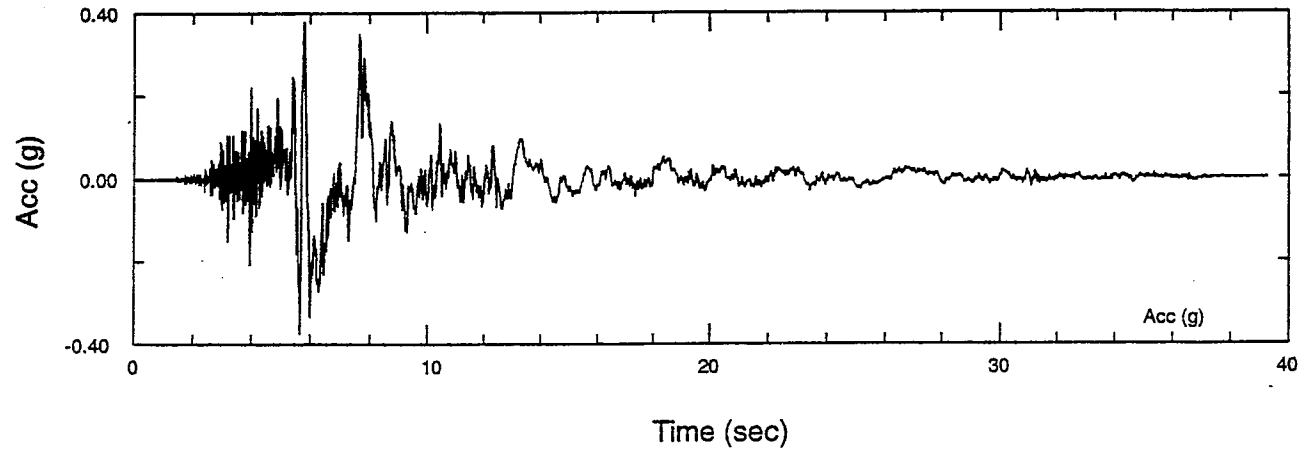

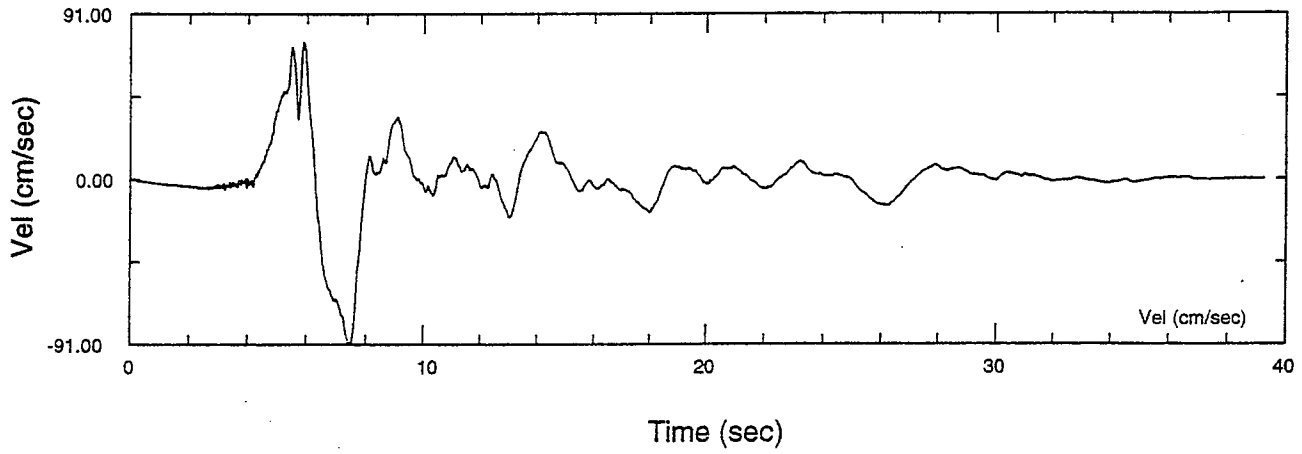

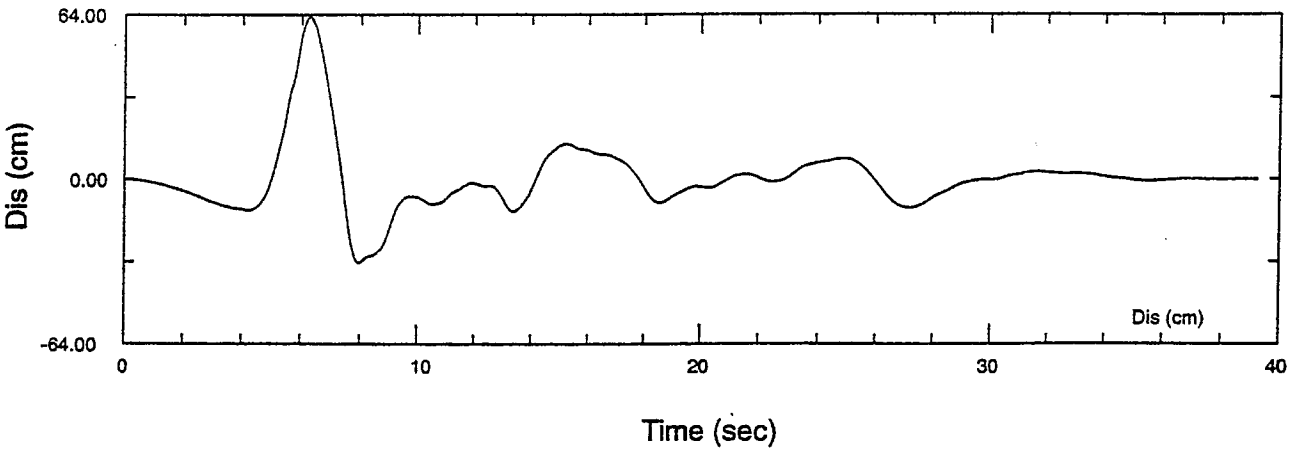

HCG
Pardee Project Team
HDR Engineering Inc.
Christensen Associates Inc.
MOH Consultants Inc.

Pardee Reservoir Enlargement Project
TIME HISTORY,
HORIZONTAL COMPONENT 230,
EL CENTRO RECORD

VOLUME
SCALE
DATE Dec. 1997

Exhibit B-2.2

REV.

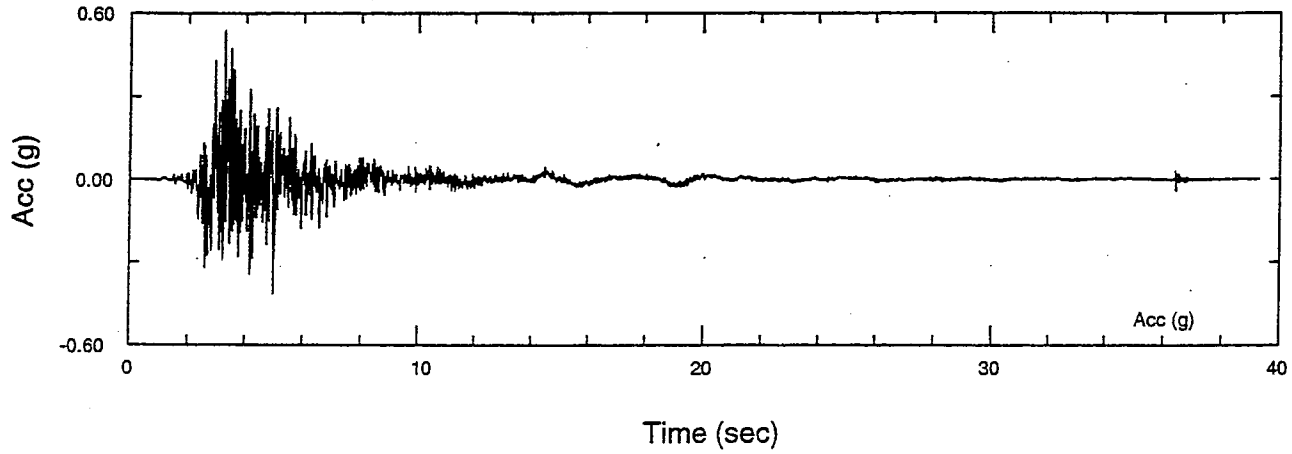

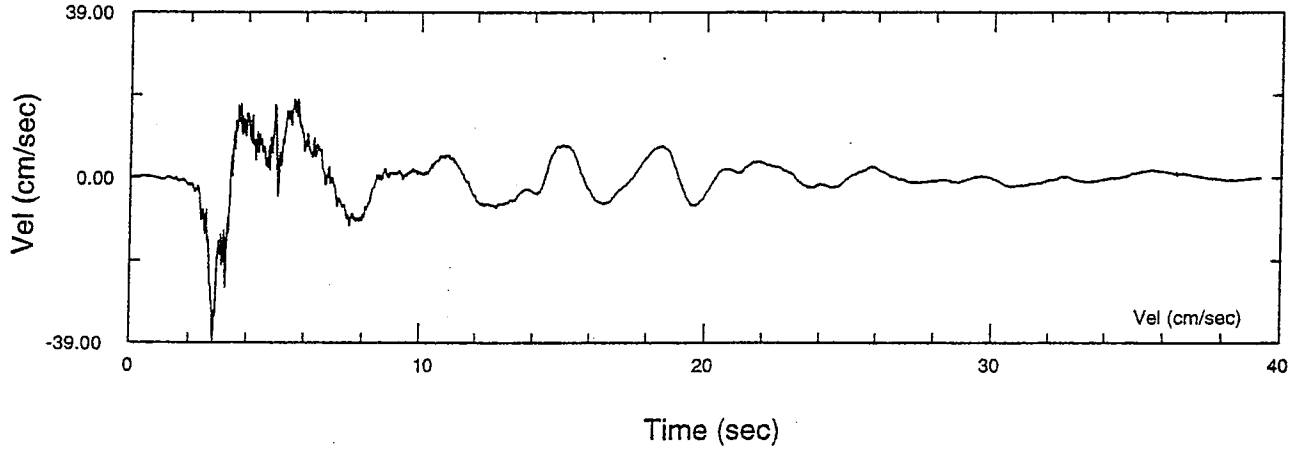

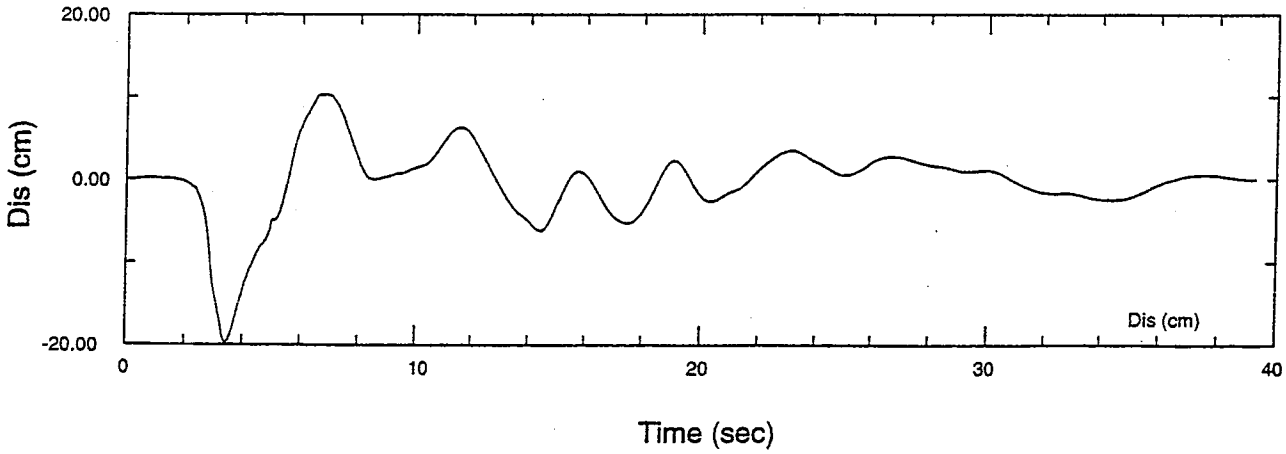

HCG
Pardee Project Team
RDR Engineering Inc.
Christensen Associates Inc.
GEI Consultants Inc.

Pardee Reservoir Enlargement Project

TIME HISTORY,
VERTICAL,
EL CENTRO RECORD

VOLUME
SCALE
DATE Dec. 1997

Exhibit B-2.3

REV.

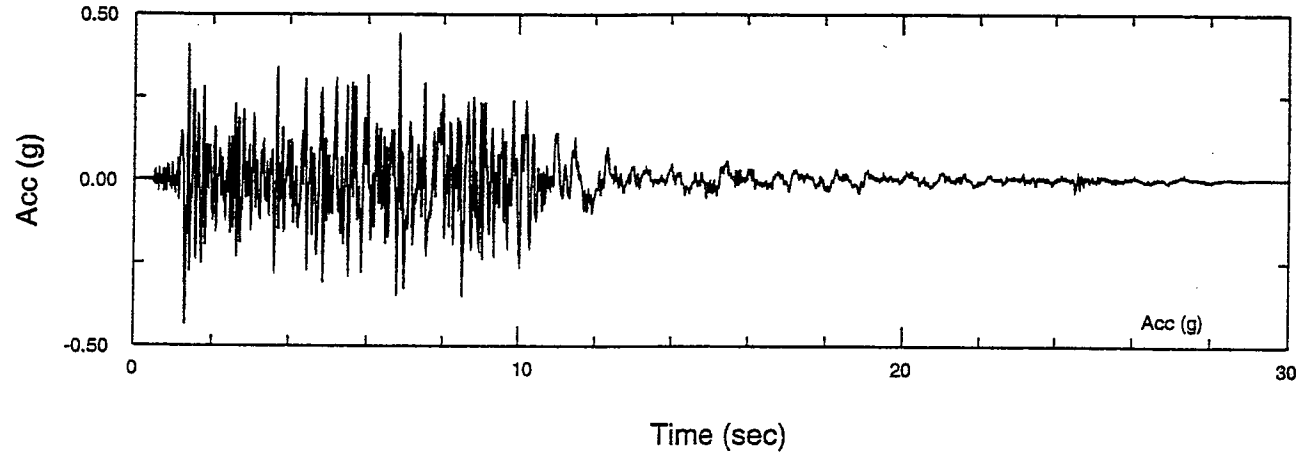

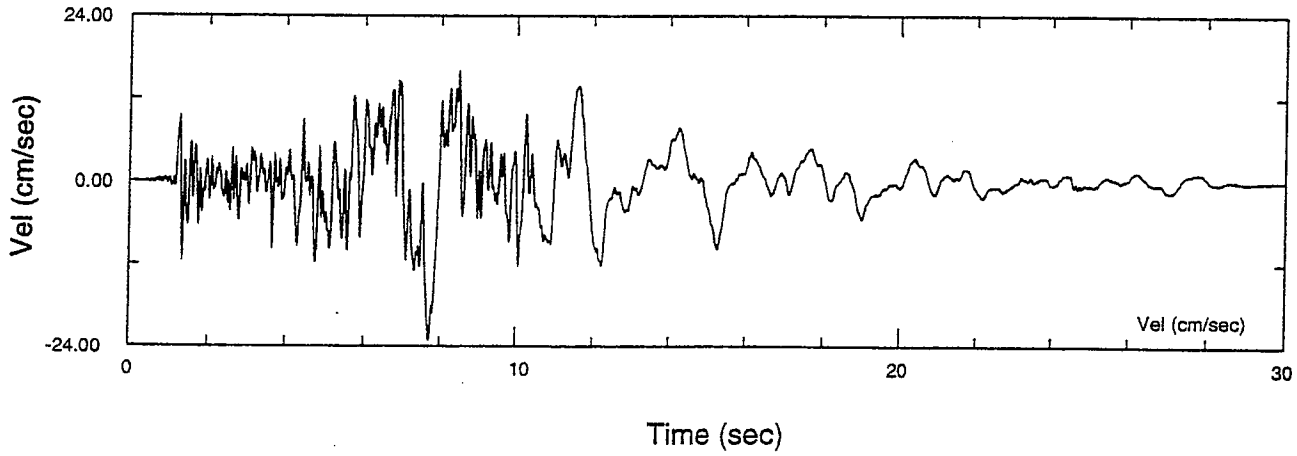

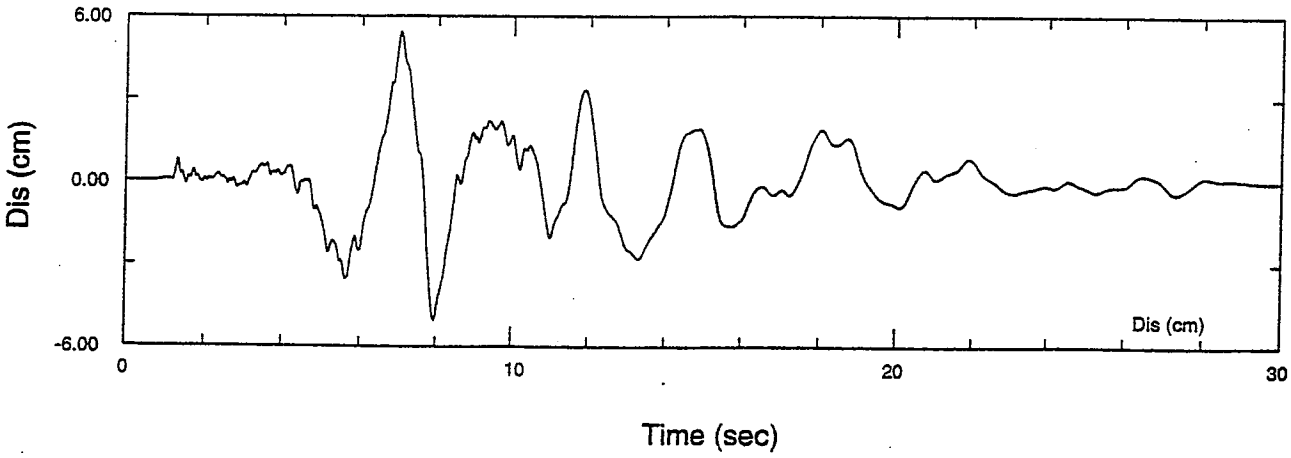

HCG

Pardee Project Team

HDR Engineering Inc.
Christensen Associates Inc.
GEI Consultants Inc.

Pardee Reservoir Enlargement Project
TIME HISTORY,
HORIZONTAL COMPONENT 180,
CONVICT CREEK RECORD

VOLUME		
SCALE		Exhibit B-3.1
DATE	Dec. 1997	REV.

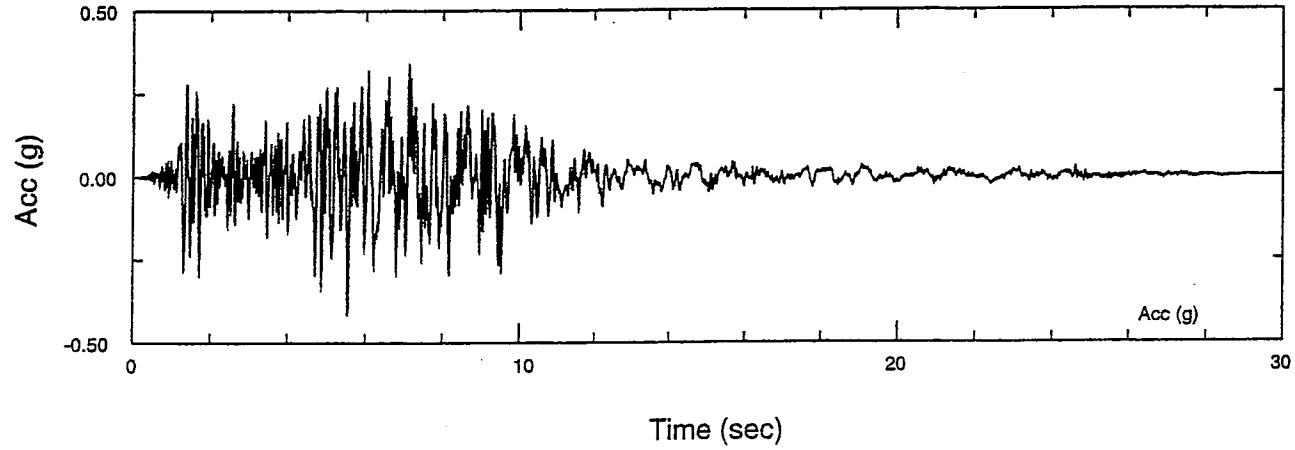

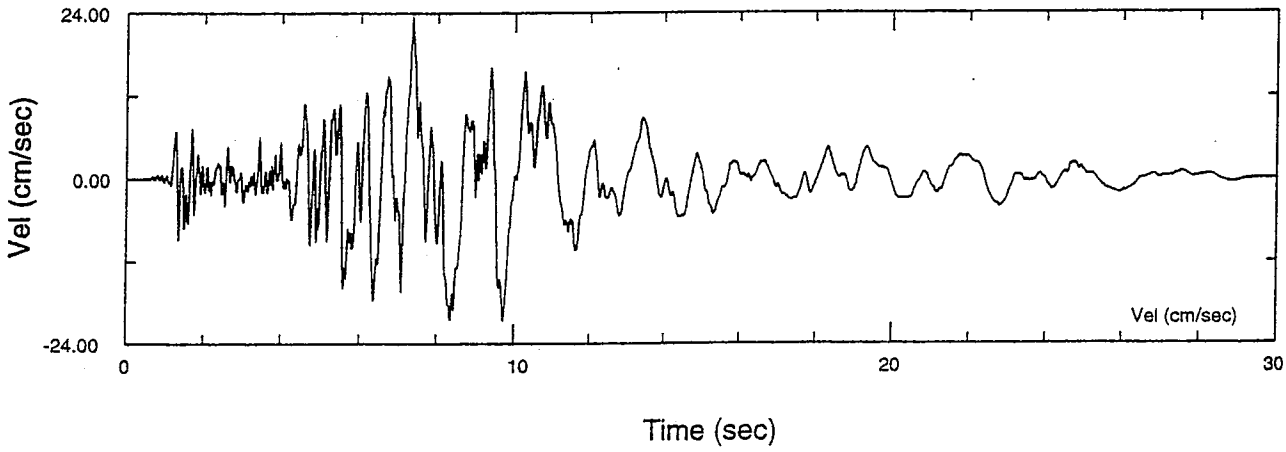

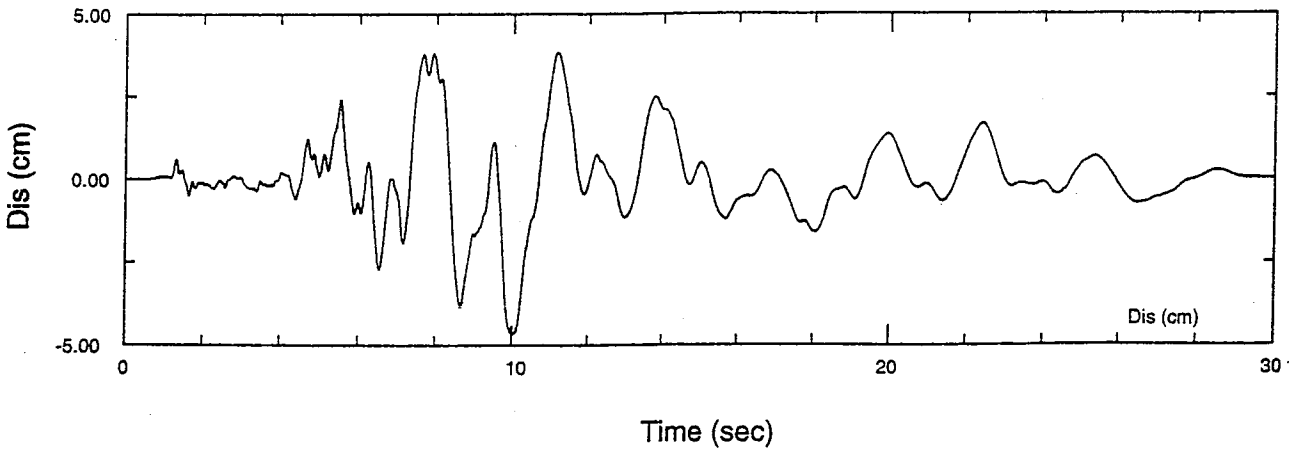

HCG

Pardee Project Team

HDR Engineering Inc.
Christensen Associates Inc.
GEI Consultants Inc.

Pardee Reservoir Enlargement Project
TIME HISTORY,
HORIZONTAL COMPONENT 090,
CONVICT CREEK RECORD

VOLUME		
SCALE		**Exhibit B-3.2**
DATE	Dec. 1997	REV.

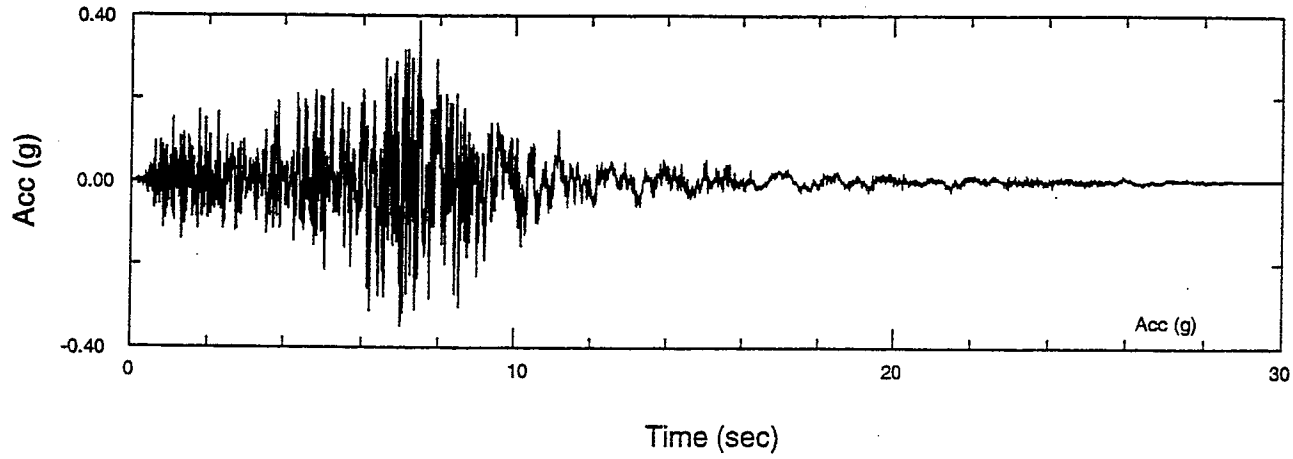

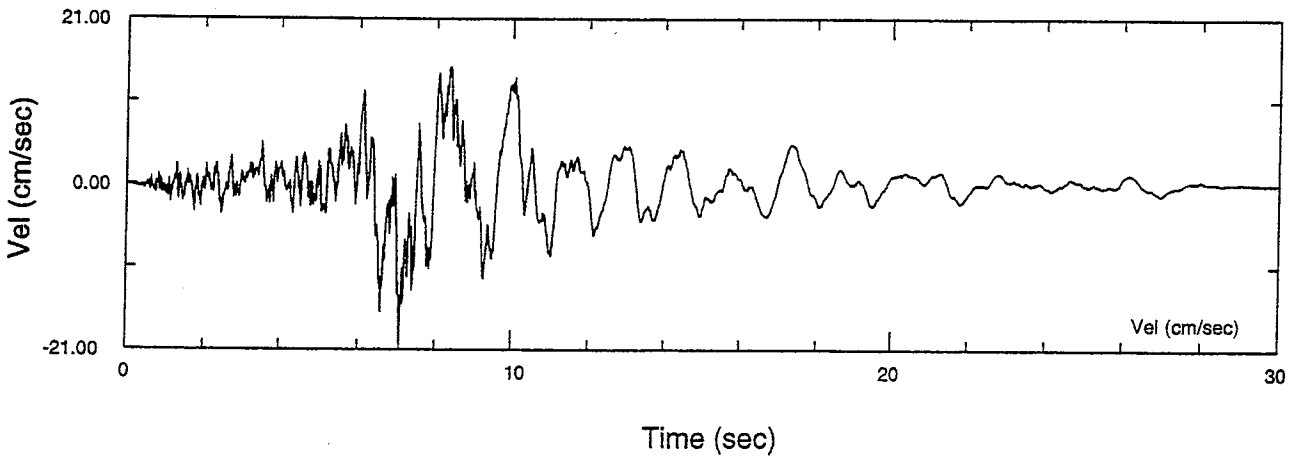

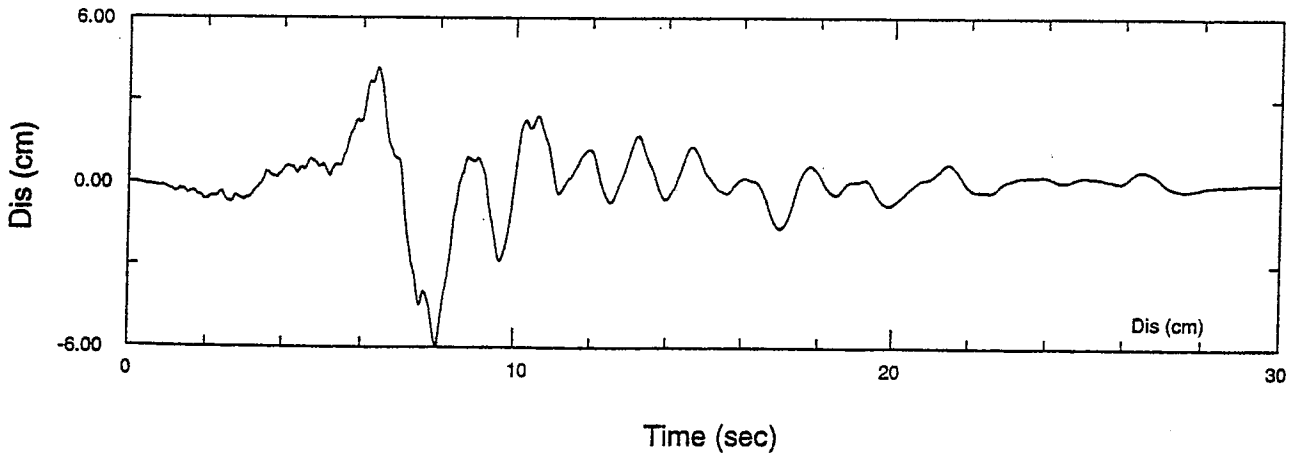

HCG

Pardee Project Team

HDR Engineering Inc.
Christensen Associates Inc.
GEI Consultants Inc.

Pardee Reservoir Enlargement Project

**TIME HISTORY,
VERTICAL,
CONVICT CREEK RECORD**

VOLUME		
SCALE	Exhibit B-3.3	
DATE Dec. 1997		REV.

APPENDIX C

PROBABILISTIC SEISMIC HAZARD ANALYSIS METHODOLOGY

Appendix C

Probabilistic Seismic Hazard Analysis Methodology

Mathematical Formulation

The probabilistic seismic hazard analysis follows the standard approach developed by Cornell (1968). The main changes from the original work are that more parameters are randomized (i.e., a more complete description of the aleatory variables) and epistemic uncertainty is considered. The basic methodology involves computing how often a specified level of ground motion will be exceeded at the site. The hazard analysis computes the annual number of events that produce a ground motion parameter, A, that exceeds a specified level, z. This number of events per year, ν, is also called the "annual frequency of exceedance". The inverse of ν is called the "return period".

The calculation of the annual frequency of exceedance, ν, involves several probability distributions for each seismic source: the frequency of occurrence of earthquakes of various magnitudes, the rupture dimension and location of the earthquakes, and the attenuation of the ground motion from the earthquake rupture to the site. The occurrence rates of the earthquakes of various magnitudes are determined by the magnitude recurrence relations. The location of the earthquake depends on the geometry of the seismic source relative to the site locations. The ground motion at the site is estimated from the attenuation relation.

If we assume that an earthquake with magnitude greater than m_L has occurred on the i^{th} seismic source, then the probability that the ground motion at the site exceeds the test level z, is given by

$$P_i(A>z|E_i) = \int_{r=0}^{\infty} \int_{m=M^L}^{M^U} f_m(m)\, f_r(r)\, P(A>z|m,r)\, dm\, dr \qquad (1)$$

where $E_i(m^L)$ indicates that an event with m^3m^L has occurred on the i^{th} source, m is magnitude, r is the closest distance measure, m^U is the maximum magnitude (for the i^{th} source), $f_m(m)$, and $f_r(r)$ are probability density functions for the magnitude, and closest distance, and $P(A>z|m,r)$ is the probability that the ground motion exceeds the test level z for magnitude m and closest distance r.

For point source models, the density function for closest distance, $f_r(r)$, is simple to compute; the hypocenters are uniformly distributed over the seismic source. For planar sources (e.g., known faults), we need to consider the finite dimension and location of the rupture in order to compute the closest distance. Specifically, we need to randomize the rupture length, rupture width, hypocenter location along strike, and hypocenter location down dip. (Since rupture width and length are correlated, it is easier to consider the rupture area and rupture width and then back calculate the rupture length.) For planar sources Eq (1) becomes

$$P_i(A>z|E_i) = \int_{W=0}^{\infty} \int_{RA=0}^{\infty} \int_{hx=0}^{1} \int_{hy=0}^{1} \int_{m=M^L}^{M^U} f_m(m)\, f_{RA}(m)\, f_{RW}(m)\, f_{hx}(h_x)\, f_{hy}(h_y)$$
$$P(A>z|m,r(h_x,h_y,RA,W))\, dm\, dh_x\, dh_y\, dRA\, dW \qquad (2)$$

where $f_{RW}(m)$, $f_{RA}(m)$, f_{hX}, f_{hY} are probability density functions for the rupture width, rupture area, hypocenter location (along strike and down dip), respectively. In Eq. (2), h_X and h_Y give the location of the energy center (hypocenter for small events) in terms of the fraction of the fault length and fault width, respectively (e.g. h_X=0 is one end of the fault and h_X=1.0 is the other end of the fault).

The annual rate of events that produce ground motions that exceed z at the site is the product of the probability given in Eq (2) and the annual rate of events with magnitude greater than M^L on the i^{th} source.

$$\nu_i(A>z) = N_i(m_L)P_i(A>z|E_i) \tag{3}$$

where $N_i(m^L)$ is the annual number of events with magnitude greater than m^L on the i^{th} source (e.g. the number of events from the magnitude recurrence relation).

For multiple seismic sources, the total annual rate of events with ground motions that exceed z at the site is just the sum of the annual rate of events from the individual sources (assuming that the sources are independent).

$$\nu(A>z) = \sum_{i=1}^{N_{source}} \nu_i(A>z) \tag{4}$$

The annual rate of events given in Eq (4) is not probability; it can exceed 1. To convert the annual rate of events to a probability, we consider the probability that the ground motion exceeds test level z at least once during a specified time interval.

At this step, a standard assumption is that the occurrence of earthquakes is a Poisson process. That is, there is no memory of past earthquakes, so the chance of an earthquake occurring in a given year does not depend on how long it has been since the last earthquake. If the occurrence of earthquakes is a Poisson process then the occurrence of peak ground motions is also a Poisson process. For a Poisson process, the probability of an event (e.g. ground motion exceeding z) occurring n times in time interval t is given by

$$p_n(t) = \exp(-\nu t)\,(\nu t)^n/n! \qquad (5)$$

The probability that at least one event occurs (e.g. $n^3 1$) is 1 minus the probability that no events occur:

$$P(n^3 1, t) = 1 - p_o(t) = 1 - \exp(-\nu t) \qquad (6)$$

So the probability of at least one occurrence of ground motion level z in t years is given by

$$P(A>z,t) = 1 - \exp(-\nu(A>z)t) \qquad (7)$$

For t=1 year, this probability is the annual hazard.

The basic part of the hazard calculation is computing the integral in Eq (2). All of the aleatory variables are inside of the hazard integral (Eq 2). The randomness of the seismic source variables is characterized by the probability density functions which are discussed below. The randomness of the attenuation relation is accounted for in the probability of exceeding the ground motion, z, for a given magnitude and closest distance (the last term in Eq 2).

Epistemic (scientific) uncertainty is considered by using alternative models and/or parameter values for the probability density functions (primarily $f_m(m)$), attenuation relation, and activity rate (usually slip rate). For each alternative model, we recalculate the hazard and compute alternative hazard curves. Epistemic uncertainty is typically handled using a logic tree approach for specifying the alternative models for the density function, attenuation relation, and activity rates.

Magnitude Recurrence Relations

The magnitude recurrence relation tells how often each magnitude earthquake is expected to occur. In this formulation, it is more convenient to separate the magnitude recurrence relation into an activity rate and a magnitude density function.

Activity Rate

There are two approaches to estimating the fault activity rate: historical seismicity and geologic (and geodetic) information.

If historical seismicity catalogs are used to estimate the activity rate, then the estimate of $N(m^L)$ is usually based on fitting the truncated exponential model (discussed below) to the historical data. Maximum likelihood procedures are generally preferred over least-squares for estimating the activity rate and the b-value.

When using geologic information on slip-rates of faults, the activity rate is computed by balancing the energy build-up estimated from geologic evidence with the total energy release of earthquakes. Knowing the dimension of the fault, the slip-rate, and the rigidity of the fault, we can balance the long term seismic moment so that the fault is in equilibrium. (e.g., Youngs and Coppersmith, 1985).

The seismic energy release is balanced by requiring the build up of seismic moment to be equal to the release of seismic moment in earthquakes. The build up of seismic moment is computed from the long term slip-rate. The seismic moment, M_o (in dyne cm), is given by

$$M_o = \mu A D \qquad (8)$$

where μ is the rigidity of the crust (in dyne/cm^2), A is the area of the fault (in cm^2), and D is the average displacement (slip) on the fault surface (in cm). The annual rate of build up of seismic moment is given by

$$\frac{dM_o}{dt} = \mu A S \tag{9}$$

where S is the slip-rate in cm/year. The seismic moment released during an earthquake is given by

$$\log_{10} Mo = 1.5 M + 16.05 \tag{10}$$

where M is the moment magnitude of the earthquake.

To balance the moment build up and the moment release, the annual moment rate from the slip-rate is set equal to the sum of the moment released in all of the earthquakes that are expected to occur each year.

$$\mu AS = N(m^L) \int_{m=M^L}^{m^U} f_m(m)\, 10^{(1.5m + 16.05)}\, dm \tag{11}$$

Given the slip-rate, fault area, and magnitude density function, the activity rate, $N(m^L)$ can be computed from Equation (11).

Magnitude Density Distribution

The magnitude density distribution describes the relative number of large magnitude and moderate magnitude events that occur on the seismic source. Two alternative magnitude density functions are usually considered: the truncated exponential model and the characteristic model.

The truncated exponential model is the standard Gutenberg-Richter model that is truncated at the minimum and maximum magnitudes and renormalized so that it integrates to unity. The density function for the truncated exponential model is given by

$$f_m(m) = \frac{\beta \exp(-\beta(m-m^L))}{1-\exp(-\beta(m^U-m^L))} \tag{12}$$

where β is ln(10) times the b-value. Regional estimates of the b-value are usually used with this model.

The characteristic model assumes that more of the seismic energy is released in large magnitude events than for the truncated exponential model. That is, there are fewer small magnitude events for every large magnitude event for the characteristic model than for the truncated exponential model. There are different models for the characteristic model. Two commonly used models are the characteristic model as defined by Youngs and Coppersmith (1985) and the "maximum magnitude" characteristic model. In this paper, we will call these two models the characteristic model and maximum magnitude model, respectively.

The density function for the generalized form of the Youngs and Coppersmith characteristic model is given by

$$f_m(m) = \begin{cases} \dfrac{\beta \exp(-\beta(m-m^L))}{1-\exp(-\beta(m^U-\Delta m_2-m^L))} \dfrac{1}{1+c} & \text{for } m < m^U-\Delta m_2 \\ \dfrac{\beta \exp(-\beta(m^U-\Delta m_1-\Delta m_2-m^L))}{1-\exp(-\beta(m^U-\Delta m_2-m^L))} \dfrac{1}{1+c} & \text{for } m \quad m^U-\Delta m_2 \end{cases} \tag{13}$$

where

$$c = \frac{\beta \exp(-\beta(m^U - \Delta m_1 - \Delta m_2 - m^L))}{1 - \exp(-\beta(m^U - \Delta m_2 - m^L))} \Delta m \qquad (14)$$

In the Youngs and Coppersmith model, Δm_1=1.0 and Δm_2=0.5.

The maximum magnitude model does not include any small earthquakes. It is typically a truncated normal distribution or uniform distribution centered about the characteristic magnitude.

Comparing the examples of the truncated exponential and characteristic density functions, the density functions themselves are similar at small magnitudes. However, when the geologic moment-rate is used to set the annual rate of events, $N(m^L)$, then there is a large impact on $N(m^L)$ depending on the selection of the magnitude density function. The characteristic model has many fewer moderate magnitude events than the truncated exponential model (up to a factor of 10 difference).

Recent studies have found that the characteristic model does a better job of matching observed seismicity than the truncated exponential model (Geomatrix, 1992, Woodward-Clyde, 1994) when the total moment rate is constrained by the geologic slip-rate. However, there is still an ongoing debate about the applicability of these two alternative models.

Rupture Dimension Density Functions

For the rupture area and rupture width, the density functions are determined from regression models, which give the rupture area and rupture width as a function of magnitude. For example, Wells and Coppersmith (1994) developed the following empirical models for rupture area and rupture width:

$$\log_{10}(RA) = -3.49 + 0.91\,M \pm 0.24 \quad (15)$$

$$\log_{10}(W) = -1.01 + 0.32\,M \pm 0.15 \quad (16)$$

The density functions, $f_{RA}(m)$ and $f_{RW}(m)$ are log normal distributions centered about the median values given by Eq. (15) and (16).

Energy Center Location Density Functions

For the energy center locations, we typically assume a uniform distribution over the fault plane. The resulting density functions for $f_{hx}(h_x)$ and $f_{hy}(h_y)$ are unity.